INFORMATION TO USERS

This manuscript has been reproduced from the microfilm master. UMI films the text directly from the original or copy submitted. Thus, some thesis and dissertation copies are in typewriter face, while others may be from any type of computer printer.

The quality of this reproduction is dependent upon the quality of the copy submitted. Broken or indistinct print, colored or poor quality illustrations and photographs, print bleedthrough, substandard margins, and improper alignment can adversely affect reproduction.

In the unlikely event that the author did not send UMI a complete manuscript and there are missing pages, these will be noted. Also, if unauthorized copyright material had to be removed, a note will indicate the deletion.

Oversize materials (e.g., maps, drawings, charts) are reproduced by sectioning the original, beginning at the upper left-hand corner and continuing from left to right in equal sections with small overlaps.

Photographs included in the original manuscript have been reproduced xerographically in this copy. Higher quality 6" x 9" black and white photographic prints are available for any photographs or illustrations appearing in this copy for an additional charge. Contact UMI directly to order.

UMI®

UNIVERSITY OF OKLAHOMA

GRADUATE COLLEGE

VIBRATION OF DISCRETELY STIFFENED SKEW PLATES

AND BRIDGE/VEHICLE INTERACTION ANALYSIS

A Dissertation

SUBMITTED TO THE GRADUATE FACULTY

in partial fulfillment of the requirements for the

degree of

Doctor of Philosophy

BY

HUAN ZENG

Norman, Oklahoma

2000

UMI Number: 9988516

UMI®

VIBRATION OF DISCRETELY STIFFENED SKEW PLATES AND BRIDGE/VEHICLE INTERACTION ANALYSIS

A Dissertation APPROVED FOR THE
SCHOOL OF AEROSPACE AND MECHANICAL ENGINEERING

BY

ACKNOWLEDGMENT

TABLE OF CONTENTS

LIST OF TABLES

LIST OF FIGURES

ABSTRACT

The interaction problem concerning bridges subjected to dynamic vehicle loading has received considerable attention. The difficulty common to a tremendous amount of efforts involves finding a suitable way to treat the dynamic coupling between the bridge and the vehicle. To be more general, skew bridges subjected to multi-axle vehicles are considered in the dissertation.

The vibration of orthogonally stiffened skew plates is studied by using the pb-2 Rayleigh-Ritz method. By minimizing the Rayleigh quotient, the natural frequencies and mode shapes are obtained. The dimensionless natural frequencies of orthogonally stiffened skew plates with different boundary conditions are determined. Since this problem has not been previously studied, the conventional finite element method is used as a comparative check. Numerical results have been presented here for different skew angles, edge ratios, and stiffener height-plate thickness ratios. The results provide rich information to better understand the dynamics of existing orthogonally stiffened plate structures and provide design information.

Then a semi-analytical method is proposed to study the vibration of the bridge under moving vehicles with the use of mode superposition. The response is expressed as the sum of the contribution of different modes. The normal coordinates can be solved explicitly. An iterative approach has been developed to treat the coupling between the bridge and the vehicle.

A general method is proposed to model multi-axle tractor-trailer type vehicles. As an example, a three-axle vehicle is considered. The vehicle model consists of two rigid mass and six wheel masses with eleven degrees of freedom (DOF), which include heave, pitch, and roll motions. The equations of motion are derived with the use of the principle of virtual work. Newmark's method is used to predict the dynamic response of the vehicle.

An existing highway bridge, the Walnut Creek Bridge, is considered. By using the pb-2 Rayleigh-Ritz method, its natural frequencies and mode shapes are obtained and compared with test results. Simulations are conducted for the Walnut Creek Bridge due to moving vehicles. The dynamic amplification factors are computed and compared with test results. The bridge/vehicle interaction problem is further discussed with examination of the effects of the bridge entrance and surface roughness. In this study, different irregularities are used, including perfectly smooth, the measured profile at the Walnut Creek Bridge entrance, and four types of road surface roughness for very good, good, average and poor roads according to the International Organization for Standardization (ISO) specifications. Other factors examined are the vehicle characteristics including vehicle type, axle spacing, vehicle model and speed, and the bridge characteristics including damping, span length and skew angle. The effect of traffic condition is also investigated. Further research is recommended.

CHAPTER ONE [1]

INTRODUCTION

The dynamic response of structures subjected to various moving loads is one of the earliest problems in the field of structural dynamics. The interaction problem concerning bridges subjected to dynamic vehicle loading has received considerable attention. The traffic has been increased significantly over time. Most existing bridges are subjected to heavier traffic than they were designed for. Meanwhile, with the development in construction and material areas, more flexible bridges with less weight have been designed and are in service. This has made it increasingly important for engineers to better understand the interaction between bridges and vehicles, and to estimate accurately the dynamic effects of vehicle on the serviceability of existing bridges and in the design of new bridges.

1.1 Comprehensive review of the bridge/vehicle interaction study

The importance and difficulty of the bridge/vehicle interaction (BVI) problem has led to a large amount of research work. Over the past 150 years, extensive research and experiments have been conducted to understand the bridge

---

[1] Figures and Tables of each chapter are listed at the end of that chapter.

dynamic response to moving vehicles. This section provides a comprehensive review of the research that has been done. Only some of the tremendous amount of work is discussed. The chronological review following provides more detailed references.

Various types of models have been developed for bridges. In the literature, bridges were modeled as a beam of single span (Timoshenko, 1922a and 1922b; Biggs et al., 1957; Humar and Kashif, 1993) or multiple spans (Wen and Toridis, 1962; Palamas et al., 1985). Grillage (Tan et al., 1998; Zeng et al., 1999) or plate models without stiffeners (Gupta and Traill-Nash, 1980; Taheri and Ting, 1990) or with stiffeners (Yener and Chompooming, 1994; Green et al., 1995) were introduced to study the vibration of bridges. Three dimensional (3D) models were usually developed with discrete methods such as the finite element method (FEM) (Bishara et al., 1993; Patten et al., 1999). The plate idealization was used only in studies of simple-span bridges, whereas the single-beam idealization was employed in studies of simple-span bridges and multiple-span continuous bridges. One dimensional (1D) beam representation was simple, but its limitation was apparent. Although 1D representation was efficient to study qualitatively the characteristic of a bridge and to identify critical parameters for BVI study, two dimensional (2D) plate modeling provided more accurate representation of a bridge. For instance, studies have shown the importance of the torsion mode (Marchesiello et al., 1999), which usually would have been ignored in 1D

2

representation. 3D modeling was more detailed oriented. The supporting conditions could be more easily involved, but the computation is more expensive.

Various models have been developed for vehicles as well. In earlier literature, moving force and moving mass approximations were considered (Timoshenko, 1922a and 1922b; Inglis, 1934; Inbanathan and Wieland, 1987). Later on, more practical models, including multiple mass systems (Ginsberg et al., 1976), and tractor-trailer vehicle with different numbers of axles, considering planar motion (Gupta and Traill-Nash, 1980) or 3D motion (Wang et al., 1996), were developed. The most general model (Fafard et al., 1997) involved degrees of freedom (DOF) in three dimensions for three rigid bodies and five axles. The models for vehicles were improved yet more complicated. The loading could include multiple vehicles (Wang et al., 1996). The vehicles were usually assumed to be moving at a constant speed, but the braking and acceleration of the vehicles were also discussed (Gupta and Traill-Nash, 1980; Chompooming and Yener, 1995).

Various methods were employed, which could be categorized into continuous methods and discrete methods. Continuous methods included series expansion (Stokes, 1849; Wilson, 1973), the Rayleigh-Ritz technique (Marchesiello et al., 1999), the Galerkin method (Nelson and Conover, 1971), modal expansion (Chiu et al., 1971) and the method of superposition (Gorman and Garibaldi, 1999). Additional references can be found in Ting and Yener (1983) and GangaRao (1984). Discrete methods, such as the finite strip method (Cheung and Cheung,

1972), the finite difference method (Mulcahy et al., 1979), and the FEM (Taheri and Ting, 1990) were used by many researchers. No method is general. Each of the various techniques has its limitation and advantages. Continuous methods have more restrictions in including details of bridge superstructures or supporting conditions, while they have the advantage of an overview of the dynamic characteristics of the structure and formulation in forced vibration. An analytical model treats a group of bridges. Discrete methods have advantages for free vibration analysis. They can be very detailed for an individual bridge. With the availability and popularity of commercial packages, such as the finite element packages, it is convenient to obtain solutions for natural frequencies and mode shapes of bridges. However, extreme difficulty arises in forced vibration study, especially interaction analysis, where the coupled forced and loading locations are time variant and unknown a priori. Bridge/vehicle interaction elements have been developed to sooth the stress for the coupling study with the use of the FEM (Yang and Lin, 1995; Yang and Yau, 1997).

Extensive studies were conducted to identify the parameters that have critical effects on the bridge dynamic response to the traffic load. The important factors included:

1. Vehicle parameters, which include damping in vehicle suspensions and interleaf friction in the springs (Eichmann, 1954; Heywood, 1996), axle weight and spacing (Ginsberg et al., 1976).

2. Characteristics of bridge superstructures, which include dimension and geometrical shape, span length, number of spans, stiffening conditions, and supporting conditions. These characteristics were often represented by the natural frequencies and mode shapes of the superstructure. In addition, bridge damping (Swannell and Miller, 1987) and bridge surface irregularities (Dodds and Robson, 1973; Wang et al., 1996) were included.

3. Initial conditions (Veletsos and Huang, 1970), vehicle speed (Tan et al., 1998), number of vehicles (Hawk and Ghali, 1981; Yener and Chompooming, 1994), traveling path (Spyrakos, 1998), and braking and acceleration of vehicles (Gupta and Traill-Nash, 1980).

4. Pavement irregularities at the abutments (Hopkins and Deen, 1970), mass ratio of vehicle to bridge, and frequency ratio of vehicle to bridge (Humar and Kashif, 1993),

It was concluded that the initial oscillation of vehicles (especially the initial displacements), matching of bridge and vehicle natural frequencies, and irregularities of bridge surface and approaches are most critical (Chompooming and Yener, 1995; Green et al., 1995).

1.2 Chronological review of the bridge/vehicle interaction study

The first reported research in bridge vibration appears to be the publication by Willis (1849). It discussed the causes of the collapse of the Chester Railway Bridge and formulating the equations of motion based on the model of a point-mass crossing with a constant velocity on a massless but flexible beam. Stokes (1849) obtained an exact solution in closed form by using power series expansion for Willis' differential equation. Robinson (1887) extended Willis' problem by including the mass of the beam.

In the early 20th century, the research emphasized the seeking of an analytical, closed form solution. Among them, Timoshenko and Inglis have to be mentioned for their classical efforts devoted to vibration study of the bridge. Timoshenko discussed the forced vibration of a beam under a moving, constant force (1922a) and a moving, pulsating force (1922b). He identified important parameters, including mass ratio, resonance, and road surface irregularities, which influenced bridge dynamics. Inglis (1934) summarized the previous work and proposed a mathematical treatise on vibrations, which was cited frequently.

Since the 1950s, great efforts have been put forward to studying vibration of bridges due to moving vehicle loading. In 1956, the Highway Research Board published a bulletin that contained a survey of all the significant research to that time. Both analytical and experimental studies were conducted on the effects of dynamic loading and impact. Most of the works can be found in the survey papers by Wright and Green (1959), Ting et al. (1975), Huang (1976), GangaRao and

Haslebacher (1981), and GangaRao (1984). To name a few, Ayre et al. investigated the vibration of a two-span beam under a moving constant force (1950a) and a moving alternating force (1950b). Edgerton and Beecroft (1955) studied the dynamics of continuous plate girder bridges. Suer (1955) studied the dynamic response of simple-span highway bridges to moving vehicle loads. Tung et al. (1956) summarized the highway bridge impact problems. In the 1960s, Wen (1960) studied the dynamic response of beams traversed by two-axle loads. Hirari (1963) modeled the bridge as orthotropic plates with two opposite edges free and the other two simply supported. With the application of high-speed computers, great progress was made in bridge/vehicle interaction study. Yamada and Kobori (1965) studied the bridge impact due to random moving vehicles. Lee (1974) investigated the effect of vehicle braking on the dynamic response of a single-span bridge. Ginsberg et al. (1976) conducted a parametric study of the interaction of bridges and moving vehicles. Discrete methods gained more popularity in the 1970s (Sridharan and Mallik, 1979), particularly, the finite element method (Fam and Trukstra, 1975; Alexandridis, 1977; Olsson, 1985). Mulcahy et al. (1979) applied the finite strip approach to study the dynamic response of bridge decks. Since the 1980s, more attention was paid to identify the parameters that have critical effects on the bridge dynamic response. The parameters included multiple vehicle loading (Hawk and Ghaili, 1981), truck suspensions (Green et al., 1995;

Heywood, 1996; Collop and Cebon, 1997), and surface irregularities (Palamas et al., 1985; Inbanathan and Wieland, 1987; Coussy et al., 1989).

More recently, researchers developed more accurate models for bridge/vehicle interaction problem. Vehicle suspensions, pavement roughness, bridge self-weight, and bridge construction details were included in the modeling (Cole and Cebon, 1992; Wang et al. 1993). Tan et al. (1994) developed a 3D vehicle model to study the bridge/vehicle interaction, while Collop and Cebon (1997) studied the effects of road-friendly suspensions. Wang and Huang (1992) provided a computer modeling analysis to evaluate bridge dynamic response. Gorman and Garibaldi (1999) employed the method of superposition to model the bridge deck. Marchesiello et al. (1999) modeled the bridge as a plate, subjected to moving vehicle with multiple DOF. The models were more reliable. It was shown that it is necessary to include the torsion mode in the model for sufficient accuracy. The simulation results of dynamic response of bridges agreed better with experimental results. Nevertheless, the models got more complicated and computational costs more expensive.

As the difficulty in treating the coupling became apparent, various techniques were proposed to solve the dynamic coupling between the bridge and vehicles. Yang and Yau (1997) developed a bridge/vehicle interaction element to solve the dynamic coupling problem. Yener and Chompooming (1991) formulated the

dynamic coupling for a discrete bridge model. Green and Cebon (1997) proposed an integral method to study the dynamic interaction between bridges and vehicles.

By reviewing the publications in the last few years, one can deduce a trend of the study of the bridge/vehicle interaction. More emphasis has been placed on proposing methods with good convergence, high accuracy, and economic computation to treat the vehicle/bridge interaction (Yang and Yau, 1997; Tan et al., 1998; Hoffmeister and Sedlacek, 2000). Meanwhile, many bridge design codes, including the American Association of State Highway and Transportation Officials (AASHTO) Specifications (1989) and the Ontario Code (1983), have adopted the same impact formula in terms of the span length and frequency of vibration. This formula has been shown to be oversimplified and, in many cases, to misrepresent the dynamics involved in the bridge/vehicle interaction (Yang et al., 1995). Many studies suggested necessary revisions for current bridge design codes or traffic regulations (Carr and Moss, 1982). Considerable efforts are being put forward to providing more practical design codes (Fafard et al., 1998; Spyrakos, 1998).

1.3 Vibration of stiffened plates

The superstructure of a girder bridge consists of a deck, girders, and diaphragms. A stiffened plate is a plate stiffened by discrete elements. The analog

between a girder bridge and a stiffened plate motivates the author to employ the stiffened plate theory to study the bridge/vehicle interaction. The following section provides a brief review of stiffened plate vibration study.

The widespread use of stiffened structural elements in engineering began in the nineteenth century, mainly with the application of steel plates for hulls of ships and with the development of steel bridges and aircraft structures. With bending and buckling being the other two, vibration is one of the three most important engineering problems associated with stiffened plates in that many stiffened plates are designed to resist vibration due to dynamic loads. These stiffened elements, representing a relatively small part of the total weight of the structures, substantially influence their strength and performance under different loading conditions. Because these structural systems can be very complex, all of the techniques of analysis proposed have included certain approximations or have been restricted to certain type of systems. Although a variety of techniques have been proposed to study the vibration of stiffened plate systems, none is completely satisfactory. There exists no exact solution for a general system. The more general the system, the greater the degree of approximation.

All methods may be generally categorized into two groups. In the first category are those methods in which the plate and the stiffeners are replaced by an equivalent system, which is then analyzed. In the second category are those methods that consider the discrete nature of the stiffeners.

A brief literature survey reveals that the most common method used in the early literature was to replace a stiffened plate with an equivalent structurally orthotropic plate. The differential equation for the free vibration of a thin naturally orthotropic plate with uniform thickness was established by Voigt (1910). More than thirty years later, Lekhnitskii (1947; translation in English, 1968) published a monograph which summarized all materials about transverse vibration of anisotropic plates available at that time. Since then, the problems of the transverse vibration of orthotropic plates have been treated in the literature rather extensively. Comprehensive references may be found in the book by Troitsky (1976). Many studies of stiffened rectangular plates have been carried out by using various methods such as the Rayleigh-Ritz method, the Galerkin method, the finite element method, and the finite difference method. Mukherjee and Mukhopadhyay (1986) provided a comprehensive review of related research. To name a few of more recent developments in vibration study of stiffened rectangular plates, Chattopadhyay et al. (1992) developed a so-called isoparametric quadratic plate bending element for free vibration analysis of eccentrically stiffened composite plates. The proposed elements had the capability to deal with plates with irregular shapes and arbitrarily located stiffeners. Palani et al. (1992) proposed two isoparametric finite element models for static and vibration analysis of plates/shells with eccentric stiffeners. The models were applicable for both thin and moderately thick plates by including transverse shear

11

deformations. Mukherjee and Chattopadhyay (1994) proposed a dynamic element method to study the vibration of stiffened plates. Economic improvement was shown for a given accuracy. Chen et al. (1994) presented a spline compound strip method, in which the displacement function was formed by revising the cubic B-splines with plate shape functions. Jin (1997) studied the dynamics of stiffened plates by using the boundary element method to treat the panel components and using the finite element method to treat the stiffening components. The proposed technique was suitable for stiffened plates with arbitrary shapes and with arbitrary boundary conditions. Bedair and Troitsky (1997) investigated the natural frequencies of concentrically and eccentrically simply supported stiffened plates. Barrette et al. (2000) presented a vibration study of stiffened plates with hierarchical finite elements with a set of local trigonometric interpolation functions. The stability and convenience for symbolic manipulation of the trigonometric functions made them potentially attractive for vibration analysis. Zeng and Bert (2000) extended the differential quadrature method to investigate the natural frequencies of rectangular stiffened plates.

Conversely, vibration studies on stiffened skew bridge are not so extensive. In the study of the free vibrations of skew plates with stiffeners running parallel to two parallel edges, the effects of the stiffeners were smeared over the plate to obtain an equivalent isotropic skew plate with uniform thickness (Srinivasan and Ramachandran, 1986) or to obtain an equivalent orthotropic plate (Naruoka et al.,

1967; Thangam Babu and Reddy, 1971; Dokainish and Kumar, 1973). It was desirable to adopt a suitable technique for the combination of the plate and the beam. Srinivasan and Munaswamy (1978) investigated the dynamic characteristics of the stiffened skew plates by using the finite strip method. Mizusawa et al. (1979) determined the natural frequencies by using the Rayleigh-Ritz method with B-spline functions as coordinate functions. The problem of stiffened skew cantilever plates was solved by Liu and Chen (1992) by using the finite element method. Xiang et al. (1995) presented a formulation for the free vibration study of stiffened skew Mindlin plates, using the Rayleigh-Ritz method with Ritz functions consisting of a set of two-dimensional polynomials.

Nevertheless, no literature has been found on the vibration study of an orthogonally stiffened skew plate (OSSP) – a skew plate with stiffeners running orthogonal to two parallel edges, as illustrated in Figure 2.1.a. An OSSP, however, can be found to be of practical importance in various engineering structures. For example, a girder bridge, constructed with a skew angle to accommodate the orientation of the creek passing underneath, has girders running parallel to two edges and diaphragms running orthogonal to the other two edges.

In the analytical study of a PSSP – a stiffened skew plate with stiffeners running parallel to two parallel edges, oblique coordinates are usually employed. Such coordinates are capable and convenient to describe both the plate and the stiffeners. For an OSSP, an oblique coordinate system is convenient for the plate;

13

however, the Cartesian coordinate system is more suitable for the description of the stiffening elements. This introduces more difficulty and extra computational effort to deal with an OSSP. This has challenged the author to study the vibrations of such orthogonally stiffened skew plate structures, then would the bridge/vehicle interaction analysis be possible.

The recently developed pb-2 Rayleigh-Ritz method was proposed as an alternative to the conventional numerical methods. It is a full-field energy technique, which eliminates the need for discretization and thus a large number of degrees of freedom. The key to the pb-2 Rayleigh-Ritz method is the definition of the trial functions, which are the product of two-dimensional orthogonal polynomials. The basic trial functions are enhanced with boundary conditions (simply supported, free, or clamped). The acquired accuracy can be obtained by increasing the number of terms of the orthogonal polynomials. Very recently, Chakraverty et al. (1999), with over 150 references, gave a comprehensive survey of the research that has been done for vibration analysis of various structures using the pb-2 Rayleigh-Ritz method. To name a few of the tremendous amount of work, Liew and Lam (1990) studied the vibration of skew plates. Liew and Wang (1993) used this method for general plate analysis. Xiang et al.(1995) studied the vibration of stiffened skew Mindlin plates. Karunasena et al. (1996) presented a free vibration study of thick arbitrary quadrilateral plates.

The pb-2 Rayleigh-Ritz method, with the FEM as a comparative check, is used in the present study.

1.4 Bridge/vehicle interaction analysis by stiffened plate theory — An overview of dissertation

Clearly, so much research towards the solution of a seemingly well-defined boundary-/initial-value problem indicates that there is common difficulty in various efforts. The difficulty involves finding a suitable way to treat the dynamic coupling between the bridge and the vehicle. In the dissertation, the author uses the skew stiffened plate theory to solve the bridge/vehicle interaction problem.

First of all, the present work studies the vibration of orthogonally stiffened skew plates by using the pb-2 Rayleigh-Ritz method. The first Ritz function is defined to satisfy both the geometry conditions of the bridge edges and the pier supports. The higher terms of the 2D orthogonal functions are generated by using the Gram-Schmidt orthogonalization process. The total energy of the plate and the stiffeners is derived and expressed in terms of the 2D orthogonal functions. By minimizing the Rayleigh quotient, the natural frequencies and mode shapes are obtained by solving the eigenvalue problem. The convergence and accuracy are dependent upon the number of terms used in the truncated series. The

dimensionless natural frequencies of orthogonally stiffened skew plates with different boundary conditions are determined. Since this problem has not been previously studied, the conventional FEM is used as a comparative check. The agreement between these two methods is very good. With additional favorable comparison with available publications, it is concluded that the pb-2 Rayleigh-Ritz method can provide accurate solution. Numerical results have been presented for different skew angles, edge ratios, and height-thickness ratios, which will be defined later. The results provide rich information to better understand the dynamics of existing orthogonally stiffened plate structures and provide design information.

A semi-analytical method is proposed to study the forced vibration of the bridge under moving vehicles with the use of mode superposition. The mode shapes are normalized according to the mass matrix such that the modes are decoupled. This procedure results in a few uncoupled equations for the normal coordinates, which have explicit analytical solutions and will be solved simultaneously. The response is expressed as the sum of the contribution of different modes. The excitation from vehicle axles is assumed to be constant in a small time increment. An iterative approach has been developed to treat the coupling between the bridge and the vehicle.

A general method is proposed to model multi-axle tractor-trailer type vehicles. As an example, a vehicle model for a tractor with semi-trailer is developed.

Without lack of generality, three axles are considered. The vehicle model consists of two rigid masses and six wheel masses with eleven DOF, which include heave, pitch and roll motions. The equations of motion are derived with the use of the principle of virtual work. Separate models are developed for AASHTO (1989) standard H series trucks, HS series trucks, and a so-called Rock Truck that was used in the bridge field test. The Newmark method is used to predict the dynamic response of the vehicle.

The vibration theory of orthogonally stiffened plates is then extended to study the vibration of an existing highway bridge, the Walnut Creek Bridge, on Interstate Highway I-35 near Purcell, Oklahoma. The four-span girder bridge is modeled as a continuous stiffened plate with point supports at the interval piers. With the use of the Rayleigh-Ritz pb-2 method, the natural frequencies and mode shapes are obtained.

Simulations are conducted for the Walnut Creek Bridge due to a moving Rock Truck. The bridge/vehicle interaction problem is further discussed with examination of the effects of the bridge entrance and surface roughness. Different irregularities are used in the study, which include perfectly smooth, the measured profile at the Walnut Creek Bridge entrance, and four types of road surface roughness generated from power spectral density function for very good, good, average, and poor roads according to the International Organization for Standardization (ISO) specifications.

More general discussions on the bridge/vehicle interaction are conducted by employing the AASHTO standard trucks. The effects of influencing factors on the dynamic amplification factor are investigated. Those factors are the vehicle characteristics including axle weight, axle spacing, vehicle model and speed, and the bridge characteristics including damping, skew angle, and span length. The effect of traffic condition is also investigated.

Further research is recommended in the last section.

CHAPTER TWO

FREE VIBRATION ANALYSIS OF

DISCRETELY STIFFENED SKEW PLATES

The stiffened plate vibration problem may be solved using either the energy functional or the governing partial differential equations. Both approaches can be attempted using standard analytical and numerical techniques. Among the methods are the finite element method, the finite difference method, the boundary element method, the differential quadrature method, the Rayleigh method, the Galerkin method, and the Rayleigh-Ritz method. In the present study, the Rayleigh-Ritz technique is adopted due to its efficiency and simplicity in numerical complementation.

The Rayleigh-Ritz method is a generalized one of the Rayleigh approximation approaches. The Rayleigh method is based on the principle that a system vibrating in one of its natural modes interchanges its energy between its potential and kinetic forms without energy dissipation. By using a trial function for the mode shapes, which satisfies at least the geometric boundary conditions, and with the assumption of harmonic motion, the minimization of the difference between the maximum potential energy and maximum kinetic energy yields the vibration frequencies and corresponding mode shapes. Ritz generalized the Rayleigh

method by assuming a set of admissible functions with independent coefficients. The frequencies and mode shapes could be obtained by a similar minimizing procedure. The Rayleigh-Ritz method is a full-field energy technique, which eliminates the need for discretization and thus a large number of degrees of freedom. It provides upper bound solutions for natural frequencies.

The most commonly used trial functions are the beam functions, the spline functions, and the beam characteristic orthogonal polynomials. Among these functions, the beam characteristic orthogonal polynomials yield the best results for rectangular plates with any combinations of boundary conditions (Liew et al. (1998). However, their application to plates in other shapes, for instance, a skew plate, may not be convenient. Thus, many intensive investigations have been focused on the use of two-dimensional polynomials associated with appropriate basic functions in the vibration analysis of plates.

The key to the pb-2 Rayleigh-Ritz method is the definition of the trial functions, which are the product of two-dimensional orthogonal polynomials. The basic trial functions are enhanced with boundary conditions such as simply supported, free, or clamped. The point support and line support can be included accordingly. The accuracy and the rate of convergence of the Rayleigh-Ritz method depend on the choice of the basic function and the finite number of approximation functions. The required accuracy can be obtained by increasing the number of terms of the orthogonal polynomials. Furthermore, since the

polynomial functions allow differentiation and integration to be carried out in an exact way, they are also easy to be implemented in computer code, and thus the computational accuracy is enhanced.

2.1 Formulation for the pb-2 Rayleigh-Ritz Method

The geometry of an isotropic elastic thin skew plate with orthogonal stiffeners is shown in Figure 2.1.a. For free vibration, the displacement of such a plate is a harmonic function of time,

$$w(x, y, t) = W(x, y)e^{i\omega t} \tag{2.1}$$

where $W(x, y)$ is the mode shape, and ω is the natural frequency in rad/s. $W(x, y)$ can be expressed in terms of two-dimensional orthogonal polynomials as

$$W(x, y) = \sum_{i=1}^{m} C_i \phi_i(x, y) \tag{2.2}$$

where m is the total number of the terms used for desired accuracy, C_i are independent coefficients, $\phi_i(x, y)$ are the two-dimensional orthogonal polynomials. The starting polynomial $\phi_1(x, y)$ is formed by the product of geometric boundary expressions. Then a recursive formula is used to obtain the subsequent polynomials (Bhat, 1987; Liew and Lam, 1990). Although an oblique coordinate system is convenient to describe the skew plate, it introduces extra difficulty and complexity in describing the stiffeners. So the Cartesian coordinate

system (x-y) is employed as the physical coordinate, meanwhile, a unit square domain (s-t) is introduced as a calculation domain for the plate.

A skew domain can be represented by three parameters a, b and ϕ, as shown in Figure 2.1.a. The special case of $\phi = 90°$ represents the rectangular domain. To generate a general set of orthogonal 2D polynomials, the following mapping is employed:

$$x = as + bt\cos(\phi) \qquad (2.3)$$

$$y = bt\sin(\phi) \qquad (2.4)$$

where x and y are coordinates for the physical domain, and s and t are mapped coordinates for calculation as shown in Figure 2.1.c. The relations between the partial derivatives are:

$$( )_{,x} = \frac{1}{a}( )_{,s} \qquad (2.5)$$

$$( )_{,y} = -\frac{1}{a\tan(\phi)}( )_{,s} + \frac{1}{b\sin(\phi)}( )_{,t} \qquad (2.6)$$

where a comma denotes partial differentiation. The inverse transform from s-t domain to x-y domain can be carried out as:

$$s = \frac{x}{a} - \frac{y}{a\tan(\phi)} \qquad (2.7)$$

$$t = \frac{y}{b\sin(\phi)} \qquad (2.8)$$

The starting polynomial is given by

$$\dot{\phi}_1(x,y) = \prod_{n=1}^{6} \varphi_n(x,y) \qquad (2.9)$$

where $\prod$ denotes the product of the terms. Suitable $\varphi_n(x,y)$ are taken for different boundary conditions:

(1) for a simply supported edge,

$$\varphi(x,y) = \begin{cases} x-a & at \quad edge \quad x=a \\ y-b & at \quad edge \quad y=b \\ y-cx-d & at \quad edge \quad y=cx+d \end{cases} \qquad (2.9a)$$

(2) for a clamped edge,

$$\varphi(x,y) = \begin{cases} (x-a)^2 & at \quad edge \quad x=a \\ (y-b)^2 & at \quad edge \quad y=b \\ (y-cx-d)^2 & at \quad edge \quad y=cx+d \end{cases} \qquad (2.9b)$$

(3) for a free edge,

$$\varphi(x,y) = 1 \qquad (2.9c)$$

(4) for a single, simple point support in the plate domain at (x_0,y_0),

$$\varphi(x,y) = (x-x_0)^2 + (y-y_0)^2 \qquad (2.9d)$$

(5) for a simple line support in the plate domain at $y=cx+d$,

$$\varphi(x,y) = y-cx-d \qquad (2.9e)$$

The starting polynomial $\dot{\phi}_1(x,y)$ is first transformed into s-t domain as $\dot{\phi}_1(s,t)$.

After forming $\dot{\phi}_1(s,t)$, the other functions can be obtained as

$$\dot{\phi}_2(s,t) = (s-a_{2,1})\dot{\phi}_1(s,t) \qquad (2.10)$$

23

Applying the Gram-Schmidt orthogonalization process gives

$$\int_0^1 \int_0^1 \phi_i(s,t)\phi_j(s,t)\,ds\,dt = \delta_{ij} \tag{2.11}$$

where δ_{ij} is the Kronecker delta function.

Multiplying Equation (2.10) by $\phi_2(s,t)$ and integrating in the plate domain results in

$$a_{2,1} = \frac{\int_0^1 \int_0^1 s\phi_1(s,t)\phi_1(s,t)\,ds\,dt}{\int_0^1 \int_0^1 \phi_1(s,t)\phi_1(s,t)\,ds\,dt} \tag{2.12}$$

Similarly, the recursion formula for higher terms $(m \ge 3)$ can be derived as:

$$\phi_m(s,t) = f_m(s,t)\phi_1(s,t) - \sum_{i=1}^{m-1} a_{m,i}\phi_i(s,t) \tag{2.13}$$

with

$$a_{m,i} = \frac{\int_0^1 \int_0^1 f_m(s,t)\phi_1(s,t)\phi_i(s,t)\,ds\,dt}{\int_0^1 \int_0^1 \phi_i(s,t)\phi_i(s,t)\,ds\,dt} \tag{2.14}$$

where $f_m(s,t)$ is the generating function, $m = \dfrac{p(p+1)}{2} + 1, \ \dots \ , \dfrac{(p+1)(p+2)}{2}$, and p is the degree of the polynomials. For example, the first six generating functions are:

$$f_1(s,t) = 1, \text{ for } p = 0,$$

$$f_2(s,t) = s, \quad f_3(s,t) = t, \text{ for } p = 1,$$

$$f_4(s,t) = s^2, \quad f_5(s,t) = st, \quad f_6(s,t) = t^2, \text{ for } p = 2.$$

After the necessary functions are generated in the *s-t* domain, they could be easily

transformed into the *x-y* domain.

2.2   Minimization of the Rayleigh quotient

The original Rayleigh method is based on Rayleigh's principle, which can be

stated as (Rao, 1995)

The frequency of vibration of a conservative system vibrating about an

equilibrium position has a stationary value in the neighborhood of a natural

mode. This stationary value, in fact, is a minimum value in the neighborhood of

the fundamental natural mode.

For an N degree-of-freedom system, the kinetic energy T is given by

$$T = \frac{1}{2}\dot{x}^T M\dot{x}$$

$$(2.15)$$

and the potential energy U is given by

$$U = \frac{1}{2}x^T Kx$$

$$(2.16)$$

with M and K being the system mass and stiffness matrices, respectively, x being

the displacement vector of the generalized coordinates, and $(\ )^T$ denotes the

transpose.

To find the natural frequency of the jth mode ω_j, one assumes harmonic motion

25

$$x(t) = X_j e^{i\omega_j t}$$

(2.17)

with X_j being the exact real eigenvector.

Then the maximum kinetic energy is

$$T_{max} = \frac{1}{2}\omega_j^2 X_j^T M X_j$$

(2.18)

and the maximum potential energy is

$$U_{max} = \frac{1}{2}X_j^T K X_j$$

(2.19)

For a conservative system, $T_{max} = U_{max}$. By equating Equations (2.18) and (2.19), one has

$$\omega_j^2 = \frac{X_j^T K X_j}{X_j^T M X_j}$$

(2.20)

The right-hand-side of Equation (2.20) is known as the Rayleigh quotient.

When applied to continuous systems, it is convenient to leave the quotient expressed in terms of energies. For convenience, define T'_{max} as

$$T'_{max} = \frac{T_{max}}{\omega_j^2}$$

(2.21)

The Rayleigh quotient can then be expressed as $\dfrac{U_{max}}{T'_{max}}$.

According to Rayleigh's principle, the Rayleigh quotient is minimized to provide a minimum value of the natural frequency. The original Rayleigh method

gives an upper-bound approximation of the lowest natural frequency. Detailed proof was given by Newland (1989), for example.

In the Rayleigh-Ritz method, the approximate modal function $w(x,y)$ is chosen as

$$w(x,y) = \sum_i^{\infty} C_i \phi_i(x,y)$$

(2.22)

Rayleigh quotient is then

$$\omega^2 = \frac{U_{max}(C_1, C_2, ...)}{T'_{max}(C_1, C_2, ...)}$$

(2.23)

which can be rewritten as

$$\omega^2 T'_{max}(C_1, C_2, ...) = U_{max}(C_1, C_2, ...)$$

(2.24)

Differentiating with respect to C_i gives

$$\frac{\partial \omega^2}{\partial C_i} T'_{max} + \omega^2 \frac{\partial T'_{max}}{\partial C_i} = \frac{\partial U_{max}}{\partial C_i}$$

(2.25)

According to differential calculus, ω is a minimum when

$$\frac{\partial \omega^2}{\partial C_i} = 0$$

(2.26)

which occurs when

$$\frac{\partial U_{max}}{\partial C_i} - \omega^2 \frac{\partial T'_{max}}{\partial C_i} = 0$$

(2.27)

Finally we have

$$\frac{\partial(U_{max} - T_{max})}{\partial C_i} = 0$$

(2.28)

which frequently appears in technical papers with Rayleigh-type methods.

2.3   Eigen solutions for vibration of an OSSP

The total energy of a stiffened plate is the sum of the total energy of the plate and that of the Bernoulli-Euler beam stiffeners. By assuming N_x X-type (perpendicular to x-axis) stiffeners (with ρ_x, E_x, I_x, and A_x) and N_y Y-type (perpendicular to y-axis) stiffeners (with ρ_y, E_y, I_y, and A_y), the strain energy U and the kinetic energy T of the system can be expressed as:

$$U = U_p + U_s$$

(2.29)

$$T = T_p + T_s$$

(2.30)

with, for a thin plate of isotropic material,

$$U_p = \iint_{\Omega_A} \frac{D}{2} \left[w_{,xx}^2 + w_{,yy}^2 + 2\nu(w_{,xx} w_{,yy}) + 2(1-\nu)w_{,xy}^2 \right] dxdy$$

(2.31)

$$U_s = \sum_{i=1}^{N_x} \int_{L_x} \frac{E_x I_x}{2} w_{,yy}^2 \bigg|_{x=x_i} dy + \sum_{i=1}^{N_y} \int_{L_y} \frac{E_y I_y}{2} w_{,xx}^2 \bigg|_{y=y_i} dx$$

(2.32)

$$T_p = \iint_{\Omega_A} \frac{\rho h}{2} w_{,t}^2 dxdy$$

(2.33)

$$T_s = \sum_{i=1}^{Nx} \int_{L_x} \frac{\rho_x A_x}{2} w_{,i}^2 \Big|_{x=x_i} dy + \sum_{i=1}^{Ny} \int_{L_y} \frac{\rho_y A_y}{2} w_{,j}^2 \Big|_{y=y_i} dx \qquad (2.34)$$

where ρ is the density of the plate, h is the plate thickness, v is the Poisson's ratio, and D is the plate flexural rigidity given by

$$D = \frac{Eh^3}{12(1-v^2)} \qquad (2.35)$$

with E being the Young's modulus of the plate.

Substitution of Equation (2.1) into Equations (2.31) to (2.34) yields

$$U_{p\,max} = \frac{D}{2} \iint_{\Omega_A} \left[W_{,xx}^2 + W_{,yy}^2 + 2v W_{,xx} W_{,yy} + 2(1-v) W_{,xy}^2 \right] dxdy \qquad (2.36)$$

$$U_{s\,max} = \frac{1}{2} \sum_{i=1}^{Nx} \int_{L_x} E_x I_x W_{,yy}^2 \Big|_{x=x_i} dy + \frac{1}{2} \sum_{i=1}^{Ny} \int_{L_y} E_y I_y W_{,xx}^2 \Big|_{y=y_i} dx \qquad (2.37)$$

$$T_{p\,max} = \frac{1}{2} \rho h \omega^2 \iint_{\Omega_A} W^2 dxdy \qquad (2.38)$$

$$T_{s\,max} = \frac{1}{2} \omega^2 \left(\sum_{i=1}^{Nx} \int_{L_x} \rho_x A_x W^2 \Big|_{x=x_i} dy + \sum_{i=1}^{Ny} \int_{L_y} \rho_y A_y W^2 \Big|_{y=y_i} dx \right) \qquad (2.39)$$

Substituting Equation (2.2) into Equations (2.34) to (2.39) gives

$$U_{p\,max} = \frac{D}{2} \left(\sum_{i=1}^{m} \sum_{j=1}^{m} C_i C_j \iint_{\Omega_A} \left[\phi_{i,xx} \phi_{j,xx} + \phi_{i,yy} \phi_{j,yy} + 2v \phi_{i,xx} \phi_{j,yy} + 2(1-v) \phi_{i,xy} \phi_{j,xy} \right] dxdy \right) \qquad (2.40)$$

$$U_{s\,max} = \frac{1}{2} \left(\begin{array}{l} \sum_{k=1}^{Nx} \int_{L_x} E_x I_x \sum_{i=1}^{m} \sum_{j=1}^{m} C_i C_j \phi_{i,yy} \phi_{j,yy}\bigg|_{x=x_k} dy \\ + \sum_{k=1}^{Ny} \int_{L_y} E_y I_y \sum_{i=1}^{m} \sum_{j=1}^{m} C_i C_j \phi_{i,xx} \phi_{j,xx}\bigg|_{y=y_k} dx \end{array} \right) \tag{2.41}$$

$$T_{p\,max} = \frac{1}{2}\omega^2 \iint_{\Omega_t} \rho h \sum_{i=1}^{m} \sum_{j=1}^{m} C_i C_j \phi_i \phi_j \, dxdy \tag{2.42}$$

$$T_{s\,max} = \frac{1}{2}\omega^2 \left(\begin{array}{l} \sum_{k=1}^{Nx} \int_{L_x} \rho_x A_x \sum_{i=1}^{m} \sum_{j=1}^{m} C_i C_j \phi_i \phi_j \bigg|_{x=x_k} dy \\ + \sum_{k=1}^{Ny} \int_{L_y} \rho_y A_y \sum_{i=1}^{m} \sum_{j=1}^{m} C_i C_j \phi_i \phi_j \bigg|_{y=y_k} dx \end{array} \right) \tag{2.43}$$

Applying the Rayleigh-Ritz minimization procedure to the difference between the maximum strain energy and the maximum kinetic energy with respect to the independent coefficients C_i

$$\frac{\partial}{\partial C_i}(U_{max} - T_{max}) = 0, \qquad i = 1,2,...,m \tag{2.44}$$

leads to the eigenvalue problem

$$\sum_j [K_{ij} - \omega^2 M_{ij}] C_j = 0 \tag{2.45}$$

where

$$K_{ij} = D \iint_{\Omega_A} \left[\begin{array}{l} \phi_{i,xx}\phi_{j,xx} + \phi_{i,yy}\phi_{j,yy} + 2(1-v)\phi_{i,xy}\phi_{j,xy} \\ + v(\phi_{i,xx}\phi_{j,yy} + \phi_{j,xx}\phi_{i,yy}) \end{array} \right] dxdy$$
$$+ E_x I_x \sum_{k=1}^{N_x} \int_{L_x} \phi_{i,yy}\phi_{j,yy}\bigg|_{x=x_k} dy + E_y I_y \sum_{k=1}^{N_y} \int_{L_y} \phi_{i,xx}\phi_{j,xx}\bigg|_{y=y_k} dx \tag{2.46}$$

$$M_{ij} = \rho_p h \iint_{\Omega_A} \dot{\phi}_i \dot{\phi}_j \, dxdy + \rho_s A_x \sum_{k=1}^{N_x} \int_{L_x} \dot{\phi}_i \dot{\phi}_j \Big|_{x=x_k} dy + \rho_s A_y \sum_{k=1}^{N_y} \int_{L_y} \dot{\phi}_i \dot{\phi}_j \Big|_{y=y_k} dx \qquad (2.47)$$

or

$$K\widetilde{C} = \omega^2 M\widetilde{C} \qquad (2.48)$$

where $\widetilde{C} = \{C_1, ..., C_m\}^T$.

Apparently, K and M are symmetric matrices. Eigen-solutions of Equation (2.45) provide the natural frequencies and mode shapes of the orthogonally stiffened skew plates.

To minimize the truncation error introduced in numerical computation, the double integral in the skew domain is carried out by transforming it into the calculation domain, while the single integral is carried out in the x-y physical domain. The mapping relations are as follows:

$$\iint_{\Omega_A} \left[\begin{array}{l} \phi_{i,xx}\phi_{j,xx} + \phi_{i,yy}\phi_{j,yy} + 2(1-\nu)\phi_{i,xy}\phi_{j,xy} \\ + \nu\left(\phi_{i,xx}\phi_{j,yy} + \phi_{i,yy}\phi_{j,xx}\right) \end{array} \right] dxdy = \frac{a^2}{\mu^3 \sin^3(\phi)} \times$$

$$\int_0^1 \int_0^1 \left[\begin{array}{l} \mu^4 \phi_{i,ss}\phi_{j,ss} + \phi_{i,tt}\phi_{j,tt} + \\ -2\mu^3 \cos\phi\left(\phi_{i,ss}\phi_{j,st} + \phi_{j,ss}\phi_{i,st}\right) + \mu^2\left(\cos^2\phi + \nu\sin^2\phi\right)\left(\phi_{i,ss}\phi_{j,tt} + \phi_{i,tt}\phi_{j,ss}\right) \\ + 2\mu^2\left(1 + \cos^2\phi - \nu\sin^2\phi\right)\phi_{i,st}\phi_{j,st} - 2\mu\cos\phi\left(\phi_{i,st}\phi_{j,tt} + \phi_{j,tt}\phi_{i,st}\right) \end{array} \right] dsdt$$

$$(2.49)$$

$$\iint_{\Omega_A} \dot{\phi}_i \dot{\phi}_j \, dxdy = \mu a^2 \sin(\phi) \int_0^1 \int_0^1 \dot{\phi}_i \dot{\phi}_j \, dsdt \qquad (2.50)$$

with μ being the edge ratio and defined by $\mu = b/a$.

2.4 Normalization of the eigenvectors with respect to the mass matrix

All the eigenvectors form the modal matrix, which is denoted by V. The jth column of the modal matrix V_j is the eigenvector corresponding to the jth mode. Equation (2.48) can be rewritten as:

$$KV_j = \omega_j^2 M V_j \qquad (2.51)$$

Multiplied by V_i^T, Equation (2.51) becomes

$$V_i^T K V_j = \omega_j^2 V_i^T M V_j \qquad (2.52)$$

Similarly,

$$V_j^T K V_i = \omega_i^2 V_j^T M V_i \qquad (2.53)$$

Take the transpose of Equation (2.52)

$$V_j^T K^T V_i = \omega_j^2 V_j^T M^T V_i \qquad (2.54)$$

Since K and M are symmetric,

$$K^T = K, \; M^T = M \qquad (2.55)$$

Subtraction Equation (2.54) from Equation (2.53) gives

$$\left(\omega_i^2 - \omega_j^2\right) V_j^T M V_i = 0 \qquad (2.56)$$

thus

$$V_j^T M V_i = 0 \text{ for } i \neq j \qquad (2.57)$$

Similarly,

$$V_j^T K V_i = 0 \text{ for } i \neq j.$$

$$(2.58)$$

Finally, if $i = j$, we let

$$V_i^T M V_i = M_i$$

$$(2.59)$$

$$V_i^T K V_i = K_i$$

$$(2.60)$$

Equations (2.57) to (2.60) define the orthogonality of the eigenvectors of Equation (2.45).

The eigenvectors can be normalized with respect to mass as:

$$\hat{V}_i^T M \hat{V}_i = 1$$

$$(2.61)$$

$$\hat{V}_i^T K \hat{V}_i = \omega_i^2$$

$$(2.62)$$

with

$$\hat{V}_i = \frac{V_i}{\sqrt{M_i}}$$

$$(2.63)$$

2.5   Convergence of solutions

The results converge differently for various boundary conditions. Skew plates with cross central stiffeners with boundary conditions as shown in Figure 2.2 were taken to study the convergence. A dimensionless natural frequency is defined as:

33

$$\Omega = \frac{\omega a^2}{2\pi} \sqrt{\frac{\rho h}{D}} \qquad\qquad\qquad (2.64)$$

A Poisson's ratio of $\nu = 0.3$, $\phi = 50^{\circ}$, $b/a = 1$, $f/h = 4$ and $e/h = 1$ have been used in the computation. The stiffeners in a plate are assumed to have the same geometry and share the material properties with the plate. Tables 2.1 to 2.3 provide the convergence patterns of the lowest six dimensionless natural frequencies Ω for CFFF, SFSF, and FSFS (C--Clamped, S--Simply supported, F--Free, see Figure 2.2) stiffened skew plates. It is apparent that more terms are required for higher frequencies. The convergence study indicates that $p = 10$ is necessary for the lowest six frequencies to converge. Thus $p = 10$ is used in subsequent frequency calculations to ensure the satisfactory accuracy of the solutions.

A general finite element code, Pro/MECHANICA, by Parametric Technology Corporation, was used to perform the modal analysis. The plate was represented by triangular and quadrilateral shell elements, while the stiffeners were represented by two-node beam elements. The function AutoGEM was used with Multi-Pass adaptive convergence method. AutoGEM automatically generates elements that provide accurate results when Pro/MECHANICA analyzes the model. By using Multi-Pass, the structure engine performs calculations and increases the polynomial order for each element edge until the difference in the results of the last two calculations is within the convergence percentage specified.

34

A frequency convergence of 1% was specified for the lowest ten natural frequencies. Actually it turned out that the lowest six frequencies converge within 0.1%.

Close agreement can be found between these two methods (see Tables 2.1 through 2.3).

2.6 Numerical results and discussion

To better understand the vibration characteristics of OSSP structures and to provide useful information for design of such structures, the lowest four dimensionless natural frequencies of two typical OSSP, with one central stiffener (see Figure 2.1.a) and with cross central stiffeners (see Figure 2.2), are discussed. For comparative purposes, corresponding skew plates without stiffeners are included. Three different types of boundary conditions, i. e., CFFF, SFSF, FSFS, are studied. For each boundary condition, studies were conducted to investigate the variation of the natural frequencies with skew angle ϕ, edge ratio b/a, and height-thickness ratio f/h. In all calculations, the stiffeners were assumed to be the same in each OSSP, and with $e/h = 1$. The eccentricity of the stiffeners was considered.

2.6.1 Frequencies vs. skew angle ϕ

Figures 2.3 through 2.5 present the frequency variation with skew angle ϕ for CFFF, FSFS, and SFSF skew plates with no stiffener (a), with one X-type stiffener (b), and with cross stiffeners (c). The ratios $b/a = 1$ and $f/h = 4$ are assumed. The reason for the selection of a ratio $f/h = 4$ will be apparent in the discussion of the effect of ratio f/h.

Figure 2.3.a presents the results obtained by using the pb-2 Rayleigh-Ritz method and the finite element method. They are compared with Leissa's (1969) results that were obtained by Claassen (1963). Very good agreement is shown. It can be concluded that the present study gives accurate results.

For the CFFF plates, the effect of stiffeners is apparent. The introduction of stiffeners increases the frequencies. The second mode is more sensitive to skew angle than other modes. For FSFS and SFSF plates, the effects of stiffeners and skew angle are slight, while the effects are more substantial on higher modes.

2.6.2 Frequencies vs. edge ratio b/a

Skew plates with different stiffener distributions as (a), (b) and (c), with $\phi = 45°$, $f/h = 4$, and various b/a are considered. The variation of frequencies with edge ratio b/a is plotted in Figures 2.6 through 2.8 for CFFF, SFSF, and FSFS plates respectively. The trends of the frequency variation vs. edge ratio are similar for the boundary supports CFFF and FSFS. As the edge ratio gets smaller,

the frequencies increase significantly. However, this is not seen in SFSF plates. This difference is because of the geometry and the supports of the plates. The constraints are in the longer edge. When the plates get narrower, the twisting constraint or stiffening effect gets much more significant and increases the frequencies substantially. Meanwhile, in SFSF plates, the longer edges are free. The bending modes are more critical. Compared to the other boundary conditions, SFSF plates have lower frequencies. Again, the figures show that the introduction of stiffeners has less effect on lower modes.

2.6.3 Frequencies vs. height-thickness ratio f/h

Skew plates with different stiffener distributions as (b) and (c) and with $b/a = 1$, $\phi = 45^{\circ}$, and various f/h are considered. The variation of frequencies with f/h is plotted in Figures 2.9 through 2.11 for CFFF, SFSF, and FSFS plates, respectively.

It should be noted that a ratio of $f/h > 6$ is not practical, where local buckling would be a problem. Here buckling is not considered. Ratios up to 10 are considered for the purpose of showing the trend of frequency variation.

Figures 2.9 to 2.11 show that for $f/h < 2$, the introduction of stiffeners does not affect the frequencies significantly. They are close to those of the corresponding skew plates without any stiffeners (This clarifies the reason for

choosing $f/h = 4$ in the other parameter studies). It is because the stiffeners occupy only a small part of the total weight. They provide the structure with more stiffness effect than mass effect. For those boundary condition sets considered in the present study, the effects of Y-type stiffeners are more significant than those of X-type stiffeners. The frequencies vary slightly with f/h for plates with X-type stiffeners, except the second mode of CFFF plates. However, for those plates with cross stiffeners, the variation is more apparent.

2.7 Summary

The free vibrations of orthogonally stiffened skew plates are extensively investigated. The parametric study indicates that the light-weight stiffeners provide more stiffness effect than mass effect to a structure. Usually, the stiffeners have larger effect on higher modes. Skew plates with various shapes (different skew angle and edge ratio) are discussed. Relatively higher frequencies are observed with higher skew angle or smaller edge ratio. The effect of the geometry of the stiffeners is investigated by varying the height of cross section. Deeper stiffeners provide more stiffness.

(a)   (c)

(b)
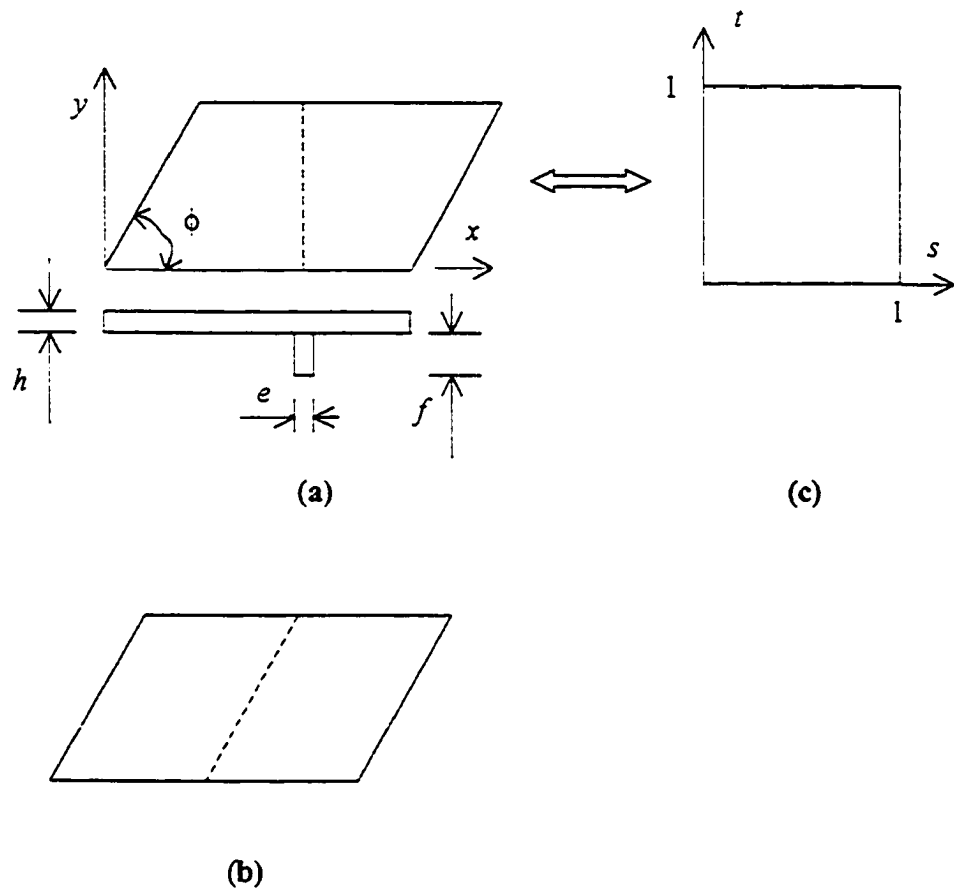
Figure 2.1: (a) Skew plate with a stiffener orthogonal to two parallel edges (OSSP);
(b) Skew plate with a stiffener parallel to two parallel edges (PSSP);
(c) Square calculation domain.

CFFF   FSFS   SFSF
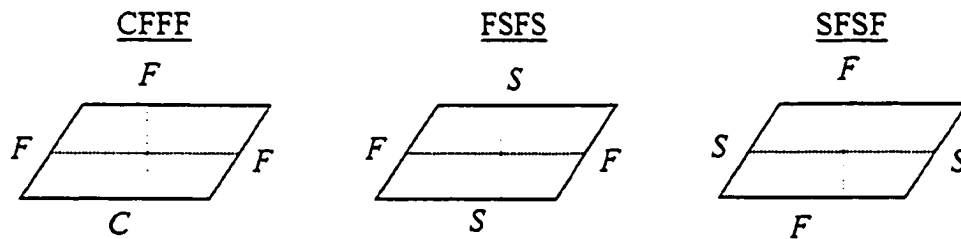
Figure 2.2:   Skew plates with cross stiffeners and various boundary conditions
(C–clamped, F–Free, S–Simply supported)

39
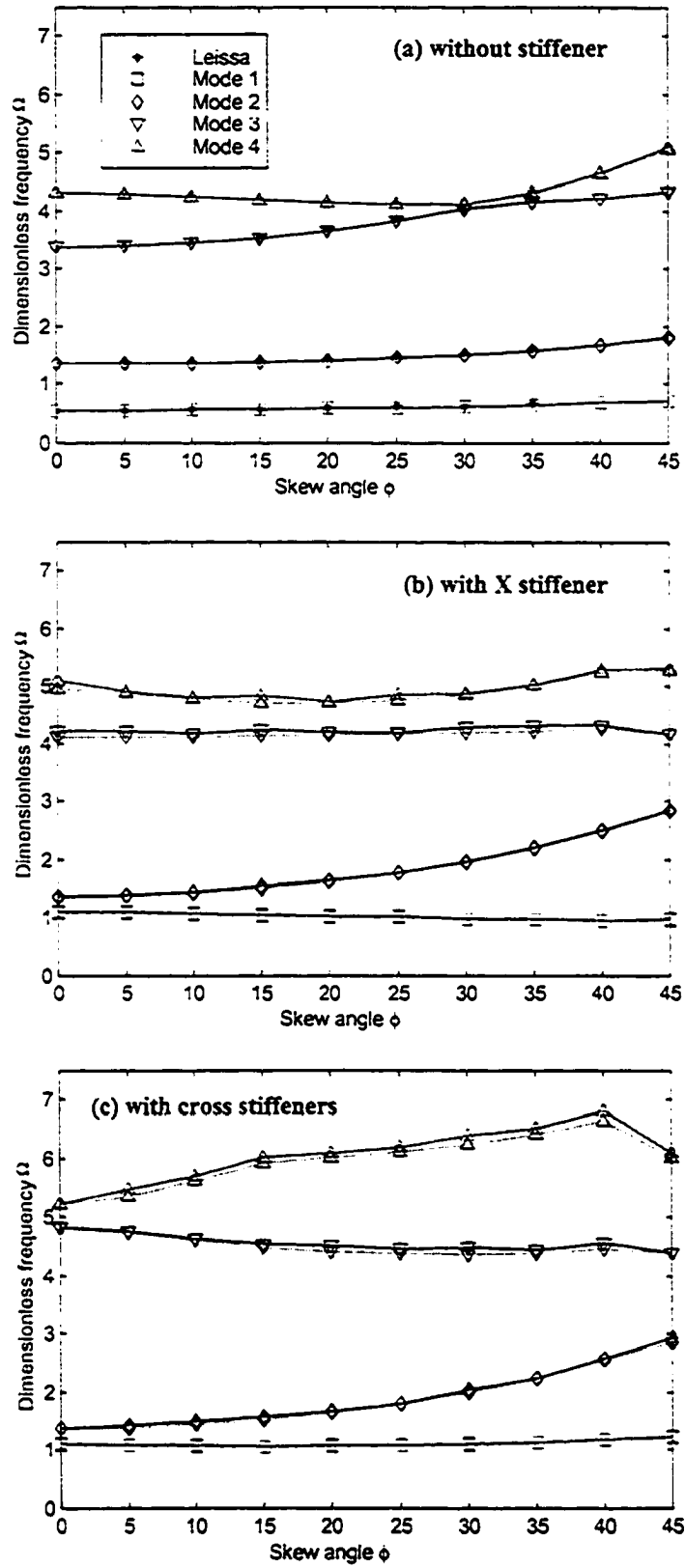
Figure 2.3: Variation of frequency Ω vs. skew angle ϕ for CFFF plates
(— pb-2 Rayleigh-Ritz; — FEM)
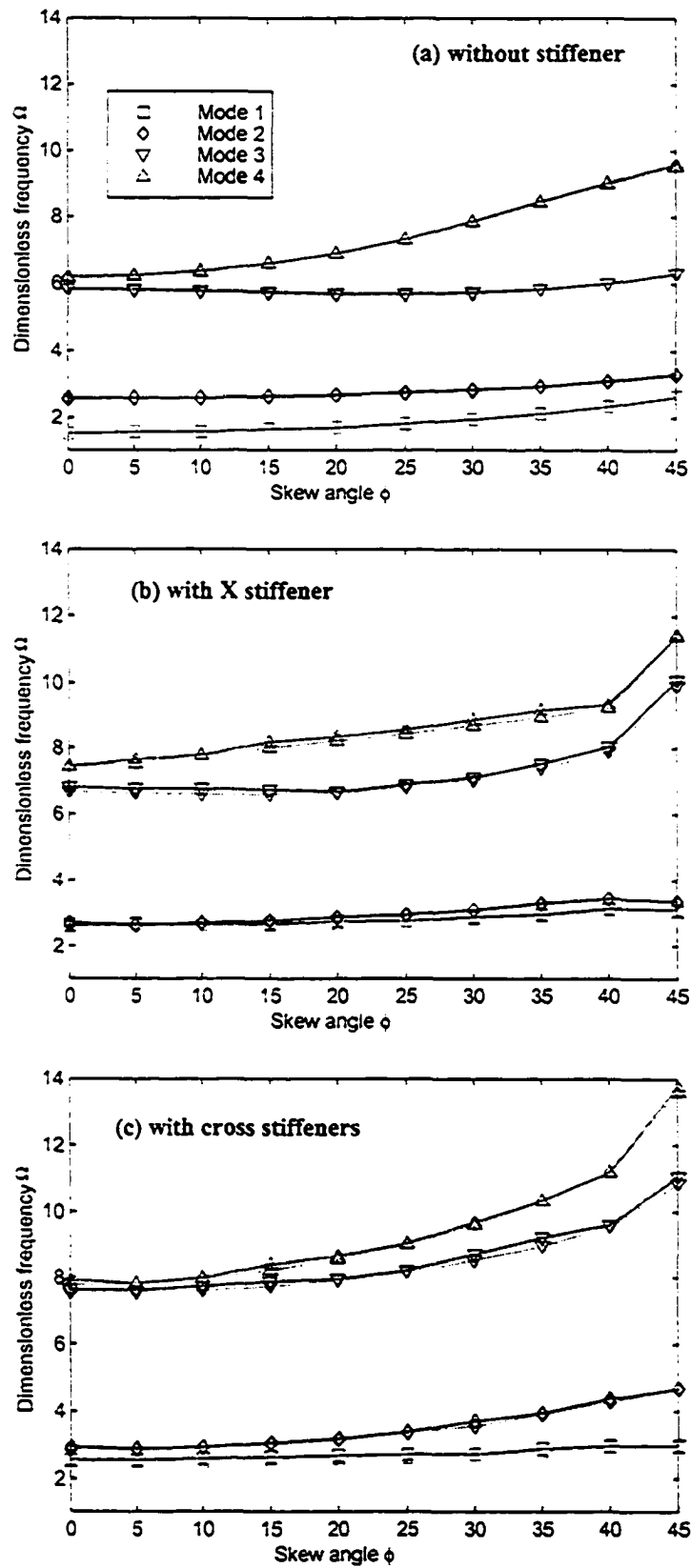
Figure 2.4: Variation of frequency Ω vs. skew angle ϕ for FSFS plates (— pb-2 Rayleigh-Ritz; --- FEM)

41
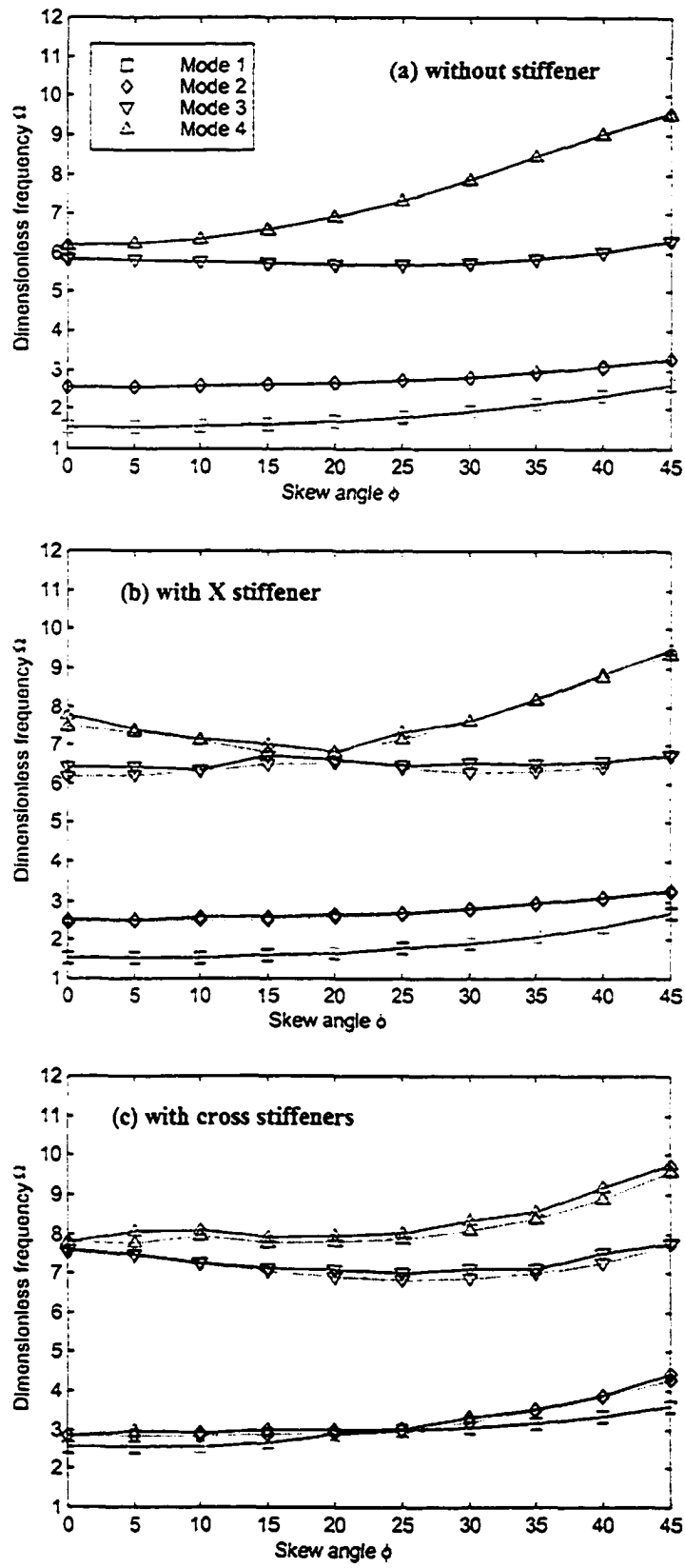
Figure 2.5: Variation of frequency Ω vs. skew angle ϕ for SFSF plates
(— pb-2 Rayleigh-Ritz; — FEM)

42
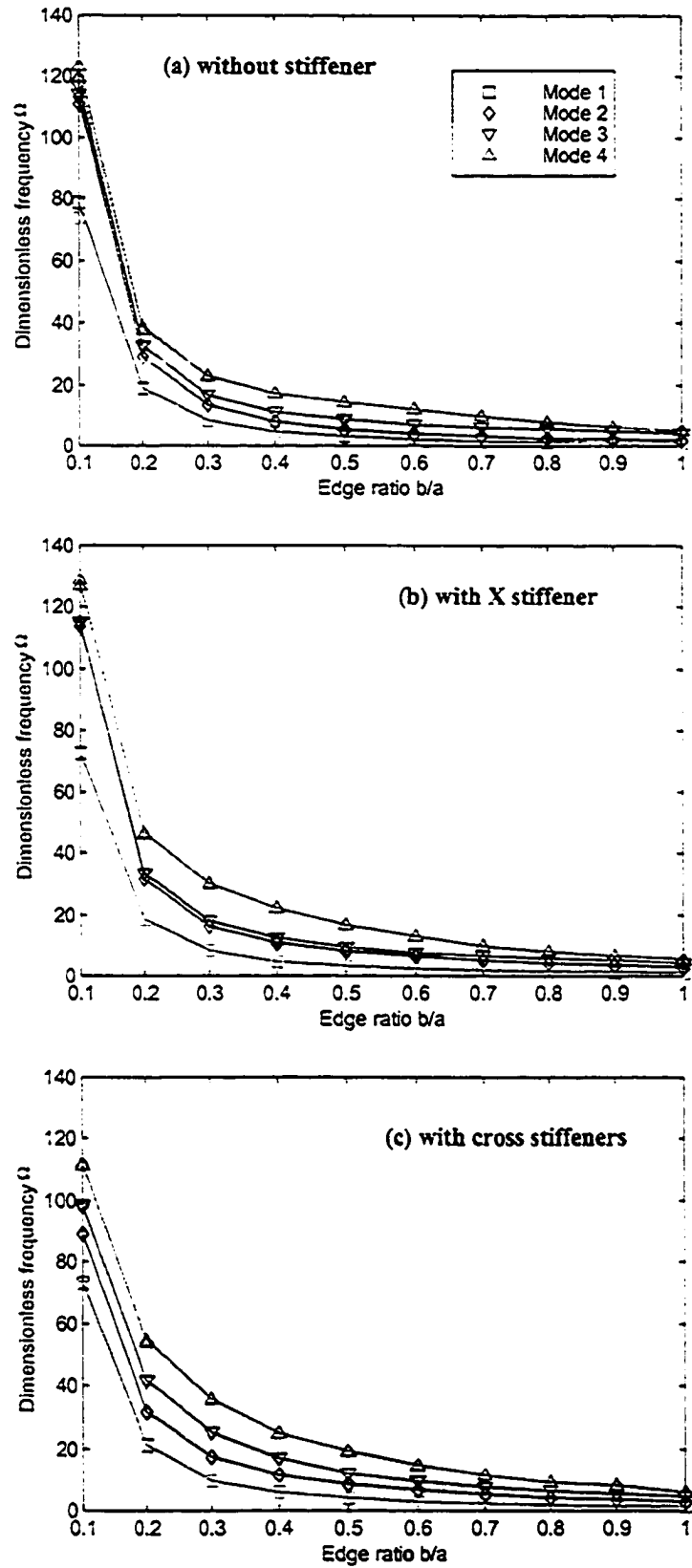
Figure 2.6: Variation of frequency Ω vs. edge ratio b/a for CFFF plates
(— pb-2 Rayleigh-Ritz; ⎯ FEM)
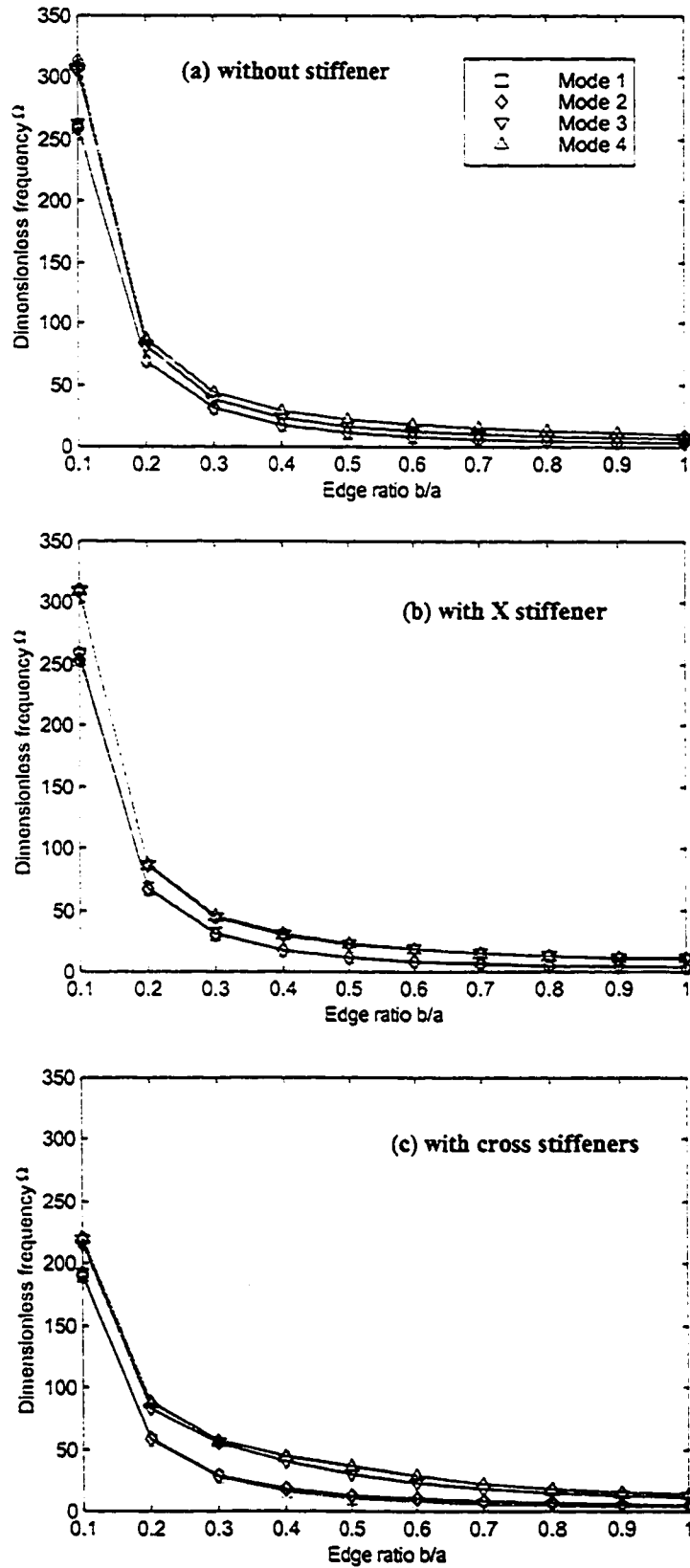
Figure 2.7: Variation of frequency Ω vs. edge ratio b/a for FSFS plates
(— pb-2 Rayleigh-Ritz; ‾‾ FEM)
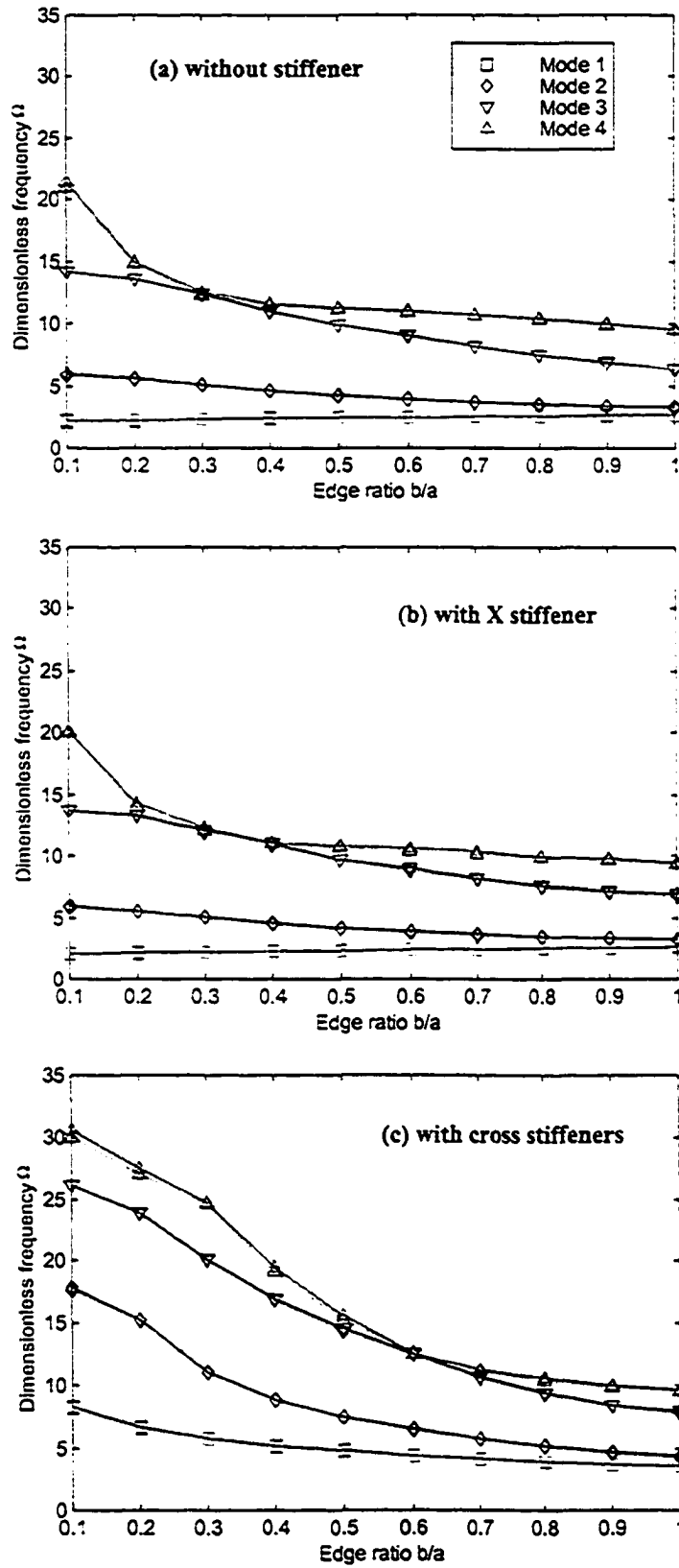
Figure 2.8: Variation of frequency Ω vs. edge ratio b/a for SFSF plates
(— pb-2 Rayleigh-Ritz; ⎯ FEM)
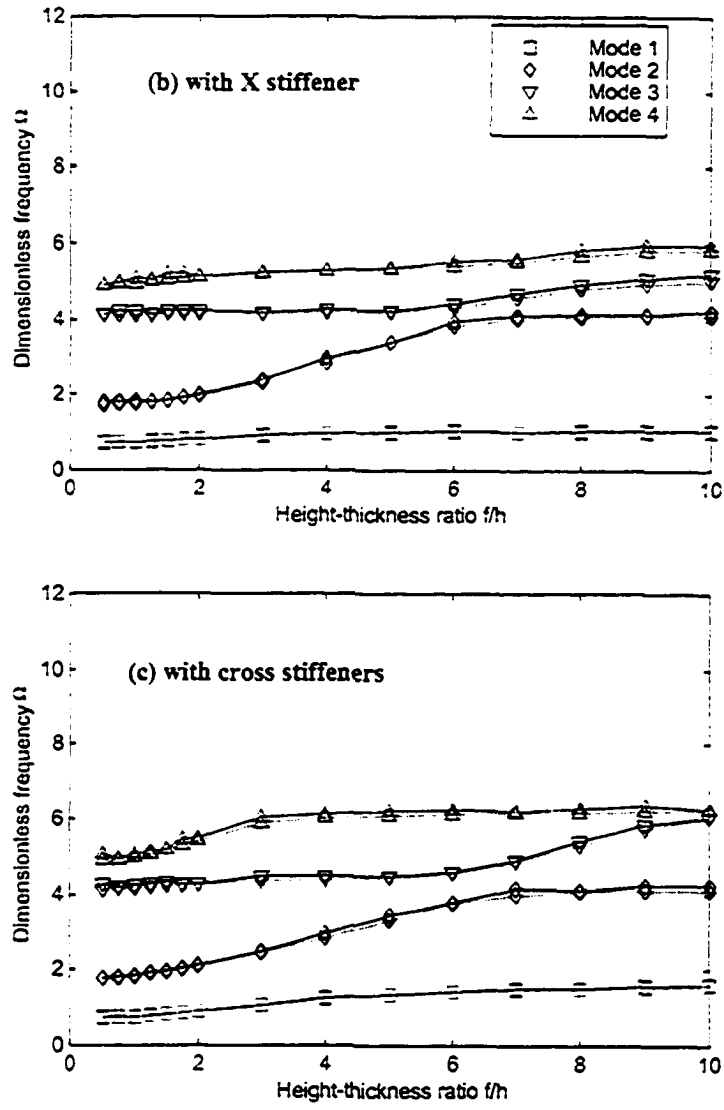
Figure 2.9: Variation of frequency Ω vs. height-thickness ratio f/h for CFFF plates (— pb-2 Rayleigh-Ritz; ⎯ FEM)
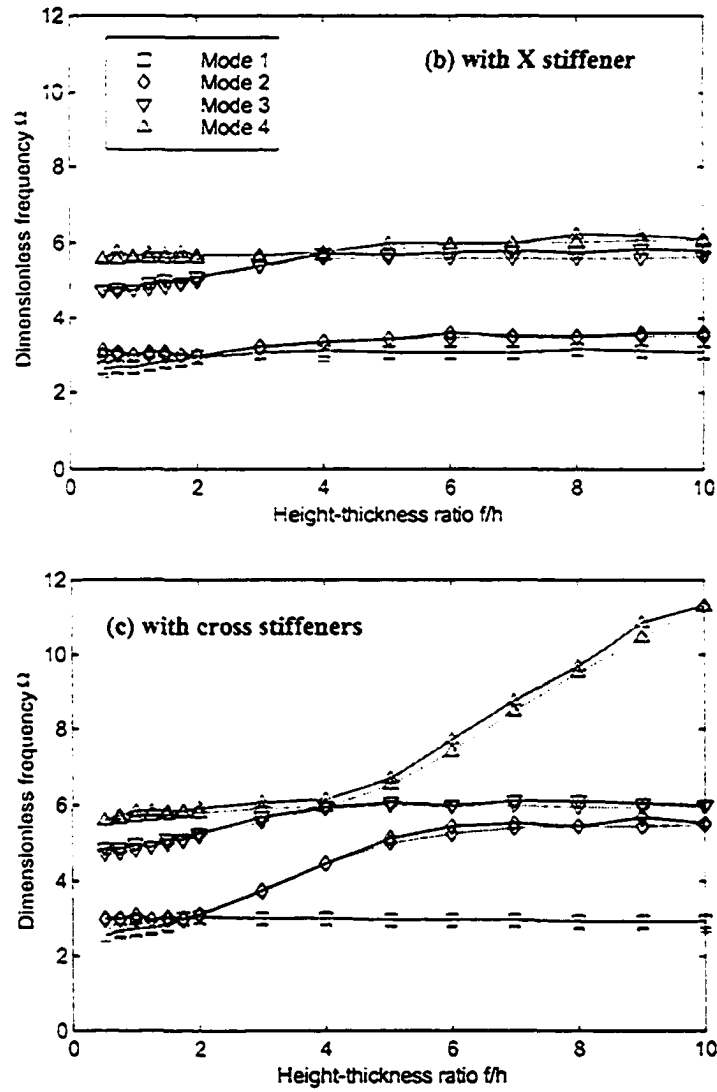
Figure 2.10: Variation of frequency Ω vs. height-thickness ratio f/h for
FSFS plates (— pb-2 Rayleigh-Ritz; — FEM)
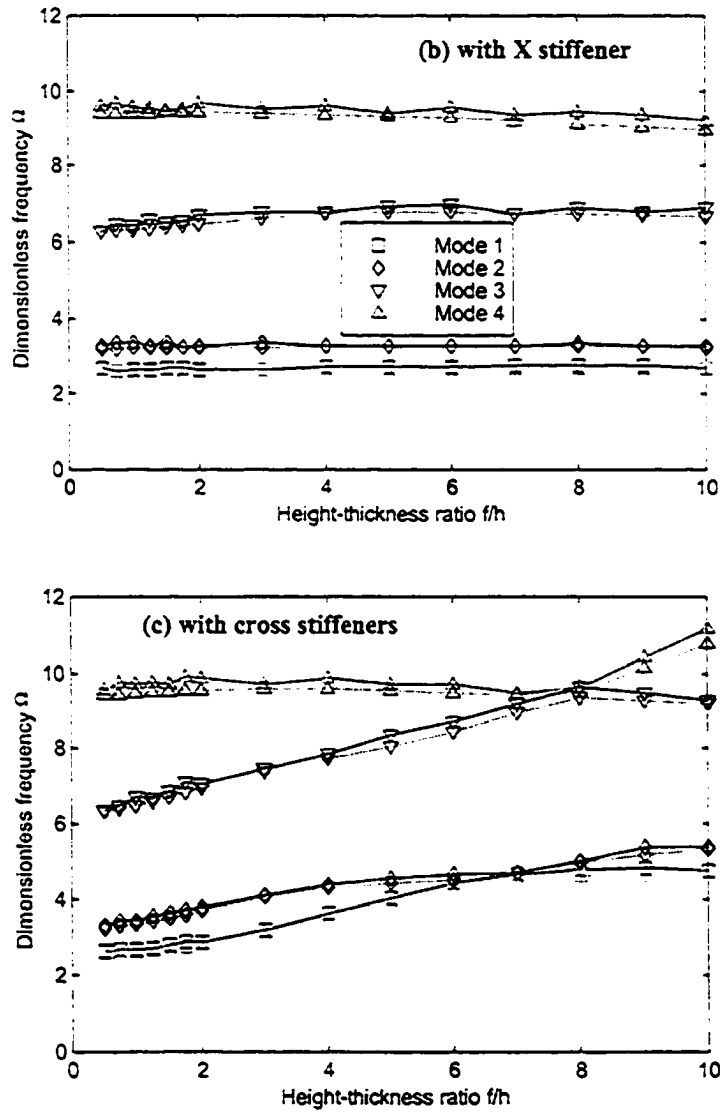
Figure 2.11: Variation of frequency Ω vs. height-thickness ratio f/h for SFSF plates (— pb-2 Rayleigh-Ritz; — FEM)

TABLE 2.1:   Convergence of dimensionless frequency Ω for CFFF skew

plates with cross stiffeners

p	Mode					
	1	2	3	4	5	6
2	1.4153	2.6118	7.1550	11.5535	14.5985	69.3942
3	1.3722	2.5693	6.0096	9.4408	11.0088	18.7626
4	1.3549	2.5434	5.2211	8.5829	10.4502	15.7487
5	1.3401	2.5239	4.8302	8.2372	9.0687	14.5700
6	1.3236	2.5133	4.7020	7.9459	8.8752	12.6259
7	1.3151	2.4947	4.6012	7.7127	8.8038	12.3436
8	1.3072	2.4738	4.5861	7.6281	8.7794	11.8152
9	1.3055	2.4665	4.5732	7.5240	8.7633	11.7673
10	1.3012	2.4556	4.5613	7.4867	8.7245	11.6821
FEM[*]	1.1756	2.5700	4.4540	6.6434	8.8848	11.8217

* 144 elements

TABLE 2.2:   Convergence of dimensionless frequency Ω for FSFS skew

plates with cross stiffeners

p	Mode					
	1	2	3	4	5	6
2	3.6996	4.8545	11.6824	20.1060	29.5365	76.2183
3	3.1878	4.8414	11.5781	14.5592	20.0899	28.0309
4	3.1865	4.6517	10.0598	14.3210	15.5468	24.6556
5	3.0533	4.6457	10.0547	12.3637	15.3689	22.9465
6	3.0478	4.5833	9.9176	12.3271	14.3879	19.0273
7	2.9792	4.5786	9.8965	12.0272	14.3549	18.2036
8	2.9775	4.5466	9.8440	11.9685	14.0032	17.9742
9	2.9548	4.5435	9.8238	11.7575	13.9768	17.1225
10	2.9545	4.5328	9.7649	11.7258	13.8278	17.0623
FEM[*]	2.9424	4.3001	9.5528	11.1750	13.4463	19.0114

* 144 elements

TABLE 2.3: Convergence of dimensionless frequency Ω for SFSF skew

plates with cross stiffeners

p	Mode					
	1	2	3	4	5	6
2	3.7337	6.3725	9.2113	20.6470	23.6733	57.3194
3	3.7233	5.3915	9.1260	12.0063	21.2051	23.3553
4	3.4608	5.3192	8.5857	11.9450	19.1594	21.2865
5	3.4512	4.1983	8.5319	9.6277	19.0060	19.9421
6	3.4032	4.1594	7.8617	9.5745	15.9686	19.7275
7	3.3949	3.9975	7.8401	9.2607	15.9177	17.7181
8	3.3811	3.9899	7.6273	9.2485	15.4685	17.7036
9	3.3768	3.9330	7.5712	9.0959	15.4170	16.8274
10	3.3758	3.9302	7.5712	9.0931	15.3651	16.6208
FEM[*]	3.2994	3.8556	7.2715	8.8807	14.4896	15.9862

* 144 elements

CHAPTER THREE

TRANSIENT VIBRATION ANALYSIS

Both analytical and numerical methods can be used to find the transient response of a system to an arbitrary excitation. Some of these methods are convolution integral, Laplace transformation, and numerical integration of the equations of motion. In a discrete system with finite number of DOFs, numerical integration is extensively used. When the bridge is modeled as a continuous system with infinite number of DOFs, the convolution integral is widely used. Green (1990) proposed an analytical technique to solve for the transient response of a continuous bridge subjected to moving vehicle excitation. The equations of motion of the bridge were written in a certain form. The present study proposes a semi-analytical method with mode superposition to find the transient response. In the proposed method, a few uncoupled equations need to be solved. The need for the convolution integral, which requires large computer storage space and computation time, is eliminated.

In a discrete system, the equations of motion are decoupled by the modal matrix to obtain the solution of forced vibration in terms of the normal coordinates of the system. In this section, the mode superposition technique is applied to continuous systems by expanding the deflection in terms of the normal modes of the system. Under certain initial conditions, only one mode is excited

$$w(x,y,t) = W_j(x,y)e^{i\omega_j t} \tag{3.1}$$

where $W_j(x,y)$ is the undamped mode shape for the jth mode, normalized with respect to the mass matrix. By representing the solution to the general problem in terms of $W_j(x,y)$

$$w(x,y,t) = \sum_{j=1}^{N_m} W_j(x,y)q_j(t) \tag{3.2}$$

where $q_j(t)$ is the response of the jth normal coordinate and N_m is the number of modes employed in the approximation.

The generalized coordinate $q_j(t)$ can be determined from Lagrange's equation by first establishing the potential and kinetic energy in terms of the generalized coordinate $q_j(t)$.

With Equation (3.2), Equations (2.15) and (2.16) can be rewritten as

$$T = \frac{1}{2}\sum_{i=1}^{N_m}\sum_{j=1}^{N_m}\dot{q}_i\dot{q}_j\left[V^T M V\right]_{ij} = \frac{1}{2}\sum_{i=1}^{N_m}\sum_{j=1}^{N_m}\dot{q}_i\dot{q}_j\delta_{ij} \tag{3.3}$$

$$U = \frac{1}{2}\sum_{i=1}^{N_m}\sum_{j=1}^{N_m}q_i q_j\left[V^T K V\right]_{ij} = \frac{1}{2}\sum_{i=1}^{N_m}\sum_{j=1}^{N_m}q_i q_j\omega_i\omega_j\delta_{ij} \tag{3.4}$$

To consider the damping of the system, the damping matrix is expressed as a linear combination of the mass and stiffness matrices:

$$C = \tilde{\alpha}M + \tilde{\beta}K \tag{3.5}$$

where $\tilde{\alpha}$ and $\tilde{\beta}$ are constants which are identified from modal tests. This type of damping is known as proportional damping or Rayleigh damping. Then Rayleigh's dissipation function R can be defined as (Rao, 1995)

$$R = \frac{1}{2}\sum_{i=1}^{N_m}\sum_{j=1}^{N_m}\dot{q}_i\dot{q}_j\left[\bar{V}^T C\bar{V}\right]_{ij} = \frac{1}{2}\sum_{i=1}^{N_m}\sum_{j=1}^{N_m}\dot{q}_i\dot{q}_j\left(\tilde{\alpha}+\omega_i\omega_j\tilde{\beta}\right)\delta_{ij} \qquad (3.6)$$

The virtual work due non-conservative force, namely, the tire forces $P(x,y,t)$ is

$$\delta W = \iint_{\Omega_A} P(x,y,t)\delta w\,dxdy = \iint_{\Omega_A} P(x,y,t)\sum_{j=1}^{N_m} W_j(x,y)\delta q_j\,dxdy$$

$$= \sum_{j=1}^{N_m}\delta q_j\iint_{\Omega_A} P(x,y,t)W_j(x,y)dxdy = \sum_{j=1}^{N_m}\delta q_j Q_j(t) \qquad (3.7)$$

thus the generalized force is

$$Q_j(t) = \iint_{\Omega_A} P(x,y,t)W_j(x,y)dxdy, \quad i = 1,2,...,N_m \qquad (3.8)$$

When the excitation is the tire force applied at point (x_f,y_f),

$$P(x,y,t) = \delta(x-x_f)\delta(y-y_f)P(x_f,y_f,t), \qquad (3.9)$$

one has

$$Q_j(t) = P_f(x_f,y_f,t)W_j(x_f,y_f), \quad j = 1,2,...,N_m \qquad (3.10)$$

Lagrange's equation, in this case (Rao, 1995), can be written as

$$\frac{d}{dt}\left(\frac{\partial T}{\partial \dot{q}_j}\right) - \frac{\partial T}{\partial q_j} + \frac{\partial R}{\partial \dot{q}_j} + \frac{\partial U}{\partial q_j} = Q_j, \quad j = 1,2,...,N_m \qquad (3.11)$$

which gives

$$\ddot{q}_j(t) + \left(\tilde{\alpha} + \omega_j^2\tilde{\beta}\right)\dot{q}_j(t) + \omega_j^2 q_j(t) = Q_j(t), \quad j = 1,2,\ldots,N_m \tag{3.12}$$

By writing

$$\tilde{\alpha} + \omega_j^2\tilde{\beta} = 2\xi_j\omega_j \tag{3.13}$$

where ξ_j is the modal damping ratio for the jth normal mode, Equation (3.12) can be rewritten as

$$\ddot{q}_j(t) + 2\xi_j\omega_j\dot{q}_j(t) + \omega_j^2 q_j(t) = Q_j(t) \tag{3.14}$$

It can be seen that each of the N_m equations represented by this expression is uncoupled from all of the others. If the damping matrix is not proportional, the equations of motion would be coupled by the damping matrix, and the equations must be solved simultaneously. The solution of Equations (3.14), when $\xi_j < 1$, can be expressed as

$$q_j(t) = e^{-\xi_j\omega_j t}\left[\cos(\omega_{d,j}t) + \frac{\xi_j}{\sqrt{1-\xi_j^2}}\sin(\omega_{d,j}t)\right]q_j(0)$$
$$+ \frac{1}{\omega_{d,j}}e^{-\xi_j\omega_j t}\sin(\omega_{d,j}t)\dot{q}_j(0) + \frac{1}{\omega_{d,j}}\int_0^t Q_j(\tau)e^{-\xi_j\omega_j(t-\tau)}\sin[\omega_{d,j}(t-\tau)]d\tau \tag{3.15}$$

where

$$\omega_{d,j} = \omega_j\sqrt{1-\xi_j^2}$$

For constant Q_j, the integral in Equation (3.15) can be carried out explicitly as

$$\int_0^t e^{-\xi_j \omega_j (t-\tau)} \sin[\omega_{d,j}(t-\tau)]d\tau$$

$$= \frac{1}{\xi_j^2 \omega_j^2 + \omega_{d,j}^2} \left\{ \omega_{d,j} - e^{-\xi_j \omega_j t} \left[\xi_j \omega_j \sin(\omega_{d,j} t) + \omega_{d,j} \cos(\omega_{d,j} t) \right] \right\} \qquad (3.16)$$

In the case in which the generalized forces are not known a priori, an iterative procedure is necessary. Provided the normal coordinates and their associated velocities in an earlier time step, with the generalized forces predicted, the normal coordinates and the corresponding velocities can be obtained by Equation (3.15). The solved normal coordinates and velocities are initial conditions for the next time step. The generalized forces for the next time step will be predicted by exciting the vehicle with the updated deflection and velocity of the bridge. This procedure is referred to as an *explicit technique* here.

Green (1990) proposed an alternative way to analyze the forced vibration, by using a convolution integral. The dynamic behavior of multi-span continuous bridges is governed by (Newland, 1989),

$$\bar{m}(x,y)\ddot{w}(x,y,t) + \bar{C}\{\dot{w}(x,y,t)\} + L\{w(x,y,t)\} = f(x,y,t) \qquad (3.17)$$

where $\bar{m}(x,y)$ is the distributed mass per unit area, L is a differential stiffness operator with respect to the spatial variables, $\bar{C}$ is a viscous damping operator with respect to the spatial variables, and $f(x,y,t)$ is the force transmitted by the vehicle onto the bridge.

It can be shown (Newland, 1989) that the response of a system governed by

Equation (3.17) to an input $f(x_f, y_f, t)$, applied at a specified position on the

bridge, (x_f, y_f), is given by the convolution integral:

$$w(x, y, t) = \int_{-\infty}^{\infty} h(x, y, x_f, y_f, t - \tau) f(x, y, \tau) d\tau \qquad (3.18)$$

where $h(x, y, x_f, y_f, t)$ is the *impulse response function* at position (x, y) for an

impulse applied at position (x_f, y_f). Therefore, to solve Equation (3.17), the

appropriate impulse response functions need to be determined.

Equation (3.14) described the response of the system in mode j. For each

mode, the *modal impulse response function*, $h_j(t)$, can be determined by setting

$Q_j(t) = \delta(t)$, where $\delta(t)$ is the Dirac delta function. By doing so, one obtains:

$$\ddot{q}_j(t) + 2\xi_j \omega_j \dot{q}_j(t) + \omega_j^2 q_j(t) = \delta(t) \qquad (3.19)$$

Solving Equation (3.19) results in a special case of $q_j(t)$, namely $h_j(t)$,

which could be expressed by:

$$h_j(t) = \frac{1}{\omega_{d,j}^2} e^{-\xi_j \omega_j t} \sin(\omega_{d,j} t) \qquad (3.20)$$

when $\xi_j < 1$.

The impulse response function for the bridge can be expressed in terms of

mode shapes and modal impulse response functions $h_j(t)$ as (Green, 1990):

57

$$h(x,y,x_f,y_f,t) = \sum_{j=1}^{\infty} \phi_j(x,y)\phi_j(x_f,y_f)h_j(t) \tag{3.21}$$

The forcing function for a vehicle with N_f tires can be described in terms of the dynamic tire loads

$$f(x_f,y_f,t) = \sum_{k=1}^{N_f} \delta(x_f - x_k)\delta(y_f - y_k)F_k(t) \tag{3.22}$$

where (x_k, y_k) is the position of the kth tire force. The forcing function is zero except at the position of contact points, where it is equal to the instantaneous tire force $F_k(t)$.

Substituting Equations (3.19) to (3.22) into the convolution integral, Equation (3.18), yields:

$$w(x,y,t) = \sum_{k=1}^{N_f} \sum_{n=1}^{\infty} \phi_n(x,y) \int_0^t h_n(t-\tau)\phi_n(x_k(\tau),y_k(\tau))F_k(t)d\tau \tag{3.23}$$

Compare these two techniques, the advantages of the explicit one are apparent. To use the convolution integral in the BVI problem, the coupled forces and the mode shapes at all contact points need to be stored. Assuming the time period is divided into N time intervals, there will be $\dfrac{N(N+1)}{2}$ integrals to obtain the time history of a single point of the bridge. Meanwhile, the calculation of the displacements of the contact points adds extra computational efforts. An additional contact point requires another $\dfrac{N(N+1)}{2}$ integrals. When there are

more than one vehicles traveling on the bridge, the required computational time and computer storage space are substantially increased. The author tried to use the convolution integral to predict the dynamic response of the bridge. The integral was carried out in the time domain. Unfortunately, the long computational time and high requirement of the computer memory allocation and storage space prevented the author from obtaining satisfactory results. Eventually, a frequency domain method was proposed by (Green and Cebon 1994) to reduce the computational time and decrease the necessary computer storage.

By using the explicit prediction, there are only N computations to predict the normal coordinates. The normal coordinates need to be stored. However, usually only a few modes (five modes in the present study) are necessary to accurately describe the dynamic response, so the storage requirement is low. The displacement of a point is obtained by summing the mode shape values at this point, weighted by the normal coordinates. Additionally, the displacements at an earlier time step act as the initial conditions for the next time step; in this case, the problem is easier to be complimented with computer programming and saves a lot of computer temporary storage space. Therefore, the explicit method is used in the present study.

CHAPTER FOUR

VEHICLE MODELING AND DYNAMICS

4.1 Vehicle models

There is a wide variety of configurations of vehicles, including the tractor with or without trailers and with different axle spacings and weights. The standard vehicles used by the American Association of State Highway and Transportation Officials (AASHTO) for highway bridge design are H trucks and HS trucks. They are designated H or HS followed by a number indicating the gross weight in tons of the standard truck. The H loadings consist of a two-axle truck as illustrated in Figure 4.1 for truck H 20-44 and for truck H 15-44. For readers' interest, "44" denotes the same designation as in the 1944 Edition of the design code. H trucks have a fixed spacing. The HS loadings consist of a tractor truck with semi-trailer as illustrated in Figure 4.2. The axle spacing is variable, from 14 ft to 30 ft.

Without loss of generality, a tractor with a semi-trailer is modeled. For a tractor with a trailer, where there are more than three axles, or a H truck where there are two axles, a similar method can be used to obtain the equations of motion without difficulty.

The body of a tractor with a semi-trailer is treated as two rigid masses, which represent the tractor (M_1) and the semi-trailer (M_2). Each of them was assigned degrees of freedom (DOF) of vertical displacement (Z_1', Z_2'), pitching rotation about the transverse axis (θ_1, θ_2), and rolling rotation about the longitudinal axis (α_1, α_2); see Figure 4.3. The supporting tire-suspension system for each axle is modeled as spring-dashpot system and six lump masses, each of which was assigned one DOF of vertical displacement (z_i, $i = 1...6$). The points supporting the vehicle body are numbered as z_i', $i = 1...6$, as shown in Figure 4.3, as well as the vehicle geometry.

The principle of virtual work is applied to derive the equations of motion. The forces include gravitational forces ($M_1 g$, $M_2 g$, $m_i g$, $i = 1...6$), inertia forces and moments ($M_j \ddot{Z}_j$, $I_{\theta j} \ddot{\theta}_j$, $I_{\alpha j} \ddot{\alpha}_j$, $j = 1,2$; $m_i \ddot{z}_i$, $i = 1...6$), suspension forces (F_i', $i = 1..6$), and tire forces (F_i, $i = 1..6$) as

$$F_i' = k_i'(z_i' - z_i) + c_i'(\dot{z}_i' - \dot{z}_i), \quad i = 1...6 \qquad (4.1\text{-}4.6)$$

$$F_i = k_i(z_i - w_i(x_i, y_i, t)) + c_i(\dot{z}_i - \dot{w}_i(x_i, y_i, t)), \quad i = 1...6 \qquad (4.7\text{-}4.12)$$

The virtual work done can be obtained by

$$\delta W_v = \sum_{i=1}^{6} m_i g \delta z_i + \sum_{j=1}^{2} M_j g \delta Z_j + \sum_{i=1}^{6} m_i \ddot{z}_i \delta z_i + \sum_{j=1}^{2} M_j \ddot{Z}_j \delta Z_j +$$

$$\sum_{j=1}^{2} I_{\alpha j} \ddot{\alpha}_j \delta \alpha_j + \sum_{j=1}^{2} I_{\theta j} \ddot{\theta}_j \delta \theta_j + \sum_{i=1}^{6} F_i' \delta(z_i' - z_i) + \sum_{i=1}^{6} F_i \delta(z_i - w_i) = 0 \qquad (4.13)$$

The displacement vector is defined in terms of basic coordinates by

$$Z_v = \{z_1, z_2, z_3, z_4, z_5, z_6, z_1', z_2', z_3', z_4', z_5'\}^T \tag{4.14}$$

With the constraint that three points determine a plane, the other displacements and rotations are related to basic coordinates as below:

$$z_6' = z_1' - z_2' + z_5' \tag{4.15}$$

$$Z_4' = (b_1 - a_2)z_2' + b_2 z_1' + a_2 z_5' \tag{4.16}$$

$$Z_3' = d_2 c_1 z_3' + a_1 c_2 z_1' + a_2 c_2 z_5' + d_1 c_1 z_4' + H_0 \tag{4.17}$$

$$\theta_1 = \frac{z_2' - z_1'}{l_b} \tag{4.18}$$

$$\alpha_1 = \frac{z_2' - z_5'}{l_a} \tag{4.19}$$

$$\theta_2 = \frac{a_1(z_3' - z_2') + a_2(z_4' - z_5') - H_0}{l_c} \tag{4.20}$$

$$\alpha_2 = \frac{z_3' - z_4'}{l_d} \tag{4.21}$$

where the dimensions a_i, b_i, c_i and d_i (i=1,2), l_a, l_b, l_c, and l_d are shown in Figure 4.3. Then eleven equations of motion can be derived from Equation (4.13) as:

$$m_j \ddot{z}_j + (k_{tj} + k_{sj})z_j + (c_{tj} + c_{sj})\dot{z}_j - k_{sj}z_j' - c_{sj}\dot{z}_j' - k_{tj}w_j - c_{tj}\dot{w}_j + m_j g = 0$$

$$j = 1,\ldots,6 \qquad (4.22\text{-}4.27)$$

$$b_2 M_1 \left[(b_1 - a_2) \ddot{z}'_2 + b_2 \ddot{z}'_1 + a_2 \ddot{z}'_5 \right] - \frac{I_{\theta 1}}{l_s^2} (\ddot{z}'_2 - \ddot{z}'_1) - k_{s1} z_1 - c_{s1} \dot{z}_1 + (k_{s6} + k_{s1}) z'_1 +$$

$$(c_{s6} + c_{s1}) \dot{z}'_1 + c_{s6} (-\dot{z}'_2 + \dot{z}'_5 - \dot{z}_6) + k_{s6} (-z'_2 + z'_5 - z_6) + b_2 M_1 g = 0$$

$$\tag{4.28}$$

$$a_1 c_2 M_2 \left[d_2 c_1 \ddot{z}'_3 + a_1 c_2 \ddot{z}'_2 + a_2 c_2 \ddot{z}'_5 + d_1 c_1 \ddot{z}'_4 + g \right]$$

$$+ (b_1 - a_2) M_1 \left[(b_1 - a_2) \ddot{z}'_2 + b_2 \ddot{z}'_1 + a_2 \ddot{z}'_5 + g \right] - k_{s2} z_2 - c_{s2} \dot{z}_2$$

$$+ \frac{I_{\alpha 1}}{q_0^2} (\ddot{z}'_2 - \ddot{z}'_5) + \frac{I_{\theta 1}}{l_s^2} (\ddot{z}'_2 - \ddot{z}'_1) - \frac{a_1 I_{\theta 2}}{l_c^2} (a_1 \ddot{z}'_3 - a_1 \ddot{z}'_2 + a_2 \ddot{z}'_4 - a_2 \ddot{z}'_5)$$

$$+ (k_{s6} + k_{s2}) z'_2 + (c_{s6} + c_{s2}) \dot{z}'_2 - c_{s6} (\dot{z}'_1 + \dot{z}'_5 - \dot{z}_6) - k_{s6} (z'_1 + z'_5 - z_6) = 0$$

$$\tag{4.29}$$

$$d_2 c_1 M_2 \left[d_2 c_1 \ddot{z}'_3 - a_1 c_2 \ddot{z}'_2 - a_2 c_2 \ddot{z}'_5 + d_1 c_1 \ddot{z}'_4 + g \right] + \frac{I_{\theta 2}}{l_d^2} (\ddot{z}'_3 - \ddot{z}'_4)$$

$$+ \frac{a_1 I_{\theta 2}}{l_c^2} (a_1 \ddot{z}'_3 - a_1 \ddot{z}'_2 - a_2 \ddot{z}'_4 - a_2 \ddot{z}'_5) - k_{s3} z_3 - c_{s3} \dot{z}_3 + k_{s3} z'_3 + c_{s3} \dot{z}'_3 = 0$$

$$\tag{4.30}$$

$$d_1 c_1 M_2 \left[d_2 c_1 \ddot{z}'_3 + a_1 c_2 \ddot{z}'_2 + a_2 c_2 \ddot{z}'_5 + d_1 c_1 \ddot{z}'_4 + g \right] - \frac{I_{\theta 2}}{l_d^2} (\ddot{z}'_3 - \ddot{z}'_4)$$

$$+ \frac{a_2 I_{\theta 2}}{l_c^2} (a_1 \ddot{z}'_3 - a_1 \ddot{z}'_2 + a_2 \ddot{z}'_4 - a_2 \ddot{z}'_5) - k_{s4} z_4 - c_{s4} \dot{z}_4 + k_{s4} z'_4 + c_{s4} \dot{z}'_4 = 0$$

$$\tag{4.31}$$

$$a_2 c_2 M_2 \left[d_2 c_1 \ddot{z}'_3 + a_1 c_2 \ddot{z}'_2 + a_2 c_2 \ddot{z}'_5 + d_1 c_1 \ddot{z}'_4 + g \right] - \frac{I_{\alpha 1}}{q_0^2} (\ddot{z}'_2 - \ddot{z}'_5)$$

$$a_2 M_1 \left[(b_1 - a_2) \ddot{z}'_2 + b_2 \ddot{z}'_1 + a_2 \ddot{z}'_5 + g \right] - \frac{a_1 I_{\theta 2}}{l_c^2} (a_1 \ddot{z}'_3 - a_1 \ddot{z}'_2 + a_2 \ddot{z}'_4 - a_2 \ddot{z}'_5)$$

$$- k_{s5} z_5 - c_{s5} \dot{z}_5 + (k_{s6} + k_{s5}) z'_5 + (c_{s6} + c_{s5}) \dot{z}'_5 + c_{s6} (\dot{z}'_1 - \dot{z}'_2 - \dot{z}_6) + k_{s6} (z'_1 - z'_2 - z_6) = 0$$

$$\tag{4.32}$$

Equations (4.22) to (4.32) can be rewritten in matrix form as:

$$M_v \ddot{Z}_v + C_v \dot{Z}_v + K_v Z_v = F_{bv} + G_v \qquad (4.33)$$

where M_v, C_v, and K_v are the vehicle mass, stiffness, and damping matrices, respectively, F_{bv} is the instantaneous coupled force vector at the points where the tires contact the bridge, and G_v is the gravity force vector. The explicit expressions for them are listed in Appendix I.

The parameters of the standard H and HS trucks are summarized in Tables 4.1 through 4.4.

A vehicle involved in the Walnut Creek Bridge test is Rock Truck, which was so called in that what it carries is rock. There is a quarry located south of the test site; it provides much of the gravel needed in the Oklahoma City area. The freight loading is considered to evenly fill the trailer to 3/4 the trailer height, which weighs approximately 20,000 kg. The total static weight of the test truck is 36,320 kg. The rolling inertia of the trailer is approximately 9,000 kg·m^2 and 1,500 kg·m^2 for the tractor. The Rock Truck is close to an HS 20-44 truck. The physical parameters for the vehicle are listed in Table 4.5.

4.2 Effect of rolling inertia on frequencies

The vehicle frequencies can be obtained by solving Equation (4.33) for eigensolutions. The natural frequencies are compared with the test results in Table 4.6. It is interesting to note that: 1) the introduction of rolling DOF doesn't affect the lowest pitch and heave frequencies, i.e. rolling is uncoupled from pitch and heave in low modes; 2) with relatively small rolling inertia, the rolling mode is a higher frequency one than a pitch or heave mode, which might not be so essential as the lower modes. However, when the rolling inertia is getting larger, the rolling frequency can be as low as second lowest, in other words, it is getting more critical in vehicle dynamics; 3) The rolling inertia introduced by the tractor $I_{\alpha 1}$ is not so essential as the trailer inertia $I_{\alpha 2}$. It is apparent $I_{\alpha 2}$ is much larger than $I_{\alpha 1}$ since the trailer is loaded with freight. Table 4.6 shows that the rolling frequency of the tractor usually is higher than that of the pitch/heave modes. However, the rolling frequency of the trailer could easily fall into the pitch/heave frequency range. Due to the lack of measurement of the rolling inertia, an example is taken here to show its magnitude. The vehicle QS-660, which is the standard vehicle for evaluation and design of bridges in the Canadian province of Quebec (Massicotte and Picard, 1990), has a semi-tractor with weight of 40,775 kg, with tractor weighing 9,060 kg and trailer weighing 28,994 kg (Fafard et al., 1998). The rolling inertias for the tractor and the trailer are 3,020 kg·m^2 and 9,661 kg·m^2, respectively. The rolling rotation DOF can not be ignored since its frequency falls into the range of the bridge frequencies, usually in the range of 2~5 Hz.

4.3 Solving the equations of motion numerically

In the bridge/vehicle coupling problem, the equations of motion for the bridge and vehicle must be solved simultaneously; thus, a direct integration method must be used to solve the equations of the vehicle. In the dissertation, the *Newmark* β-*method* (Newmark, 1959) with $\alpha = 1/6$ and $\beta = 1/2$ is used. In the Newmark β-method, the acceleration between two instants of time is assumed to vary linearly. It's noted that at time t_i, the displacement vector $Z_{v,j}$ is calculated first, followed by the acceleration vector $\ddot{Z}_{v,j}$, and finally the velocity vector $\dot{Z}_{v,j}$. The resulting expressions for the displacement, velocity, and acceleration vectors are written as (Rao, 1995):

$$Z_{v,i+1} = \left(\frac{1}{\alpha(\Delta t)^2} M_v + \frac{\beta}{\alpha \Delta t} C_v + K_v \right)^{-1} \times$$

$$\left(\begin{array}{l} M_v \left(\frac{1}{\alpha(\Delta t)^2} Z_{v,i} + \frac{1}{\alpha \Delta t} \dot{Z}_{v,i} + \left(\frac{1}{2\alpha} - 1 \right) \ddot{Z}_{v,i} \right) + \\ C_v \left(\frac{1}{\alpha \Delta t} Z_{v,i} + \left(\frac{\beta}{\alpha} - 1 \right) \dot{Z}_{v,i} \right) + \left(\frac{\beta}{\alpha} - 1 \right) \frac{\Delta t}{2} \ddot{Z}_{v,i} + F_{bv,i+1} \end{array} \right)$$

(4.34)

$$\dot{Z}_{v,i+1} = \dot{Z}_{v,i} + (1 - \beta) \ddot{Z}_{v,i} \Delta t + \beta \ddot{Z}_{v,i+1} \Delta t$$

(4.35)

$$\ddot{Z}_{v,i+1} = \frac{1}{\alpha(\Delta t)^2}(Z_{v,i-1} - Z_{v,i})Z_{v,i} - \frac{1}{\alpha\Delta t}\dot{Z}_{v,i} - \left(\frac{1}{2\alpha} - 1\right)\ddot{Z}_{v,i} \qquad (4.36)$$

An algorithm named VehiclePack (Appendix II) has been developed to predict the instantaneous response of the vehicle.
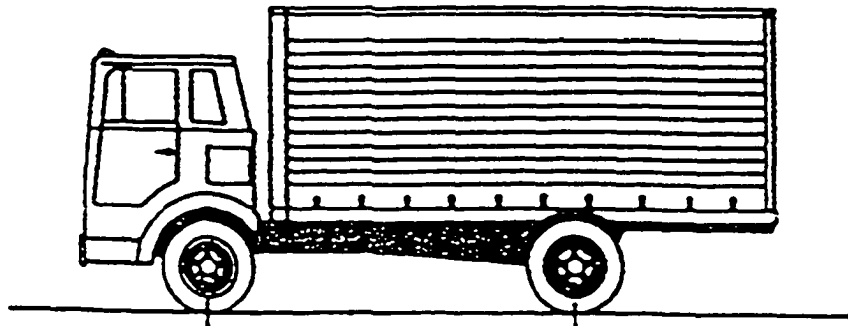
| H 20-44 | 8,000 LB | 32,000 LB |
| H 15-44 | 6,000 LB | 24,000 LB |

14'-0"

0.2W

W = TOTAL WEIGHT OF
TRUCK AND LOAD

0.8 W

0.1 W   0.4 W

0.1 W   0.4 W

CLEARANCE AND
LOAD LANE WIDTH

10'-0"

2'-0"   6'-0"   2'-0"
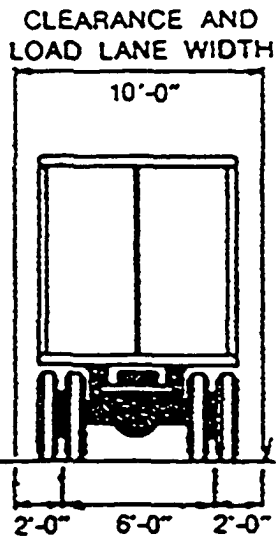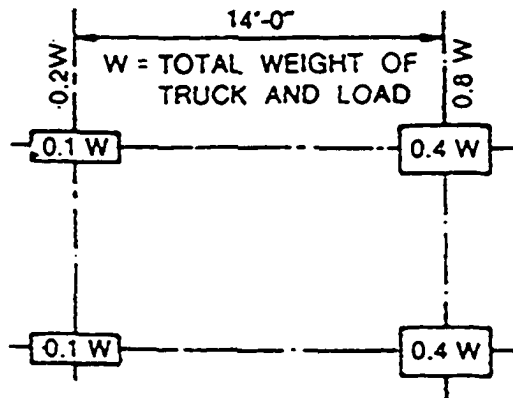
Figure 4.1: Standard H trucks

HS20-44 8.000 LB   32.000 LB   32.000 LB
HS15-44 6.000 LB   24.000 LB   24.000 LB

0.2W   0.8 W   0.8 W

14'-0"   V

| 0.1 W | | 0.4 W | | 0.4 W |

| 0.1W | | 0.4 W | | 0.4 W |
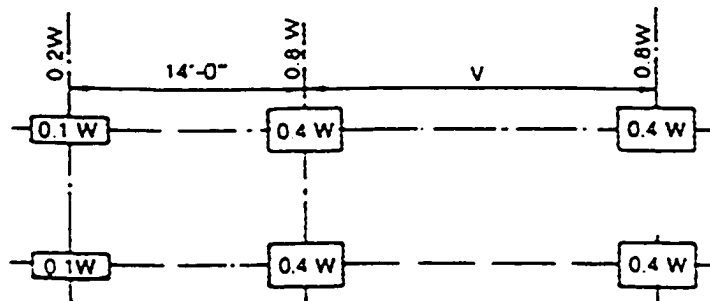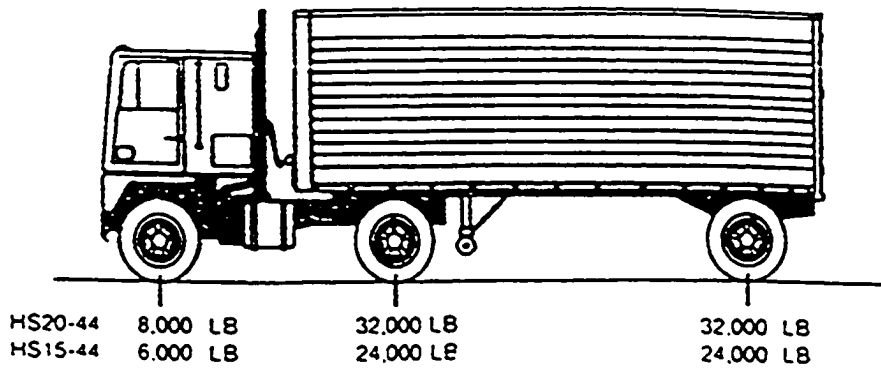
W = COMBINED WEIGHT ON THE FIRST TWO AXLES WHICH IS THE SAME
AS FOR THE CORRESPONDING H TRUCK.

V = VARIABLE SPACING — 14 FEET TO 30 FEET INCLUSIVE. SPACING TO BE
USED IS THAT WHICH PRODUCES MAXIMUM STRESSES.

CLEARANCE AND
LOAD LANE WIDTH
10'-0"

2'-0"   6'-0"   2'-0"
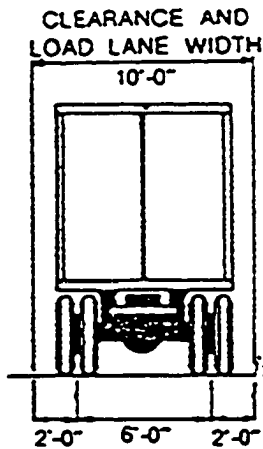
Figure 4.2: Standard HS trucks

69
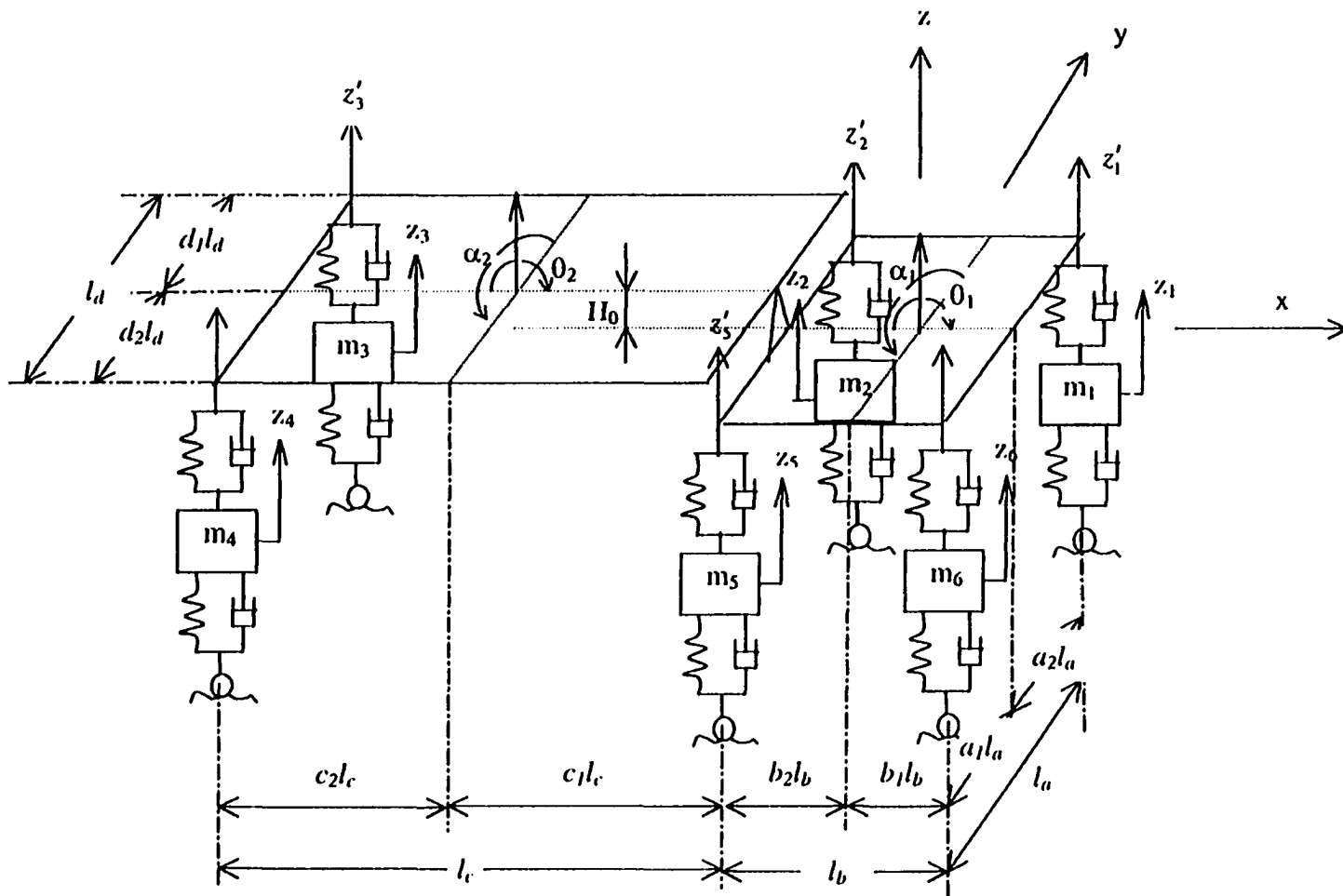
Figure 4.3: Three-dimensional model of a three-axle tractor-trailer

70

TABLE 4.1: Properties of standard H 20-44 truck

$$m_1 = m_6 = 250 kg\,,\ m_2 = m_5 = 1,000 kg\,,\ M_t = 16,910 kg\,,\ k_{s1} = k_{s6} = 4 \times 10^6\,N/m\,,$$

$$k_{s2} = k_{s5} = k_{t2} = k_{t5} = 8 \times 10^6\,N/m\,,\ k_{t1} = k_{t6} = 2.25 \times 10^6\,N/m\,,$$

$$c_{s1} = c_{s2} = c_{s5} = c_{s6} = c_{t1} = c_{t2} = c_{t5} = c_{t6} = 2 \times 10^4\,N \cdot s/m$$

$$I_{\theta t} = 2.4 \times 10^4\,kg \cdot m^2\,,\ I_{\alpha t} = 9 \times 10^3\,kg \cdot m^2\,,\ l_a = 1.83 m\,,\ l_b = 4.27 m\,,$$

$$a_t = 1 - a_2 = 0.50\,,\ b_t = 1 - b_2 = 0.65$$

TABLE 4.2: Properties of standard H 15-44 truck

$$m_1 = m_6 = 250kg \,, \quad m_2 = m_5 = 1,000kg \,, \quad M_: = 12,683kg \,,$$

$$k_{s1} = k_{s6} = 4 \times 10^6 \, N/m \,, \quad k_{t1} = k_{t6} = 2.25 \times 10^6 \, N/m \,,$$

$$k_{s2} = k_{s5} = k_{t2} = k_{t5} = 8 \times 10^6 \, N/m \,,$$

$$c_{s1} = c_{s2} = c_{s5} = c_{s6} = c_{t1} = c_{t2} = c_{t5} = c_{t6} = 2 \times 10^4 \, N \cdot s/m$$

$$I_{\theta 1} = 1.8 \times 10^4 \, kg \cdot m^2 \,, \quad I_{\alpha 1} = 6,750kg \cdot m^2 \,, \quad l_c = 1.83m \,, \quad l_b = 4.27m \,,$$

$$a_1 = 1 - a_2 = 0.50 \,, \quad b_1 = 1 - b_2 = 0.65$$

TABLE 4.3: Properties of standard HS 20-44 truck

$$m_1 = m_6 = 250kg \,, \quad m_2 = m_3 = m_4 = m_5 = 1{,}000kg \,,$$

$$M_1 = 3{,}323kg \,, \quad M_2 = 27{,}821kg$$

$$k_{s1} = k_{s6} = 4 \times 10^6 \, N/m \,, \quad k_{t1} = k_{t6} = 2.25 \times 10^6 \, N/m \,,$$

$$k_{s2} = k_{s3} = k_{s4} = k_{s5} = k_{t2} = k_{t3} = k_{t4} = k_{t5} = 8 \times 10^6 \, N/m \,,$$

$$c_{s1} = c_{s2} = c_{s3} = c_{s4} = c_{s5} = c_{s6} = c_{t1} = c_{t2} = c_{t3} = c_{t4} = c_{t5} = c_{t6} = 2 \times 10^4 \, N \cdot s/m \,,$$

$$I_{\theta 1} = 14{,}055kg \cdot m^2 \,, \quad I_{\theta 2} = 24{,}934kg \cdot m^2 \,, \quad I_{\alpha 1} = 1{,}108kg \cdot m^2 \,, \quad I_{\alpha 2} = 9{,}274kg \cdot m^2 \,,$$

$$l_c = l_d = 1.83m \,, \quad l_b = 4.27m \,, \quad l_c = 4.27 \sim 9.14m \,,$$

$$a_1 = 1 - a_2 = 0.50 \,, \quad b_1 = 1 - b_2 = 0.3 \,, \quad c_1 = 1 - c_2 = 0.50 \,, \quad d_1 = 1 - d_2 = 0.50$$

TABLE 4.4: Properties of standard HS 15-44 truck

$$m_1 = m_6 = 250 kg, \quad m_2 = m_3 = m_4 = m_5 = 1,000 kg,$$

$$M_1 = 2,492 kg, \quad M_2 = 20,866 kg$$

$$k_{s1} = k_{s6} = 4 \times 10^6 N/m, \quad k_{t1} = k_{t6} = 2.25 \times 10^4 N/m,$$

$$k_{s2} = k_{s3} = k_{s4} = k_{s5} = k_{t2} = k_{t3} = k_{t4} = k_{t5} = 8 \times 10^6 N/m,$$

$$c_{s1} = c_{s2} = c_{s3} = c_{s4} = c_{s5} = c_{s6} = c_{t1} = c_{t2} = c_{t3} = c_{t4} = c_{t5} = c_{t6} = 2 \times 10^4 N \cdot s/m,$$

$$I_{\theta 1} = 10,541 kg \cdot m^2, \quad I_{\theta 2} = 18,700 kg \cdot m^2, \quad I_{\alpha 1} = 831 kg \cdot m^2, \quad I_{\alpha 2} = 6,955 kg \cdot m^2,$$

$$l_a = l_d = 1.83m, \quad l_b = 4.27m, \quad l_c = 4.27 \sim 9.14m,$$

$$a_1 = 1 - a_2 = 0.50, \quad b_1 = 1 - b_2 = 0.3, \quad c_1 = 1 - c_2 = 0.50, \quad d_1 = 1 - d_2 = 0.50$$

TABLE 4.5: Properties of the Rock Truck

$$m_1 = m_6 = 250kg \, , \; m_2 = m_5 = 1000kg \, , \; m_3 = m_4 = 794kg$$

$$M_1 = 4,232kg \, , \; M_2 = 2.8 \times 10^4 kg$$

$$k_{s1} = k_{s6} = 421.510N/m \, , \; k_{s2} = k_{s5} = 1.854.996N/m \, , \; k_{s3} = k_{s4} = 643.613N/m$$

$$k_{t1} = k_{t6} = 473.851N/m \, , \; k_{t2} = k_{t5} = 4,132,964N/m \, , \; k_{t3} = k_{t4} = 5,583,154N/m$$

$$c_{s1} = c_{s6} = 3,065 N \cdot s/m \, , \; c_{s2} = c_{s3} = c_{s4} = c_{s5} = 8,750 N \cdot s/m \, ,$$

$$c_{t1} = c_{t6} = 437.5 N \cdot s/m \, , \; c_{t2} = c_{t3} = c_{t4} = c_{t5} = 1,750 N \cdot s/m \, ,$$

$$I_{\theta 1} = 5.260kg \cdot m^2 \, , \; I_{\theta 2} = 1.26 \times 10^5 kg \cdot m^2 \, ,$$

$$I_{\alpha 1} = 1.5 \times 10^3 kg \cdot m^2 \, , \; I_{\alpha 2} = 9 \times 10^3 kg \cdot m^2$$

$$l_a = 2.29m \, , \; l_b = 4.71m \, , \; l_c = 5.84m \, , \; l_d = 2.44m$$

$$a_1 = 1 - a_2 = 0.50 \, , \; b_1 = 1 - b_2 = 0.39 \, , \; c_1 = 1 - c_2 = 0.48 \, , \; d_1 = 1 - d_2 = 0.50$$

TABLE 4.6: Rock Truck natural frequencies vs. rolling inertia

Rolling inertia (kg·m^2)	Vehicle natural frequencies (Hz)				
	1	2	3	4	5
$I_{\alpha 1} = I_{\alpha 2} = 0$	1.63	2.28	2.68	8.66	9.84
$I_{\alpha 1} = 1000$, $I_{\alpha 2} = 0$	1.63	2.28	2.68	**7.48**	9.84
$I_{\alpha 1} = 2000$, $I_{\alpha 2} = 0$	1.63	2.28	2.68	**6.20**	9.84
$I_{\alpha 1} = 3000$, $I_{\alpha 2} = 0$	1.63	2.28	2.68	**5.32**	9.78
$I_{\alpha 1} = 0$, $I_{\alpha 2} = 3000$	1.63	2.28	2.68	**3.79**	8.66
$I_{\alpha 1} = 0$, $I_{\alpha 2} = 5000$	1.63	2.28	2.68	**2.94**	8.66
$I_{\alpha 1} = 0$, $I_{\alpha 2} = 10000$	1.63	**2.08**	2.28	2.68	8.66
$I_{\alpha 1} = 1000$, $I_{\alpha 2} = 3000$	1.63	2.28	2.68	**3.79**	7.48
$I_{\alpha 1} = 1000$, $I_{\alpha 2} = 5000$	1.63	2.28	2.68	**2.94**	7.48
$I_{\alpha 1} = 2000$, $I_{\alpha 2} = 5000$	1.63	2.28	2.68	**2.94**	6.20
$I_{\alpha 1} = 1500$, $I_{\alpha 2} = 9000$	1.63	**2.19**	2.28	2.68	6.79
Test	1.62[1]	-	2.26[2]	2.68[3]	-

*Patten, 1997.

[1] trailer pitch; [2] tractor pitch; [3] entire vehicle heave; - not measured.

CHAPTER FIVE

TREATING DYNAMIC BRIDGE/VEHICLE INTERACTION

As discussed previously. there is a common difficulty in the many studies in finding a suitable method to deal with the kinematic coupling term, which arises in the mathematical formulation of the problem (Ting et al., 1975). To illustrate the kinematic relationship involved, consider the interaction of a bridge due to a moving vehicle where the system is modeled as a Bernoulli-Euler beam carrying a single mass particle. The governing differential equation for the beam can be written as

$$EI\frac{\partial^4 w}{\partial x^4} + m\frac{\partial^2 w}{\partial t^2} = f(x,t) \tag{5.1}$$

where $w(x,t)$ is the deflection of the beam at point x and at time t, EI is the flexural rigidity of the beam, m is the mass per unit length of the beam, and $f(x,t)$ is the reaction force exerted by the mass particle m_0. When the mass is at position $\tilde{x}(t)$, the interaction force $f(x,t)$ can be written by Newton's second law as:

$$f(x,t) = -m_0\left(g + \frac{d^2 w(\tilde{x},t)}{dt^2}\right)\delta(x-\tilde{x}) \tag{5.2}$$

Since the force is convective, i.e., the particle position is time-dependent, the explicit form of the second complete derivative with respect to $w(x,t)$ is

$$\frac{d^2w}{dt^2} = \frac{\partial^2 w}{\partial t^2} + 2\left(\frac{d\bar{x}}{dt}\right)\frac{\partial^2 w}{\partial x \partial t} + \left(\frac{d\bar{x}}{dt}\right)^2 \frac{\partial^2 w}{\partial x^2} + \frac{d^2\bar{x}}{dt^2}\frac{\partial w}{\partial x} \qquad (5.3)$$

The mathematical difficulty involves dealing with the Dirac delta function and the mixed derivative on the right hand side of Equation (5.3). By assuming that the vehicle travels at a constant speed, the right hand side of Equation (5.3) is simplified, but the mixed derivative can not be avoided unless the vehicle were not moving. This is one reason why many studies are limited to the case of moving loads with *constant* speeds.

To fully consider the basic kinematic characteristics, the analysis becomes considerably involved, which was demonstrated by Stanisic et al. (1974). As they concluded, the exact analytical solution is almost beyond hope. In most of the existing studies, the relationship described in Equation (5.3) was replaced with the satisfaction of the equilibrium and compatibility conditions at the interface. This is somehow an analog to a black box problem. What it does is more important than how it works that out.

Due to the various methods used, various types of governing differential equations have been obtained for the coupled system.

1. Coupled equations with an infinite number of DOF for the bridge and a few DOF for the vehicles. They are generally obtained by modeling the bridge as a beam. The system is then solved by analytical methods, such

as the infinite series expansion method. Timoshenko and Young (1955) gave details of early applications.

2. Coupled equations with a few DOF for both the bridge and the vehicle. They are normally obtained by prescribing the bridge a given mode shape. The system can be solved analytically or numerically without difficulty, due to the small number of DOF involved. More details can obtained by referring to Jacobsen and Ayre (1958).

3. Coupled equations with large number of DOF for either the bridge or the vehicle. Usually, such equations are obtained when the bridge is treated as a discrete system, for example, with use of the finite element method. The vehicle model can be very complicated, but can be expressed in a matrix form. The coupled equations are solved by direct time integration, namely step-by-step method, such as Runge-Kutta, Newmark, and Wilson-θ methods. Chu et al. (1979) gave all the formulas in detail.

4. Two uncoupled sets of equations for the bridge and the vehicles, respectively, and with the compatibility and equilibrium conditions at the interface between the bridge and vehicles included. The two sets of equations are solved separately and the interface conditions are satisfied in an iterative way.

The first two methods can be used only when the bridge has a simple shape. Nowadays, sophisticated models are deemed necessary for the bridge and the vehicles. Hence these two methods are rarely used today.

The third method is not recommended due to some apparent inconvenience. For instance, a single parameter change, either in the bridge or the vehicles, requires an update of the whole system; the more vehicles on the bridge, the more coupled DOF and also the more DOF in the coupled equations for the system; etc. All these inconveniences render the coupled equations very difficult to solve in view of memory allocation or computational effort.

This fourth method was first used by Veletsos and Huang (1970). Since then, it has been widely used. Usually these equations are solved by direct time integration. However, more recently, Green (1990) developed an involution integration procedure. Green and Cebon (1994) developed a calculation procedure in the frequency domain. Similar iterative methods have been used by other researchers. Hawk and Ghali (1981) proposed a similar procedure, called the "iterative dynamic substructuring method (IDSM)". They compared their method with solutions obtained by Runge-Kutta-Nystrom numerical integration and found good agreement.

The fourth technique is employed in the present study. The bridge and vehicle is considered as two separate structures connected at the time-dependent contact points. The interaction is considered in an iterative way, in which the

equilibrium and compatibility conditions are satisfied. The input to the vehicle is the roughness of its travel path, or more precisely, the displacements and the velocities of what the tires contact. When a vehicle travels on a bridge, the input is the sum of the irregularities of the pavement surface and the deflection of the bridge. The input excites the vehicle and results in dynamic tire forces, which in turn act as inputs to the bridge. The bridge deflects accordingly. The interactive force coupled the dynamic response of the vehicle to that of the bridge. An iterative procedure is used to realize this, and an algorithm, BVPack (included in Appendix III), has been developed to simulate the interaction. The algorithm incorporates the equations describing the dynamics of the bridge and the equations for the vehicle, which are solved simultaneously in the procedure. The procedure for a single vehicle moving at a constant speed over a bridge is described as followed:

(i)   Initialization of the program, including identifying the bridge and vehicle parameters, time increment, initializing memory allocation, etc.;

(ii)   Obtain the mode shapes of the bridge;

(iii)   Obtain the equilibrium conditions for the bridge and the vehicle and take them as the starting conditions;

(iv)   The vehicle is excited by the bridge entrance profile. The tire forces at the entrance are predicted;

(v)   With the tire forces as inputs to the bridge, carry out the computation described in Equation (3.15) and obtain the dynamic response of the normal coordinates;

(vi)   Use mode superposition to obtain the displacements and velocities of the contact points;

(vii) Running VehiclePack to update the dynamic response of the vehicle and predict the new tire forces;

(viii) Steps (iv) to (vi) are repeated until the vehicle has passed over the entire bridge.

(ix)   Compute the bridge response at an arbitrary point by use of Equation (3.2).

If there are more vehicles running over the bridge, a similar procedure is carried out to simulate the interaction.

CHAPTER SIX

HIGHWAY BRIDGE/VEHICLE INTERACTION ANALYSIS

The dynamic effect resulting from the passage of vehicles is of most concern in the design of highway bridges in that it provides a measure for the dynamic interaction between a bridge and moving loads. To allow for such a dynamic effect, it is required that the static load be increased by a dynamic allowance factor, which is known as the impact factor. The impact factor (also known as dynamic index and dynamic amplification factor) reflects a ratio of the maximum dynamic response to the maximum static response of the bridge. Usually, it is defined by

$$I(\%) = (I_d - I_s)/I_s \tag{6.1}$$

where I_d is the maximum dynamic response and I_s is the maximum static response of the bridge.

Many bridge design codes, including the Standard Specifications for Highway Bridges (1989) by the American Association of State Highway and Transportation Officials (AASHTO) and the Ontario Highway Bridge Design Code by the Ministry of Transportation and Communication (1983), have adopted the same impact formula for various dynamic responses, and have related the impact factor to a single parameter of the bridge, such as the span length or

fundamental frequency of vibration. For example, AASHTO provides a formula for the impact factor, which is only a function of the length of the span. The formula is written as

$$I = \frac{50}{L + 125} \qquad (6.2)$$

where L is "the length in feet of the portion of the span that is loaded to produce the maximum stress in the member". The maximum allowance of I is 0.3. This approach to design is certainly an oversimplification and, in many cases, misrepresentation of the complex physical phenomena involved in the vehicle-bridge/vehicle interactions. The literature demonstrated that the dynamic amplification of vehicle loads depends on a wide range of factors including the velocity and dynamic properties of the moving vehicle, the dynamic properties and supporting conditions of the bridge, and the roughness of the road pavement.

Recently the use of the term impact has been dropped in some codes; the Ontario Highway Bridge Design Code (1983) deleted the term in 1979 and other countries have followed. The Australian Draft Bridge Design Specification (1987) uses the term dynamic-load allowance. The definition of the dynamic factor or dynamic amplification factor remains the same.

In this chapter, the terminology of dynamic amplification factor (DAF) is employed and defined as:

$$DAF = I_d / I_s \qquad (6.3)$$

The influence of various factors on DAF is extensively investigated.

6.1 Model of the bridge entrance and surface roughness

The effects of the roughness of the bridge entrance and surface will be examined shortly. A pavement profile may be considered as a realization of a random process that can be described by a power spectral density (PSD) function (Wang et al., 1996):

$$S(\gamma) = A_r \left(\frac{\gamma}{\gamma_0} \right)^{-2} \tag{6.4}$$

where $S(\gamma)$ is the PSD value (m^3/cycle) for the pavement evaluation, γ is the wave number or the spatial frequency (cycle/m), A_r is the roughness coefficient (m^3/cycle), and γ_0 is the discontinuity frequency, which takes the value of $1/2\pi$ (cycle/m). According to International Organization for Standardization (ISO) specifications (Dodds, 1972), the roughness coefficient A_r takes the value of 5×10^{-6}, 20×10^{-6}, 80×10^{-6}, and 260×10^{-6} for the classes of very good, good, average and poor roads, respectively.

When modeled as a stationary Gaussian random process, a sample road pavement profile can be generated as (Solnes, 1997)

$$r(x) = \sum_{n=1}^{N} \sqrt{2S(f_n)\Delta f} \cos(f_n x + \theta_n) \tag{6.5}$$

where N is a large number that defines the number of the data points generated and is taken as 2^{10} in the simulation, $f_n = (n - 1/2)\Delta f$ is the nth frequency, Δf is the frequency increment, which is a measure of the desired or possible frequency resolution, and θ_n are random phase angles, independent and uniformly distributed from 0 to 2π.

Sample profiles according to the four classes of roads are shown in Figures 6.1 to 6.4. The roughness profiles of the bridge approach and surface are generated by the same procedure. The end of the bridge is assumed to be perfectly smooth.

6.2 Modal parameters of the Walnut Creek Bridge

The Walnut Creek Bridge (Figure 6.5) is located on I-35 and crosses Walnut Creek near Purcell, Oklahoma. It has four spans and consists of five 122 m long continuous steel girders. It is supported by three sets of piers. The bridge deck is skewed at 45° to the longitudinal central line of the roadway. The composite concrete deck is 11.6 m wide, including two lanes of traffic, west lane and east lane, carrying north bound traffic. The lane locations are shown in Figure 6.6. The deck is stiffened with diaphragms at 6.1 m intervals. The diaphragms are perpendicular to the longitudinal central line of the bridge.

In the pb-2 Rayleigh-Ritz method, the bridge superstructure is idealized as an orthogonally stiffened skew plate, as shown in Figure 6.7. The following features have been assumed:

1. The bridge deck is made of linearly elastic isotropic materials with uniform thickness such that the thin plate theory is valid. Shear deformability and rotatory inertia are ignored. Two edges are simply supported while the other two (the long side edges) are free.

2. The girders are continuous wide-flange I-beams without rotatory inertia and shear deformability.

3. The pier supports are simple point supports.

4. The concrete deck is made of high strength concrete. All steel members are made from high-strength, low-alloy structural steel.

5. Small deflections are assumed so that the linear strain-displacement relations may be used.

Following the same procedure as previously discussed, the lowest five frequencies are obtained and compared with test results in Table 6.1, where the modal damping ratios are also included. The lowest six mode shapes are illustrated in Figure 6.8. The first two modes are mainly bending. The torsion mode appears from the third mode. Higher modes are combinations of bending and torsion.

6.3 The Walnut Creek Bridge subjected to Rock Truck

By using the procedure described previously, the dynamic amplification factors of the Walnut Creek Bridge due to a moving Rock Truck at different locations can be obtained. The west lane and east lane with the truck relative location on the bridge are shown in Figure 6.6. The truck is assumed to be traveling on the east lane at the posted speed of 29.2 m/s (65 mph) for dynamic analysis. For static analysis, the vehicle is modeled as six dead weights moving at a low speed 0.45 m/s (1 mph).

The bridge responses at the second mid-span points in the central girder (#3) due to static and dynamic excitation are demonstrated in Figures 6.9. Figures 6.10.a and 6.10.b show the contribution of various modes to the bridge response. Figure 6.10.a illustrates the variation of the first six normal coordinates with time. Those modes higher than the fifth have substantially smaller amplitudes. Figure 6.10.b shows the deflection of the fourth mid-span on the central girder (Figure 6.7) vs. the superposition of different number of modes. The representation by the summation of the lowest five modes and the lowest ten modes are so close that the difference can hardly be distinguished. It is apparent that the lowest five modes are enough to describe the bridge response accurately. It is noted that the torsion mode appears at the third mode; thus, it is important to consider the torsion effect of a bridge.

According to the impact factor formula defined by AASHTO (1989), the Walnut Creek Bridge, with $L = 100\,ft$, results in an impact factor of 0.22, or a DAF of 1.22. Table 6.2 lists the DAF at the four mid-span points along the central girder with sampled irregularities of bridge entrance and surface according to perfect (0), very good (VG), good (G), average (A) and poor (P) roads. It is apparent that the roughness results in larger bridge dynamic response. The poor entrance with poor surface results in the largest DAF.

In general, with the bridge entrance in the same class of roads, the roughness of the bridge surface causes slightly larger dynamic increment. The effect is not significant. With perfect entrance, the poor surface results in approximately 0.8 percent higher DAF than the perfect surface. With poor entrance, the poor surface results in approximately 3.8 percent higher DAF than the perfect surface. The effect of the roughness of the bridge surface may be considered negligible. However, with perfect surface, the poor entrance results in approximately 16.8 percent higher DAF than the perfect entrance. With poor surface, the poor entrance results in approximately 20.3 percent higher DAF than the perfect entrance. Thus, the effect of the bridge entrance roughness is noticeably more significant than that of the bridge surface. Many previous researchers agreed that the initial conditions of the vehicle affect substantially the dynamic response of the bridge. The effect is evident in the current study.

Table 6.3 compares the effects of bump type and depressed type profile for bridge entrance. The DAF along the central girder (#3) and the east girder (#1) are listed. The bridge entrance profile was measured by Patten et al. (1999). Figure 6.11 illustrates the depressed type roughness measured (WCB). The analytical DAF are close to those obtained from tests. A bump type profile has been generated by simply revising the sign of the measured profile (-WCB). The bump-type profile causes larger DAF at the first and second mid-span points and smaller DAF at the other two mid-span points. However, the largest DAF often occurs at the first and second mid-span points. The bump-type profile tends to result in worse dynamic response of the bridge. In general, a dump-type or depressed-type profile yields larger DAF than the profiles generated as random processes.

Figure 6.12 demonstrates the bridge response at the fourth mid-span of the central girder, with and without the consideration of the bridge damping. The appearance of damping lowers the peak of the deflection.

6.4 Parametric studies of dynamic amplification factor

In this subsection, several examples are studied to illustrate the effects of vehicle characteristics, bridge layouts, and traffic conditions. The vehicle parameters chosen for the sensitivity studies include axle weight, axle spacing,

and speed. The bridge parameters chosen are those that could be directly and easily retrieved from a review of bridge layouts, including span length and skew angle. The effects of multiple trucks are investigated as well. In the following illustration, the roadway surface irregularities are excluded.

6.4.1 Effects of vehicle type and axle spacing

In this subsection, for the purpose of illustration, four standard trucks are chosen. The trucks are assumed to be traveling on east lane at a speed of 30 m/s. The minimum axle spacing of 14 ft is chosen for the HS trucks. In Figure 6.13, the DAF are plotted for the four mid-span points along the central girder. In general, HS trucks result in larger DAF and HS 20-44 yields the largest DAF. However, the changes of DAF at different locations are not similar. The effect of axle spacing on DAF is plotted in Figure 6.14, where the spacing of the HS 20-44 truck varies within its allowance. As the spacing increases, the DAF decreases slightly in the investigated range; however, the change is not significant. Figure 6.14 indicates that the pattern of variation of DAF with axle spacing for different locations at the bridge is not generally the same. The HS 20-44 standard truck is chosen in the discussions hereafter.

6.4.2 Effects of vehicle model and speed

As discussed in Chapter Three, rolling motion of the vehicle introduces a frequency close to the natural frequency of the bridge. In a 3D model of the vehicle, there exists a coupling between the wheels of any axle, in addition to the coupling between the axles as in the case of a 2D model. Thus, the tire forces are dependent upon the heaving, pitching and rolling of the vehicle. Figure 6.15 compares the DAF vs. vehicle speed. It shows that 3D model produces small difference for speed under 40 mph. However, for higher speeds, the difference between the DAF from these two vehicle models becomes significant. Further, the 2D model generally yields higher values of DAF. Figure 6.15 also indicates higher DAF for higher speed, especially in the range of 40 to 80 mph.

6.4.3 Effect of traffic condition

For the purpose of examining the DAF under various traffic conditions, six traffic patterns are considered. As indicated in Figure 6.18, Case 1 refers to one vehicle running on the east lane, while in Case 2, one vehicle running on the west lane. In Cases 3 to 6, two vehicles are considered. Case 3 considers two vehicles running side by side. In Case 4, one vehicle leads the other. Case 5 considers two vehicles with one-span length in between, and Case 6 considers two vehicles running on adjacent spans. In all cases, HS 20-44 trucks running at the speed of 30 m/s is assumed.

6.4.4 Effect of span length

In Figure 6.18, the maximum DAF of the central girder is plotted against L in order to make a comparison with the impact factor defined by AASHTO ($50/(L+125) \div 1$). The span length varies from 70 ft to 120 ft (21.3 m to 36.6 m). It is surprising to note that the simple formula actually provides a very good evaluation of the dynamic factor, although only one parameter is considered.

6.4.5 Effect of skew angle

The skew angle of a bridge is one of the most critical parameters that affect the *natural frequencies* of the bridge. However, Figure 6.19 indicates that the variation of DAF vs. skew angle from 0° to 60° is not significant, although it increases slightly with increasing skew angle.
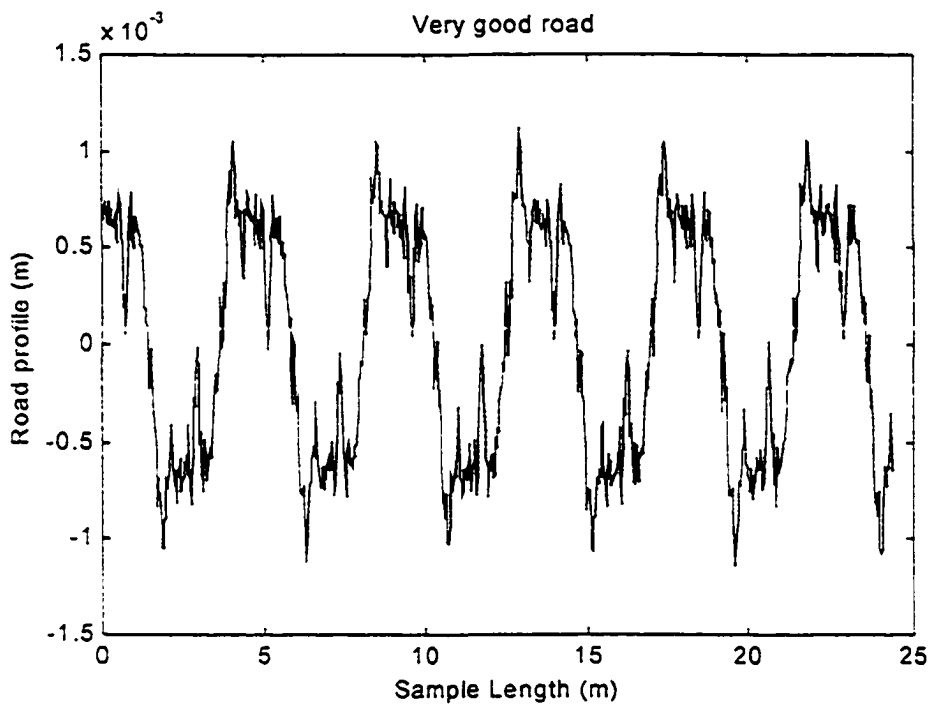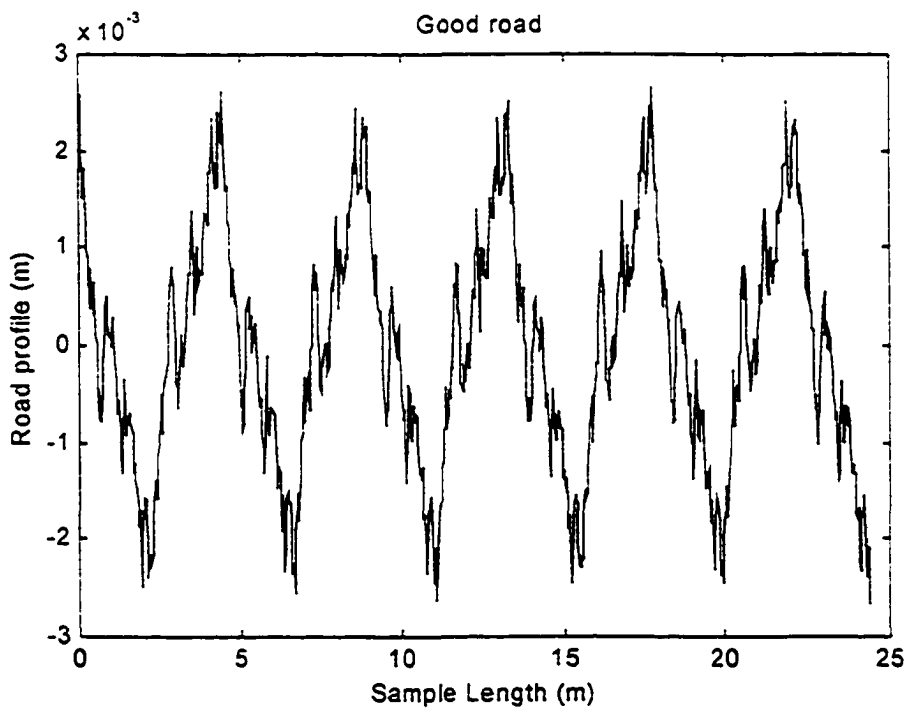
Figure 6.1: Sample profile for very good road

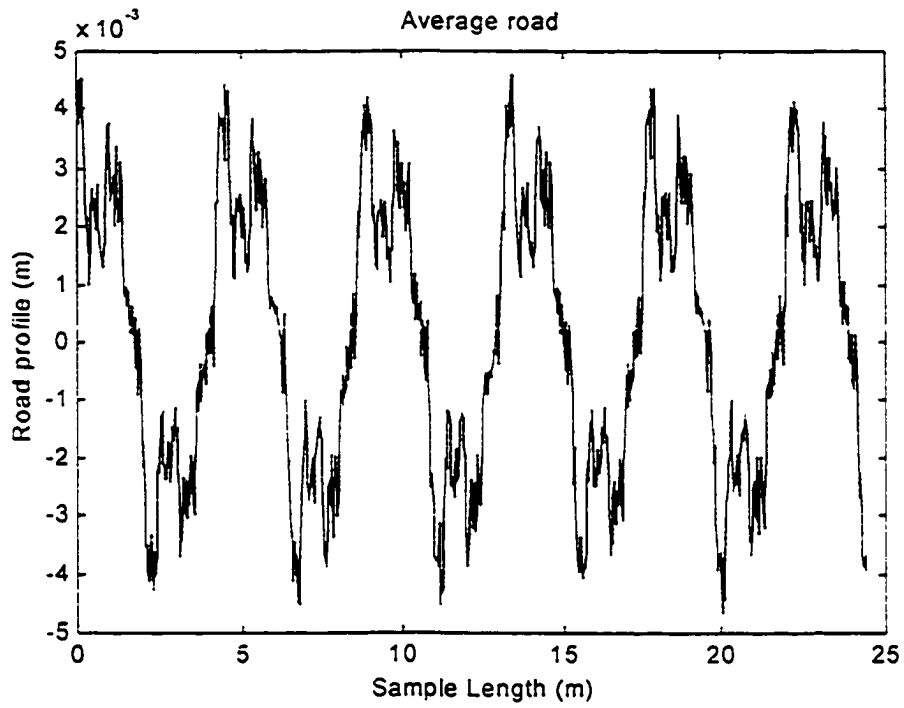Figure 6.2: Sample profile for good road

Figure 6.3: Sample profile for average road

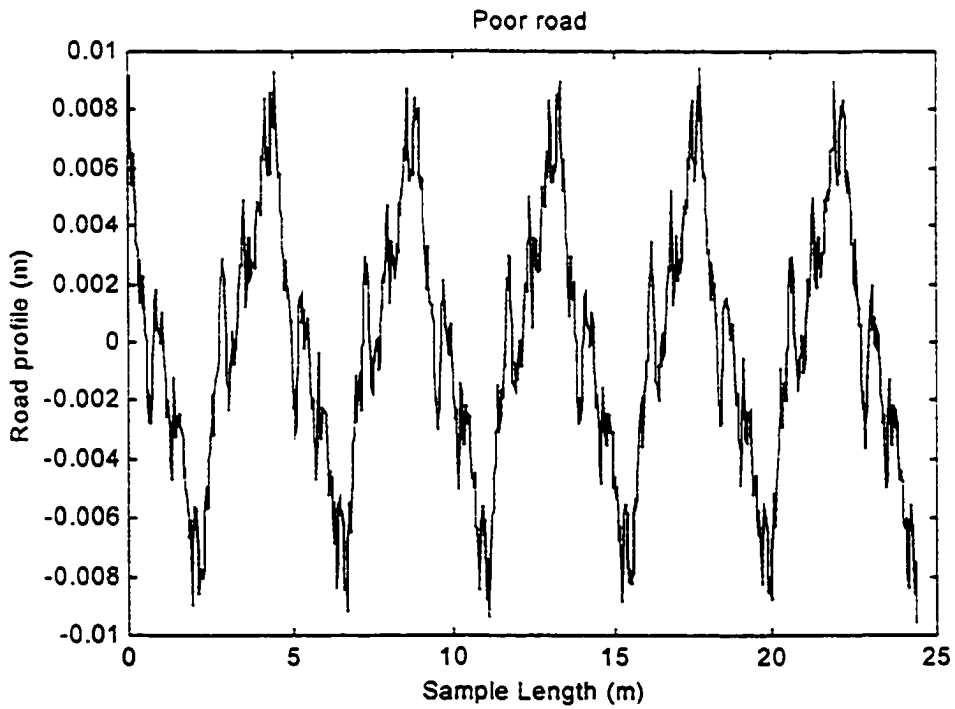**Figure 6.4: Sample profile for poor road**

South   Concrete Deck   Traffic Direction →

North

10.4m

5.2m

Abutment   Expanded Shoes   Piers   Fixed shoes

#5
#4
45   #3
#2

Steel Girder #1
W54x132

30.5m

122m

11.6m

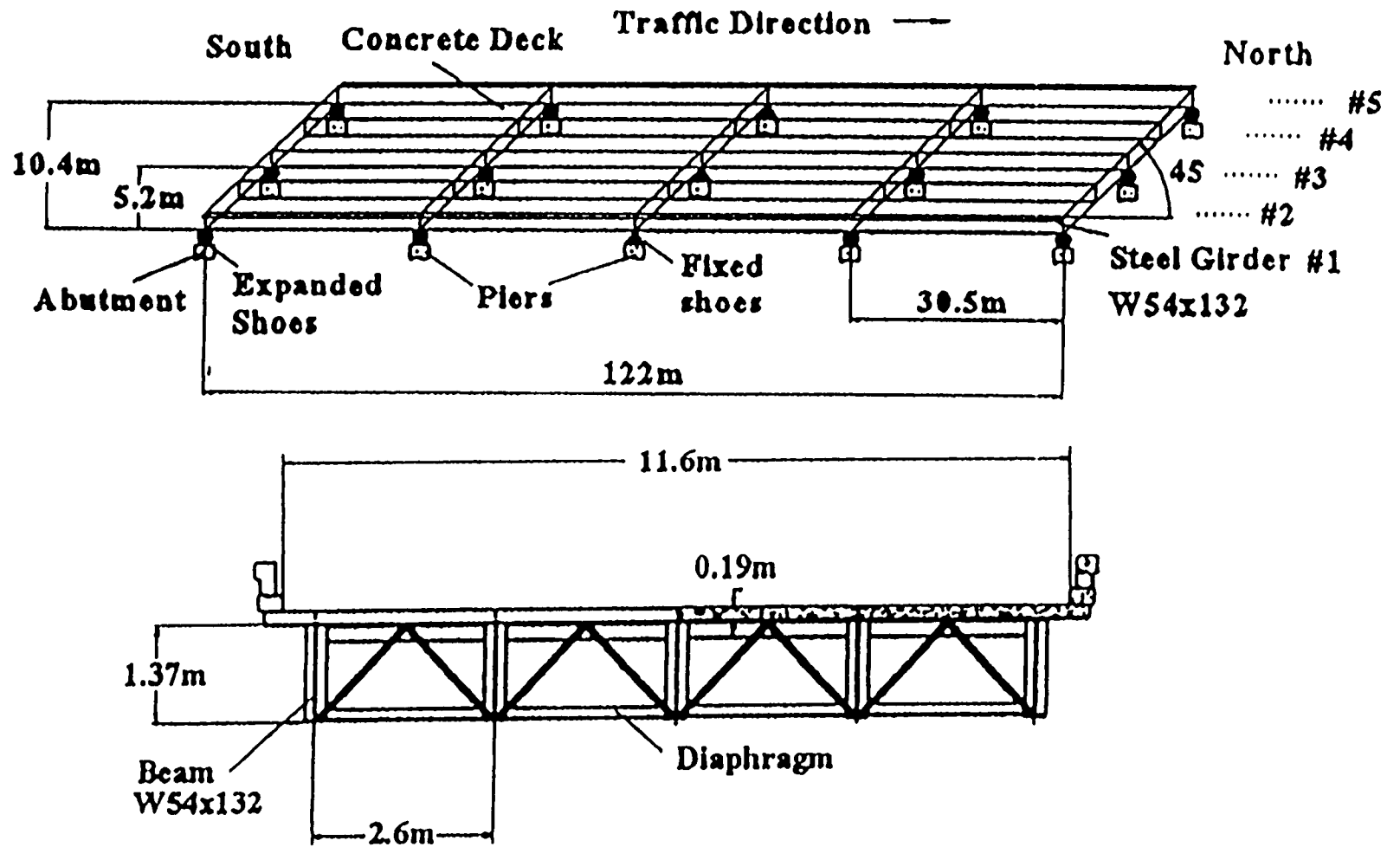0.19m

1.37m

Beam
W54x132

Diaphragm

2.6m

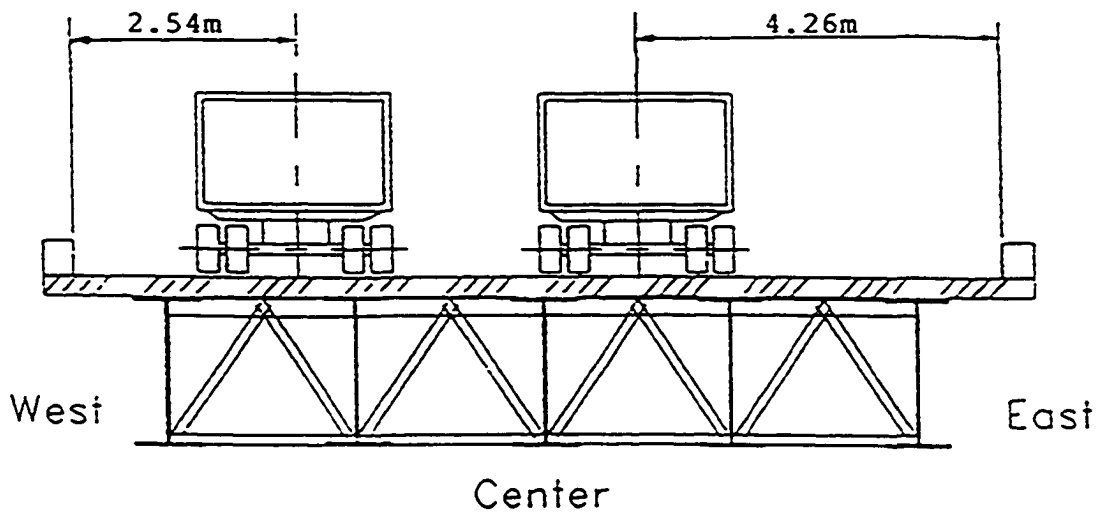Figure 6.5: Superstructure of the Walnut Creek Bridge

Figure 6.6: Lane location on the deck of the Walnut Creek Bridge
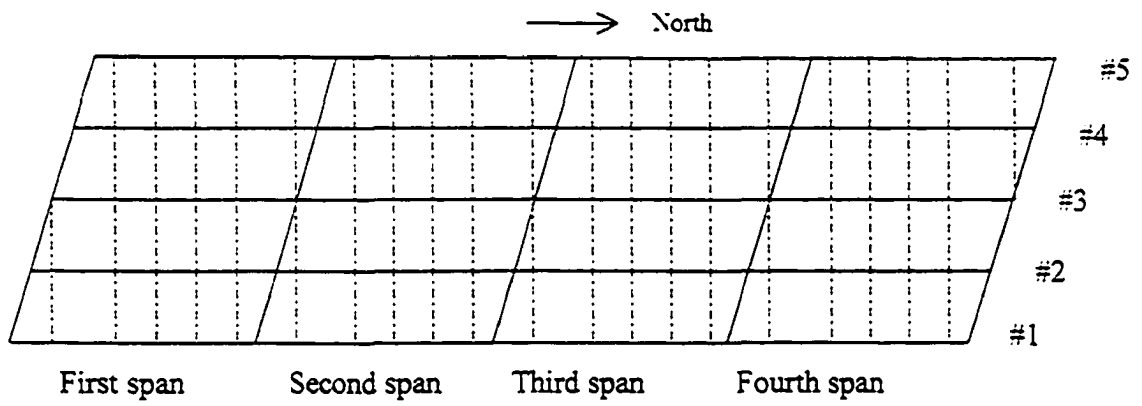
Figure 6.7: Model of the Walnut Creek Bridge superstructure

Mode 1: 2.63 Hz

Mode 2: 3.04 Hz
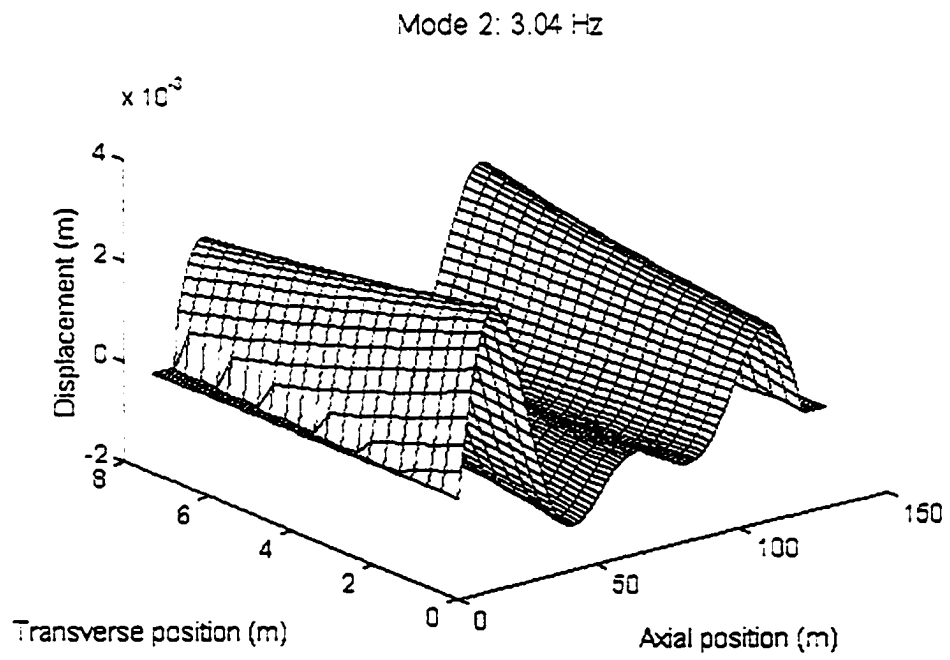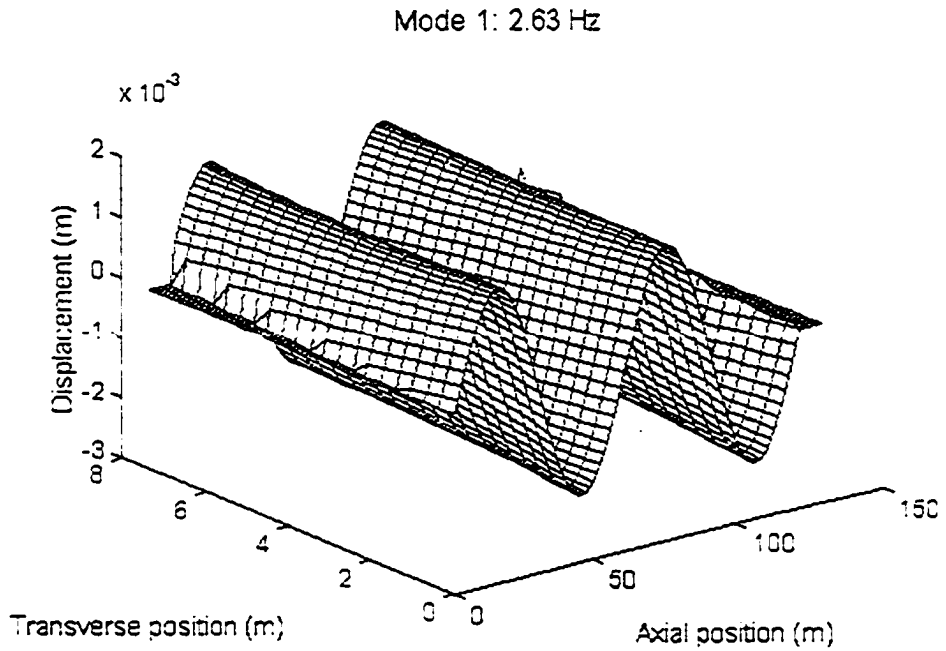
Figure 6.8: First six modes of the Walnut Creek Bridge

Mode 3: 3.22 Hz
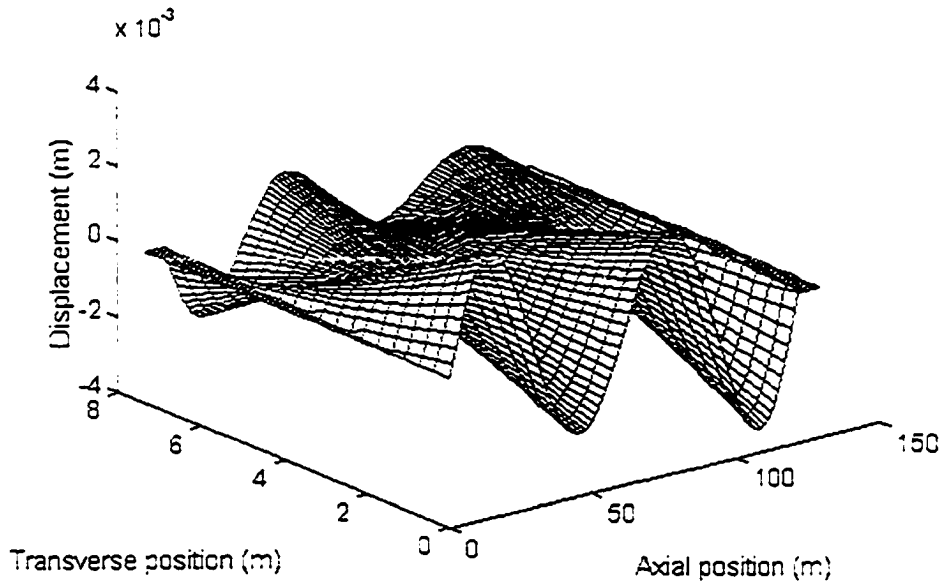
Mode 4: 3.67 Hz
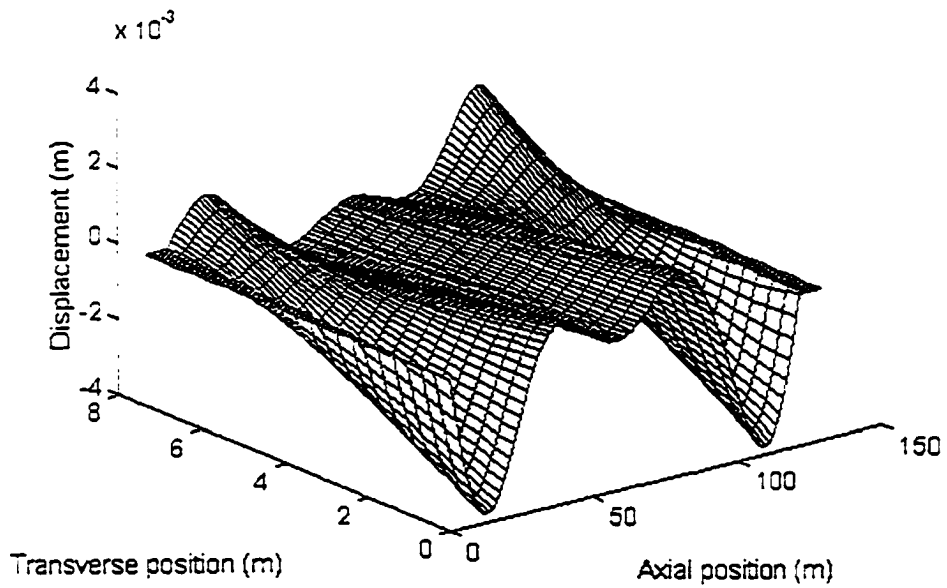
Figure 6.8: First six modes of the Walnut Creek Bridge (cont'd)

Mode 5: 3.93 Hz
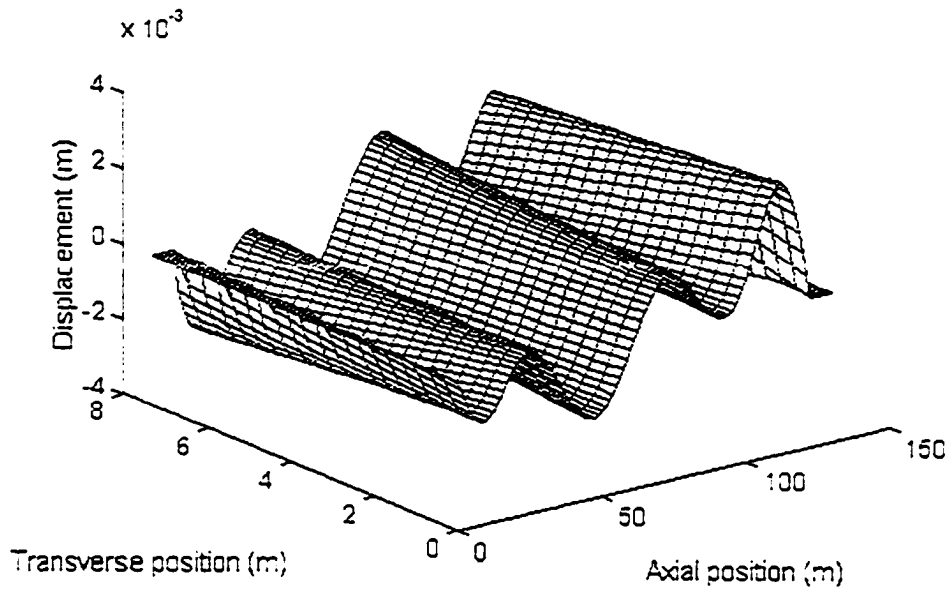
Mode 6: 4.58 Hz
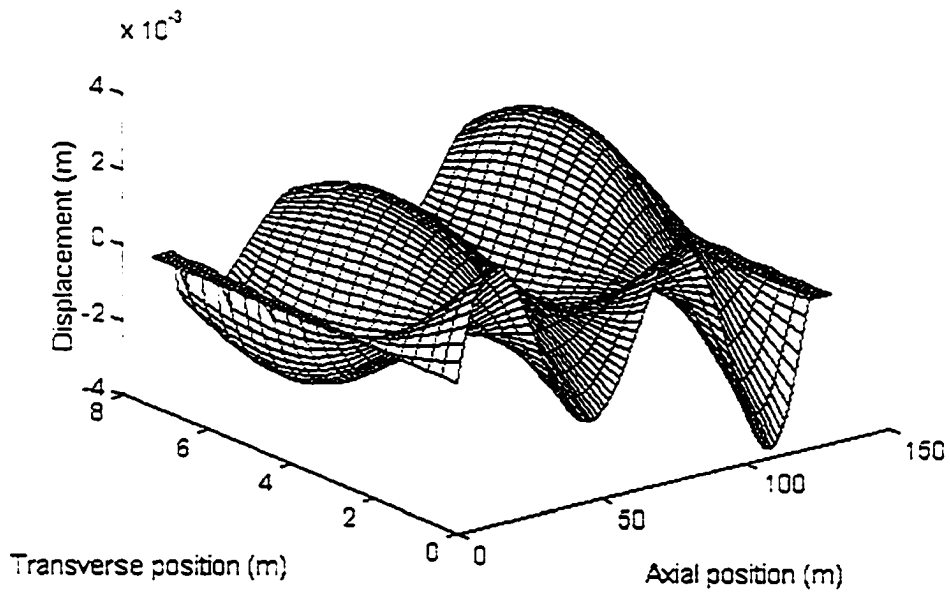
Figure 6.8: First six modes of the Walnut Creek Bridge (cont'd)
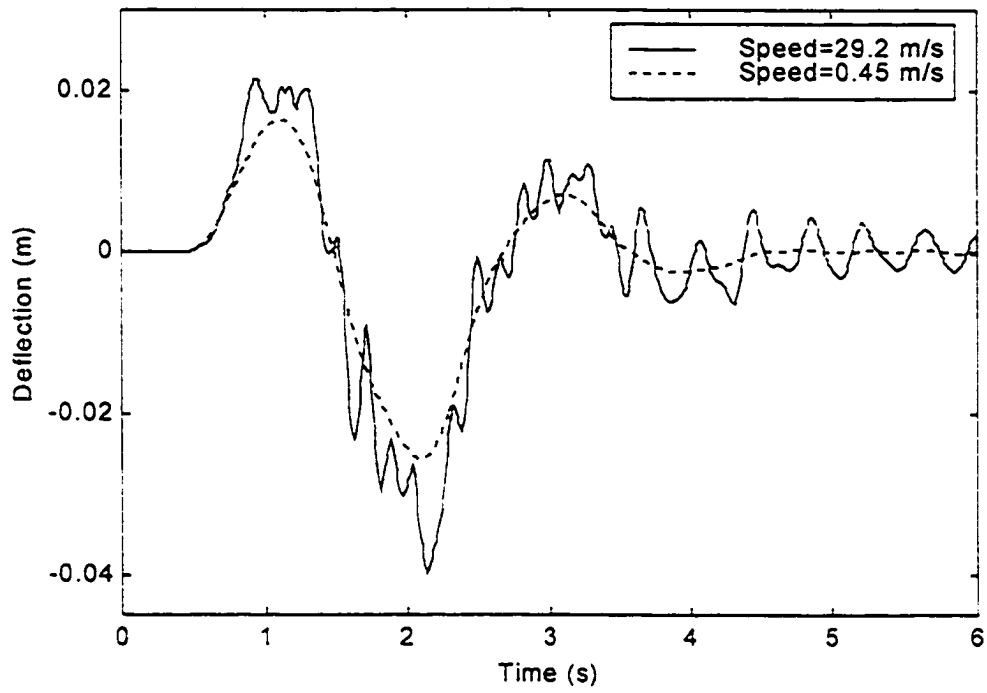
Figure 6.9: Bridge dynamic and static response at the second mid-span point of the central girder
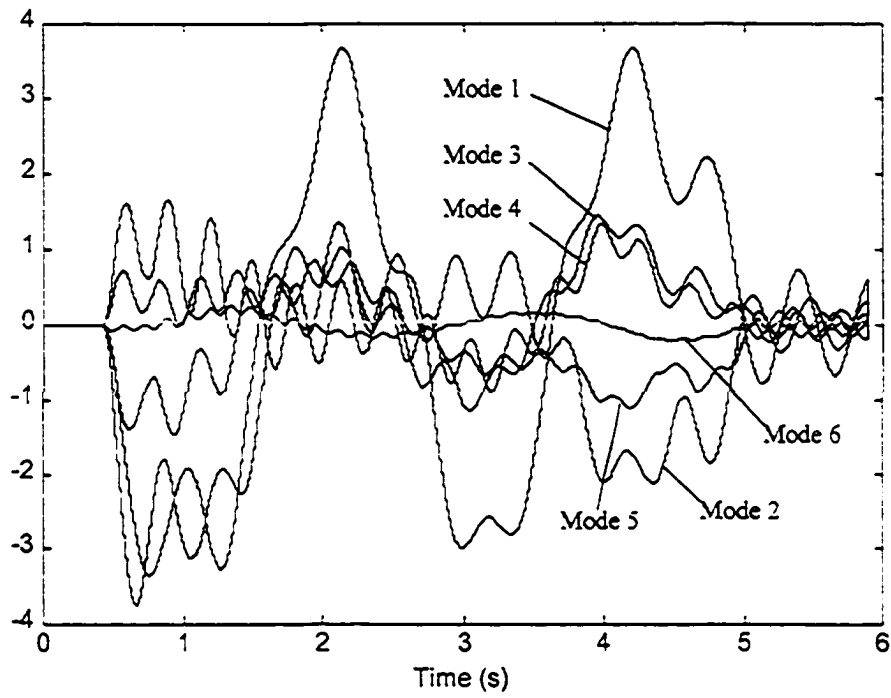
(a)
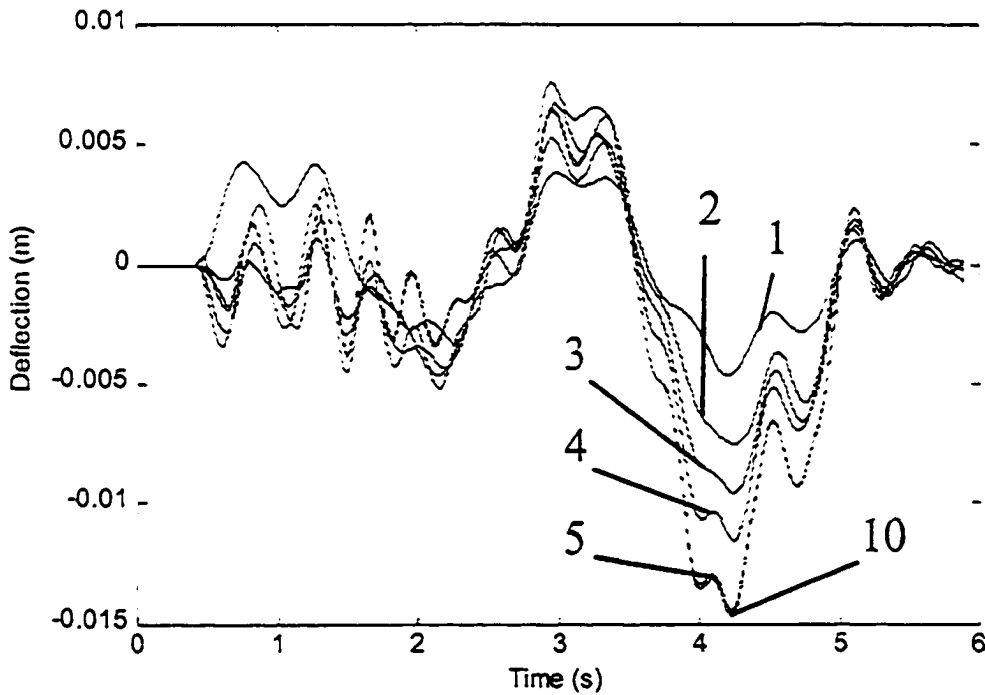
(b)

Figure 6.10: Mode contributions:
(a) Time history of normal coordinates;
(b) Mode contributions to the deflection of a mid-span point.
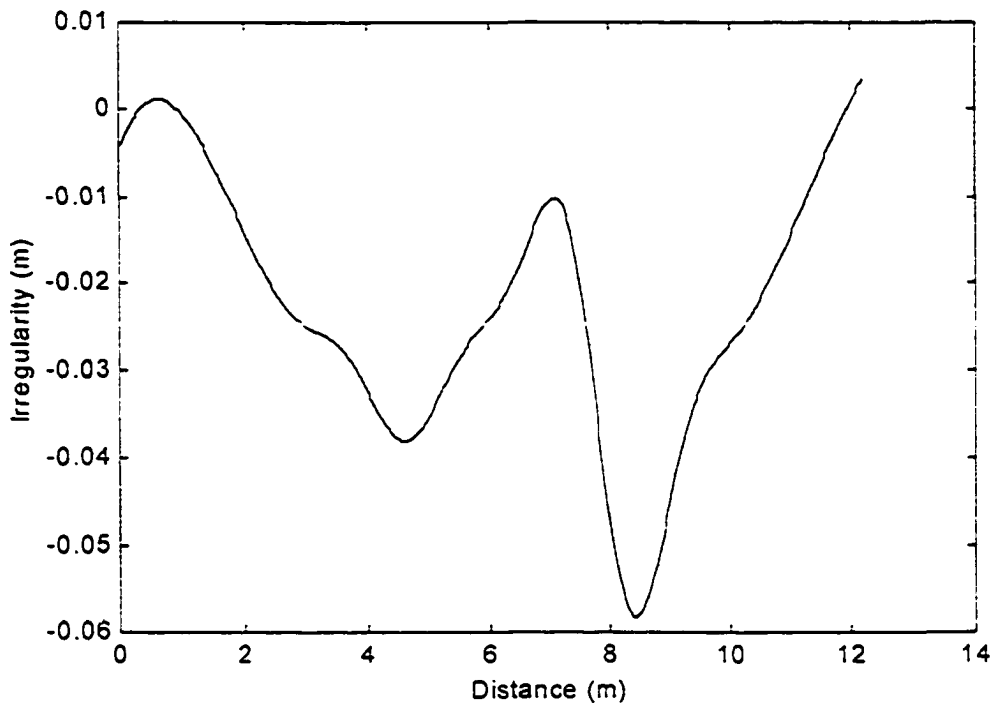
Figure 6.11: The Walnut Creek Bridge entrance profile (measured)
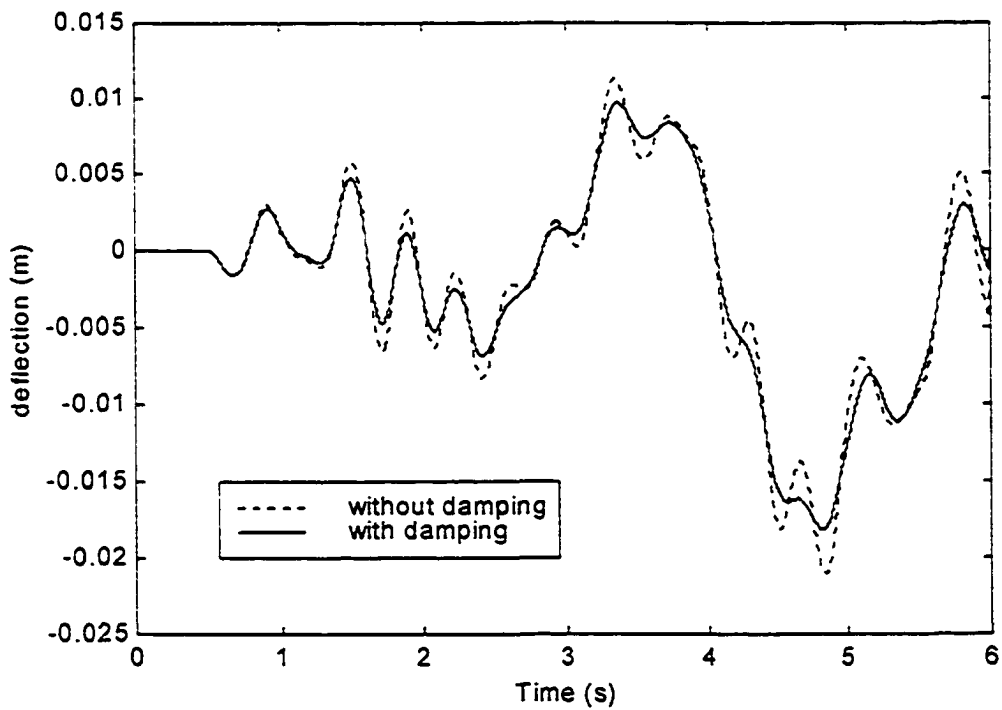
Figure 6.12: Bridge response at the fourth mid-span point
on the central girder
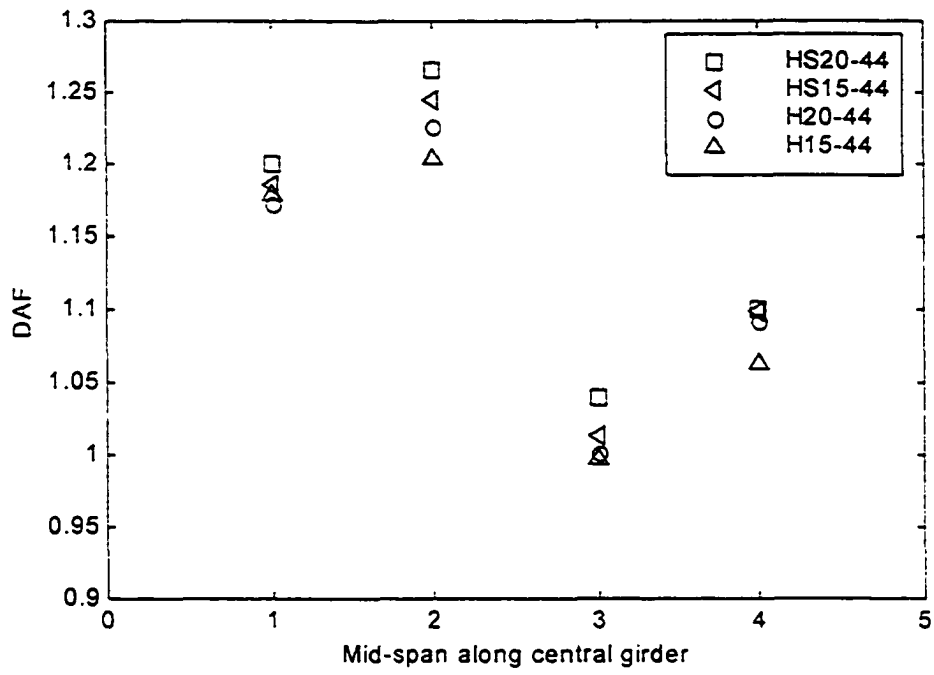
Figure 6.13: Bridge subjected to four different standard trucks, each moving at 30 m/s
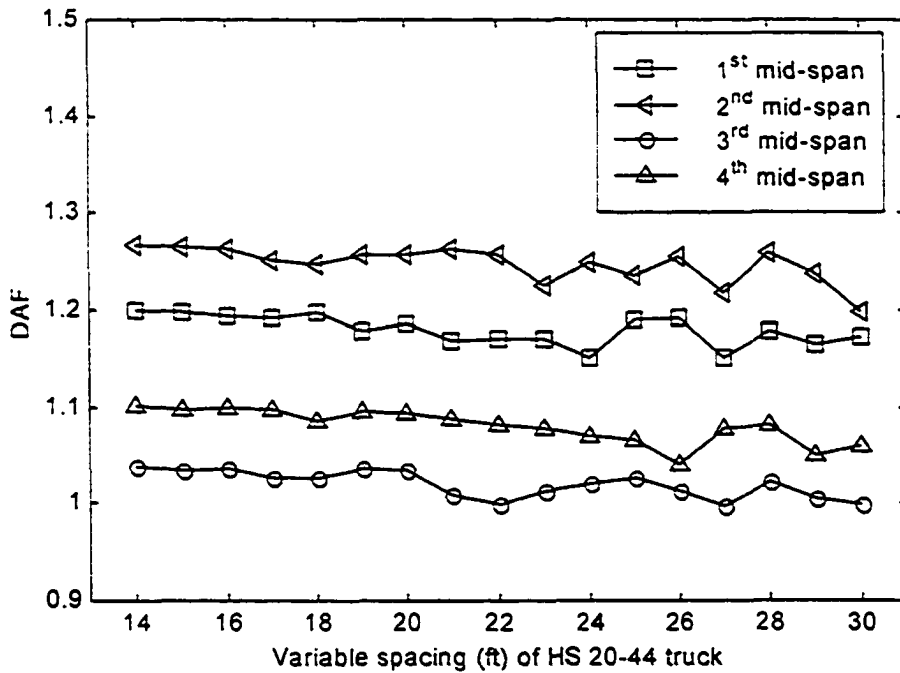
Figure 6.14: DAF vs. axle spacing along the central girder
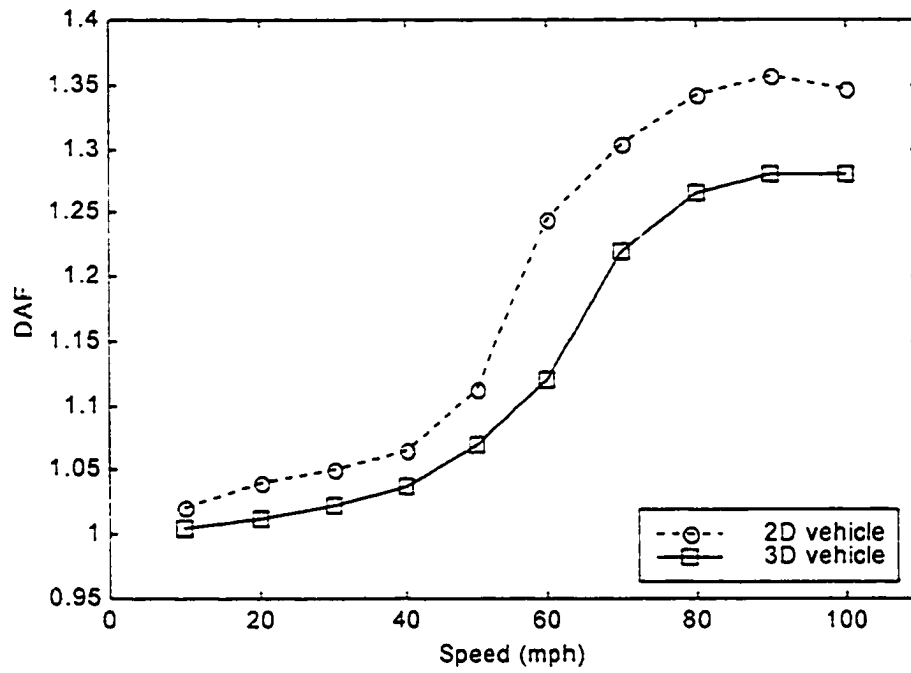
Figure 6.15: DAF vs. speed with different vehicle models
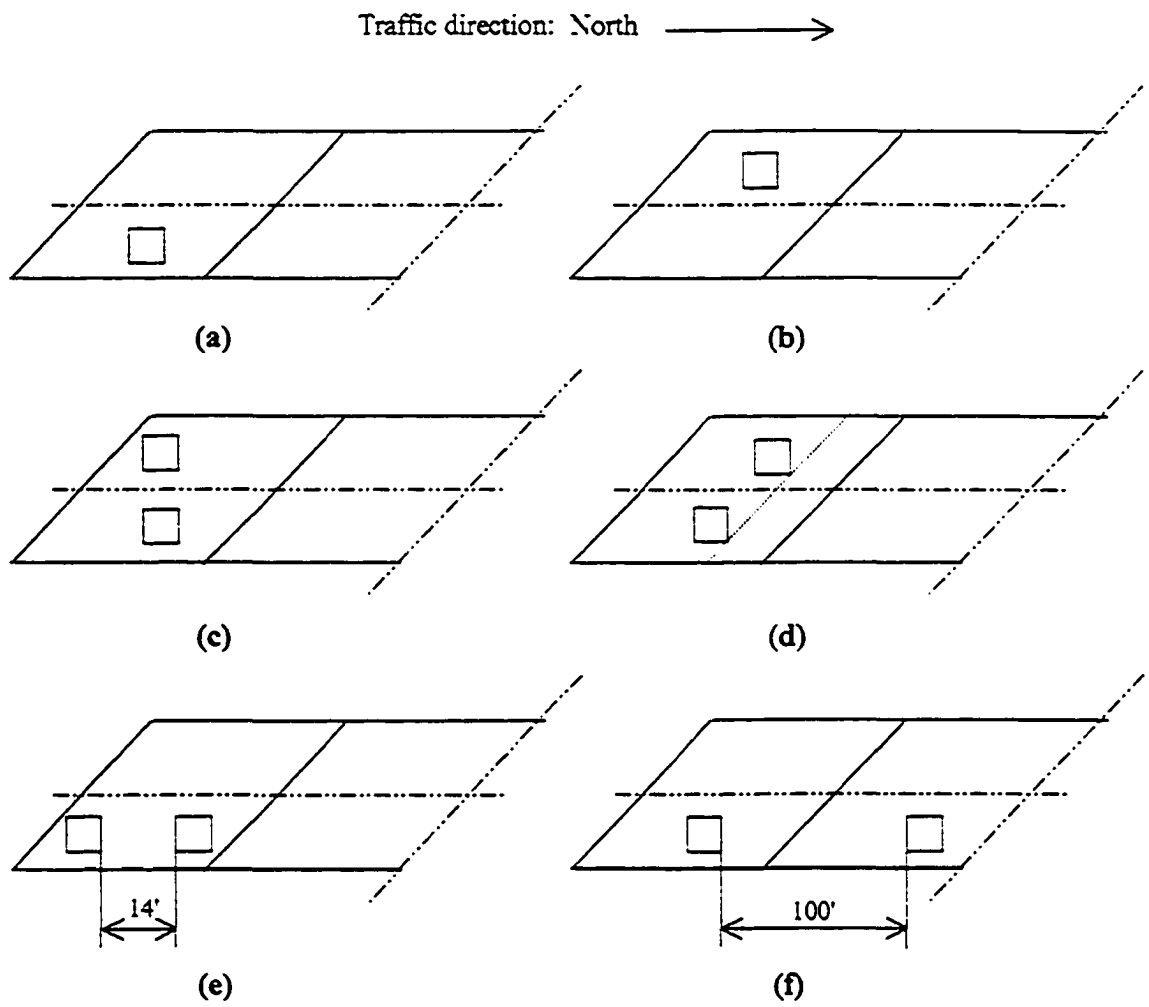
Figure 6.16: Traffic conditions: (a) Case 1; (b) Case 2; (c) Case 3;
(d) Case 4; (e) Case 5; (f) Case 6.
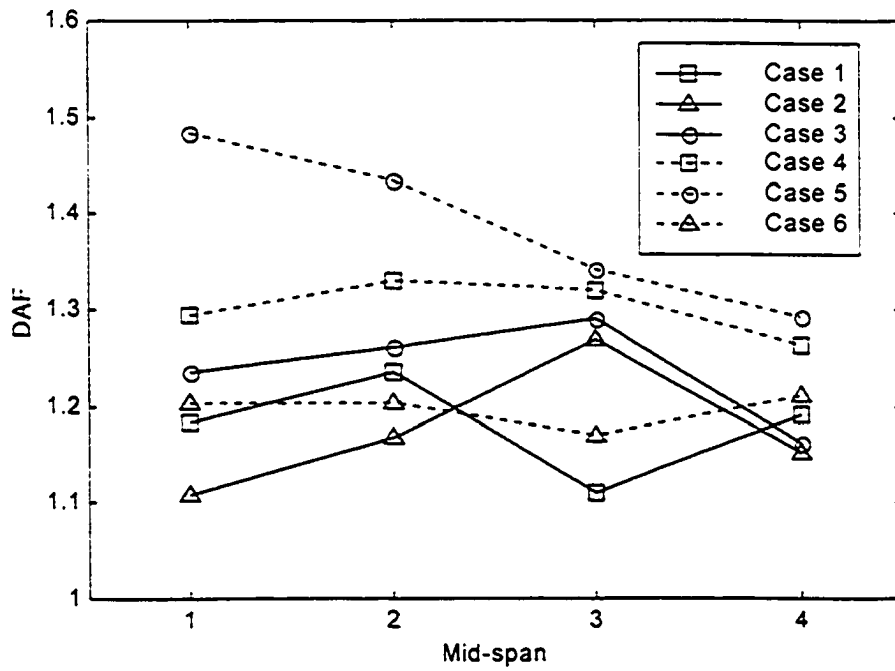
Figure 6.17: DAF vs. traffic condition
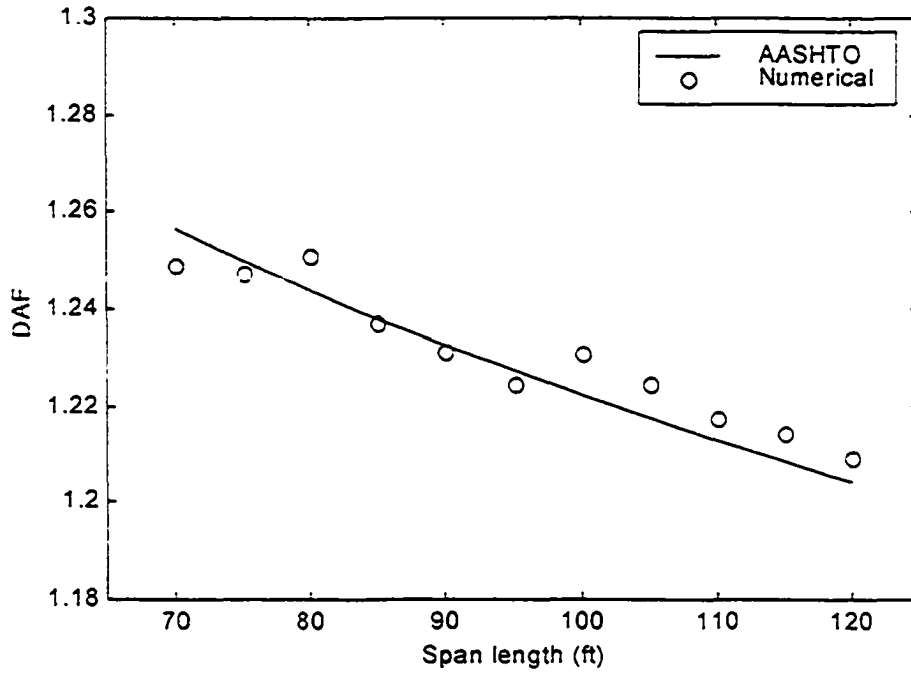
Figure 6.18: DAF vs. span length of bridge
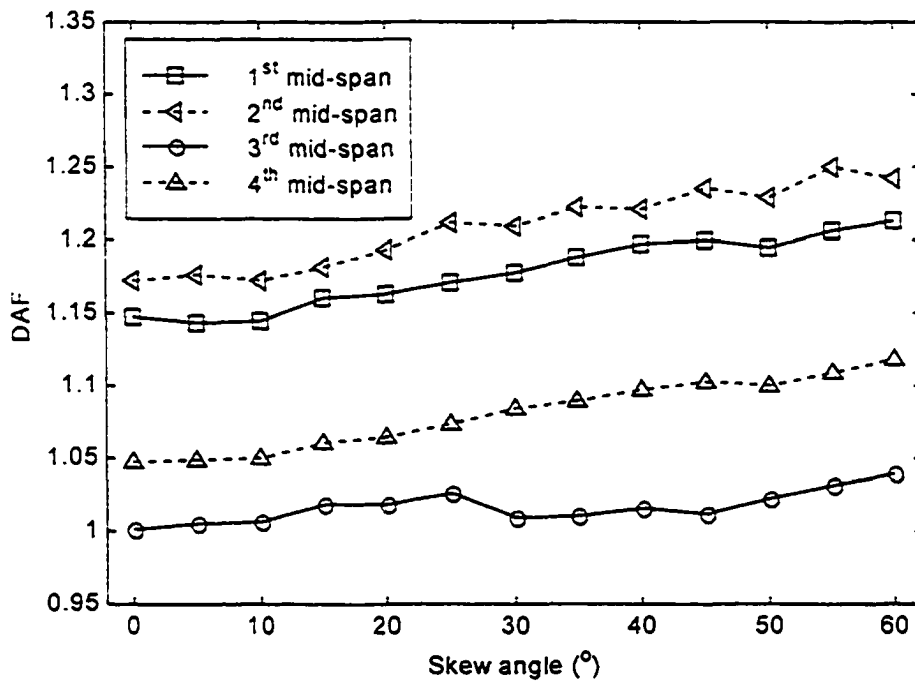
Figure 6.19: DAF vs. skew angle of bridge

TABLE 6.1: Natural frequencies (Hz) and modal damping ratios

of the Walnut Creek Bridge

Mode	pb-2 Rayleigh-Ritz	Test*	Test* damping
1	2.63	2.50	0.024
2	3.04	3.02	0.014
3	3.22	3.20	0.016
4	3.67	3.57	0.018
5	3.93	3.85	0.014
6	4.58	4.21	0.014

*Patten et al., 1999

TABLE 6.2: DAF with different roughness conditions along the central girder

		Mid-span points			
Entrance	Surface	First	Second	Third	Fourth
0	0	1.1837	1.2341	1.0105	1.0918
0	VG	1.1836	1.2378	1.0112	1.0938
0	G	1.1836	1.2390	1.0115	1.0944
0	A	1.1835	1.2403	1.0118	1.0951
0	P	1.1832	1.2441	1.0127	1.0972
VG	0	1.1925	1.2736	1.0128	1.1114
VG	VG	1.1918	1.2787	1.0150	1.1139
VG	G	1.1916	1.2804	1.0158	1.1148
VG	A	1.1915	1.2821	1.0166	1.1156
VG	P	1.1910	1.2876	1.0193	1.1183
G	0	1.1912	1.3102	1.0314	1.1293
G	VG	1.1919	1.3172	1.0356	1.1327
G	G	1.1922	1.3197	1.0371	1.1338
G	A	1.1926	1.3222	1.0386	1.1350
G	P	1.1938	1.3301	1.0435	1.1387
A	0	1.2064	1.3797	1.0767	1.1614
A	VG	1.2105	1.3924	1.0856	1.1670
A	G	1.2120	1.3968	1.0887	1.1690
A	A	1.2135	1.4014	1.0920	1.1710
A	P	1.2187	1.4160	1.1025	1.1774
P	0	1.2155	1.4416	1.1332	1.1896
P	VG	1.2227	1.4605	1.1473	1.1977
P	G	1.2253	1.4673	1.1524	1.2006
P	A	1.2280	1.4743	1.1577	1.2035
P	P	1.2368	1.4967	1.1746	1.2129

TABLE 6.3: DAF with different entrance profiles

		Mid-span points on central girder			
Entrance	Surface	First	Second	Third	Fourth
-WCB	0	1.8483	1.7889	1.4602	1.1953
WCB	0	1.5487	1.3852	1.5068	1.3642
Test		1.55	1.20	1.52	1.22
		Mid-span points on eastern girder			
-WCB	0	1.9160	1.6674	1.1560	1.2723
WCB	0	1.7219	1.5007	1.4791	1.4301
Test		1.57	1.30	1.04	1.41

Patten, 1997

CHAPTER SEVEN

CONCLUSIONS AND RECOMMENDATIONS

7.1 Conclusions

The present work proposed a semi-analytical method to study the bridge/vehicle interaction problem. A skew bridge was modeled as a plate with stiffeners running parallel and orthogonal to two opposite edges. The vibration of such plates was first studied by using the pb-2 Rayleigh-Ritz method. The influence of skew angle, edge ratio, and stiffener height-plate thickness was examined. It was shown that the light-weight stiffeners provide more stiffness effect than mass effect to the plate structure. The stiffeners affect the higher modes more significantly. Relatively higher frequencies are observed with larger skew angle or smaller edge ratio. Without consideration of buckling, deeper stiffeners yield higher frequencies.

A general model was developed for trucks with trailers. The model had eleven degrees of freedom and included three-dimensional motion including heave, pitch, and roll. The principle of virtual work was employed to derive the equations of motion.

A semi-analytical technique was proposed to deal with the dynamic interaction. The proposed semi-analytical technique substantially decreases the

computation cost and was shown to be efficient in dealing with the bridge/vehicle interaction problem with an iterative procedure. In the preceding chapter, the effects of the following factors on the dynamic amplification factor of a bridge due to moving vehicles were examined: bridge damping, bridge entrance roughness, bridge surface roughness, span length, skew angle, vehicle axle weight, axle spacing, vehicle model, vehicle speed, and traffic condition. Among these factors, the bridge entrance roughness, span length, vehicle speed and traffic condition influenced the bridge dynamic response relatively more significantly.

7.2 Recommendations

Usually the bridge deck is made of reinforced concrete, which has mechanical behavior close to orthotropic material. It is worth studying the bridge/vehicle interaction problem by remodeling the bridge superstructure as an orthotropic stiffened plate.

The bridge/vehicle interaction problem can be viewed in the frequency domain. It was claimed that when the natural frequencies of the bridge and the vehicle are close, resonance occurred. The author disagreesz. For instance, model the bridge as a one-DOF mass-spring system (S1) with natural frequency of $\sqrt{m/k}$. When an identical mass-spring system (S2), modeling the vehicle excitation, is connected with it in series, it results in a two-DOF system (S3). The

114

resonance frequencies of system S3 are $\left(\dfrac{3\pm\sqrt{5}}{2}\right)^{1/2}\sqrt{\dfrac{k}{m}}$, or $0.618\sqrt{\dfrac{k}{m}}$ and

$1.618\sqrt{\dfrac{k}{m}}$, which are away from the natural frequency of the one-DOF system.

Moreover, the resonance frequency is defined for external excitation. The two-DOF system S3 vibrates wildly when an ideal external excitation has the same frequency of one of natural frequencies of system S3. It does not mean that the excitation from system S2 causes system S1 to vibrate at resonance when their frequencies are close.

When resonance is a concern, it is worth having a look at the frequency changes of the coupled system as the vehicle travels across the bridge. The natural frequencies vary with the vehicle's position on the bridge. To the author's knowledge, no one has looked at the frequencies of the coupled system in this way. The natural frequencies of the bridge are not changed by the vehicle, and vice versa. What are changed are the frequencies of the coupled bridge/vehicle system.

It was concluded that the initial condition of the vehicle upon the entrance to the bridge is very critical. Lots of work has been done to show this. Usually, the simulation is conducted with the vehicle running on a profile. After it is excited, it passes over the bridge. The present work treats the initial condition in a similar way. However, this raises the question: can we directly look at the vehicle

condition at the entrance and propose an index, such as the vehicle initial energy plus Rayleigh's dissipation function, to evaluate the initial conditions quantitatively?

Some research proposed more practical formulas for DAF evaluation. Most of them include the span length, vehicle speed and bridge frequency (Yang et al., 1995). As the derivation of a formula that is valid for various bridges due to all kinds of conditions, more comprehensive work should be carried out to test the proposed formulas.

REFERENCES

A.A. Alexandridis. (1977) *The Coupled Response of a Dynamic Element Riding on a Continuously Supported Beam*, Ph.D. dissertation, Princeton University.

R.S. Ayre, G. Ford, and L.S. Jacobsen. (1950a) "Transverse vibration of a two-span beam under action of a moving constant force", *Journal of Applied Mechanics*, ASME, 17(1), pp. 1-12.

R.S. Ayre and L.S. Jacobsen. (1950b) "Transverse vibration of a two-span beam under action of a moving alternating force", *Journal of Applied Mechanics*, ASME, 17(3), pp. 283-290.

M. Barrette, A. Berry, and O. Beslin. (2000) "Vibration of stiffened plates using hierarchical trigonometric functions", *Journal of Sound and Vibration*, 235(5), pp. 727-747.

O.K. Bedair and M.S. Troitsky. (1997) "Study of the fundamental frequency characteristics of eccentrically and concentrically simply supported stiffened plates", *International Journal of Mechanical Sciences*, 39(11), pp. 1257-1272.

R.B. Bhat. (1987) "Flexural vibration of polygonal plates using characteristic orthogonal polynomials in two variables", *Journal of Sound and Vibration*, 114(1), pp. 65-71.

J.M. Biggs, H.S. Suer, and J.M. Louw. (1957) "Vibration of simple-span highway bridges", *Journal of the Structural Division*, ASCE, 83(ST2), Proceedings Paper 1186, pp. 291-318.

A.G. Bishara, M.C. Liu, and N.D. El-Ali. (1993) "Wheel load distribution on simply supported skew I-beam composite bridges", *Journal of Structural Engineering*, ASCE, 119(2), pp. 399-419.

A.J. Carr and P.J. Moss. (1982) "Review of impact factors for design of highway bridges", *Dept. Civil Engrg. Rept. 82-14*, University of Canterbury, Christchurch, New Zealand.

S. Chakraverty, R.B. Bhat, and I. Stiharu. (1999) "Recent research on vibration of structures using boundary characteristic orthogonal polynomials in the Rayleigh-Ritz method", *The Shock and Vibration Digest*, 31(3), pp.187-194.

B. Chattopadhyay, P.K. Sinha, and M. Mukhopadhyay. (1992) "Finite element free vibration analysis of eccentrically stiffened composite plates", *Journal of Reinforced Plastics and Composites*, 11(9), pp. 1003-1034.

C.J. Chen, W. Liu, and S.M. Chern. (1994) "Vibration analysis of stiffened plates", *Computers and Structures*, 50(4), pp. 471-480.

Y.K. Cheung and M.S. Cheung. (1972) "Free vibration of a curved and straight beam-slab or box-girder bridges", *International Association of Bridge and Structural Engineering*, 32(II), pp. 41-52.

W. Chiu, R. Smith, and D.N. Wormley. (1971) "Influence of vehicle and distributed guide-way parameters on high-speed vehicle-guideway dynamic interactions", *Journal of Dynamic Systems, Measurement, and Control*, Transactions of ASME, 93(1), p. 25.

K. Chompooming and M. Yener. (1995) "The influence of roadway surface irregularities and vehicle deceleration on bridge dynamics using the method of lines", *Journal of Sound and Vibration*, 183(4), pp. 567-589.

K.H. Chu, V.K. Garg, and L.D. Chaman. (1979) "Railway-bridge impact: simplified train ad bridge model", *Journal of Structure Division*, ASCE, 105, 1823-1844.

R.W. Claassen. (1963) "Vibration of skew cantilever plate", *Pacific Missile Range Tech. Rept.* PMR-TR-62-1, Pacific Missile Range.

D. Cole and D. Cebon. (1992) "Validation of an articulated vehicle simulation", *Vehicle System Dynamics*, 21, pp. 197-223.

A.C. Collop and D. Cebon. (1997) "Effects of 'road friendly' suspensions on long-term flexible pavement performance", *Proc. Instn. Mech. Engrs.*, 211(Part C).

O. Coussy, M. Said, and J.P.V. Hoove. (1989) "The influence of random surface irregularities on the dynamic response of bridges under suspend moving loads", *Journal of Sound and Vibration*, 130, pp. 313-320.

Draft Bridge Design Specification. (1987) National Association of Australian State Road Authorities, Sydney, Australia.

C.J. Dodds. (1972) *BSI Proposals for Generalized Terrain Dynamic Inputs to Vehicles*, ISO/TC/108/WG9, Document No. 5, International Organization for Standardization (ISO).

C.J. Dodds and J.D. Robson. (1973) "The description of road surface roughness", *Journal of Sound and Vibration*, 31(2), pp. 175-183.

M.A. Dokainish and K. Kumar. (1973) "Vibrations of orthotropic parallelogramic plates with variable thickness", *AIAA Journal*, 11(12), pp. 1618-1621.

R.C. Edgerton and G.W. Beecroft. (1955) "Dynamic stresses in continuous plate girder bridges", *ASCE Proc. 82*, Paper No. 973.

E.S. Eichmann. (1954) "Influence of vehicle suspension systems on highway bridge impact", *Structural Research Series No. 70*, University of Illinois, Urbana, IL, pp. 359-364.

M. Fafard, M. Bennur, and M. Savard. (1997) "A general multi-axle vehicle model to study the bridge-vehicle interaction". *Engineering Computations*, 14(5), pp. 491-508.

M. Fafard, M. Laflamme, M. Savard, and M. Bennur. (1998) "Dynamic analysis of existing continuous bridge", *Journal of Bridge Engineering*, ASCE, 3(1), pp. 28-37.

A. Fam and C. Turkstra. (1975) "A finite element scheme for box bridge analysis", *Computers and Structures*, 48, pp. 179-186.

H.V.S. GangaRao. (1984) "Research in vibration analysis of highway bridges", *The Shock and Vibration Digest*, 16(7), pp. 17-22.

H.V.S. GangaRao and C.A. Haslebacher. (1981) "Vibration analysis of highway bridges", *The Shock and Vibration Digest*, 13(1), pp. 3-8.

J.H. Ginsberg, J. Genin, and E.C. Ting. (1976). "Parametric study of the interaction of bridges and moving vehicles", *Applied Scientific Research*, 32, pp. 355-370.

D.J. Gorman and L. Garibaldi. (1999) "A study of multi-span bridge deck free vibration by the method of superposition", *Proceedings of the 2nd International Symposium on Vibrations of Continuous Systems*, Grindelwald, Switzerland, July 11-16.

M.F. Green. (1990) *Dynamic Response of Short-Span Highway Bridges to Heavy Vehicle Loads*, Ph.D. dissertation, University of Cambridge, UK.

M.F. Green and D. Cebon. (1994) "Dynamic response of highway bridges to heavy vehicle loads: theory and experimental validation", *Journal of Sound and Vibration*, 170(1), pp. 51-78.

M.F. Green and D. Cebon. (1997) "Dynamic interaction between heavy vehicles and highway bridges", *Computers and Structures*, 62(2), pp. 253-264.

M.F. Green, D. Cebon, and D.J. Cole. (1995) "Effects of vehicle suspension design on dynamics of highway bridges", *Journal of Structural Engineering*, ASCE, 121(2), pp. 272-282.

R.K. Gupta and R.W. Traill-Nash. (1980) "Bridge dynamic loading due to road surface irregularities and braking of vehicle", *Earthquake Engineering and Structural Dynamics*, 8, pp. 83-96.

H. Hawk and A. Ghali. (1981) "Dynamic response of bridges to multiple truck loading", *Canadian Journal of Civil Engineering*, 8, pp. 392-401.

R.J. Heywood. (1996) "Influence of truck suspensions on the dynamic response of a short span bridge over Cameron's Creek", *Heavy Vehicle Systems*, 3(1-4), pp. 222-239.

I. Hirari. (1963) "Dynamic response of orthortropic plates with two opposite free edges and two simply supported edges under the action of a constant moving force", *Transactions of the Japan Society of Civil Engineers*, 92, pp. 13-20.

B. Hoffmeister and G. Sedlacek. (2000) " Dynamic bridge behaviour under traffic", *The Shock and Vibration Digest*, 32(1), p. 26.

T.C. Hopkins and R.C. Deen. (1970) "The bump at the end of the bridge", *Highway Research Record*, Highway Research Board No. 302, pp. 72-75.

T. Huang. (1976) "Vibration of bridges", *The Shock and Vibration Digest*, 8(1), pp. 61-76.

J.L. Humar and A.M. Kashif. (1993) "Dynamic response of bridges under traveling loads", *Canadian Journal of Civil Engineering*, 20, pp. 287-298.

M.J. Inbanathan and M. Wieland. (1987) "Bridge vibrations due to vehicle moving over rough surface", *Journal of Structural Engineering*, ASCE, 113(9), pp. 1994-2008.

C.E. Inglis. (1934) *A Mathematical Treatise on Vibrations in Railway Bridges*, Cambridge University Press, London, England.

L.S. Jacobsen and B.S. Ayre. (1958) *Engineering Vibrations*, McGraw-Hill, New York, pp. 534-536.

K. Jin. (1997) "Dynamic analysis of stiffened plates using BEM-FEM" (in Chinese), *Gong Cheng Li Xue/Engineering Mechanics*, 14(2), pp. 134-138.

W. Karunasena, K.M. Liew, and F.G.A. Al-Bermani. (1996) "Natural frequencies of thick arbitrary quadrilateral plates using the pb-2 Ritz method", *Journal of Sound and Vibration*, 196(4), pp. 371-385.

S.G. Lekhnitskii. (1947) *Anizotropnye plastinki*, Russia (in Russian).

S.G. Lekhnitskii. (1968) *Anisotropic Plates*, translated by S.W. Tsai and T. Cheron, Gordon and Breach Science Publishers, Inc., New York.

S.S. Lee. (1974) *The Dynamic Response of a Uniform Single Span Bridge under Vehicle Loading with Braking*, Master of Engineering Science thesis, The University of New South Wales, Kensington, New South Wales, Australia.

A.W. Leissa. (1969) *Vibration of Plates*, U.S. Government Printing Office, NASA SP-160, p. 172.

K.M. Liew and K.Y. Lam. (1990) "Application of two-dimensional orthogonal plate function to flexural vibration of skew plates", *Journal of Sound and Vibration* **139(2)**, pp. 241-252.

K.M. Liew and C.M. Wang, (1993) "Pb-2 Rayleigh–Ritz method for general plate analysis", *Engineering Structures*, **15(1)**, pp. 55-60.

K.M. Liew, C.M. Wang, Y. Xiang, and S. Kitipornchai. (1998) *Vibration of Mindlin Plates: Programming the p-version Ritz Method*, Elsevier Science Ltd., Oxford, UK.

W.H. Liu and W.C. Chen. (1992) "Vibration analysis of skew cantilever plates with stiffeners", *Journal of Sound and Vibration*, **159(1)**, pp. 1-11.

S. Marchesiello, A. Fasana, L. Garibaldi, and B.A.D. Piombo. (1999) "Dynamics of multi-span continuous straight bridges subjected to multi-degrees of freedom moving vehicle excitation", *Journal of Sound and Vibration*, **224(3)**, pp. 541-561.

B. Massicotte and A. Picard. (1990) "Developpement d'un camion de calcul adapte aux camions circulant au Quebec", *Conference de l' Association des routes et tranports du Canada (ARTC)*, *Calgary, Canada*, **2**, pp. 619-635 (in French).

T. Mizusawa, T. Kajita, and M. Naruoka. (1979) "Vibration of stiffened skew plates by using B-spline functions", *Computers and Structures*, **10**, pp.821-826.

N. Mukherjee and T. Chattopadhyay. (1994) "Improved free vibration analysis of stiffened plates by dynamic element method", *Computers and Structures*, 52(2), pp. 259-264.

A. Mukherjee and M. Mukhopadhyay. (1986) "A review of dynamic behavior of stiffened plates", *The Shock and Vibration Digest*, 18, pp. 3-8.

N.L. Mulcahy, V.A. Pulmano, and R.W. Traill-Nash. (1979) "Dynamic resonse of bridge decks to vehicle loads by the finite strip approach", *Proceedings of the Third International Conference in Australia on Finite Element Methods*, Sydney, Australia.

M. Naruoka, H. Ohmura, K. Nakagawa, and T. Yamaguchi. (1967) "Free vibration of skew girder bridges with right grillage system", *Transactions of the Japan Society of Civil Engineers*, 139, pp. 1-8.

H.D. Nelson and R.A. Conover. (1971) "Dynamic stability of a beam carrying moving masses", *Journal of Applied Mechanics*, ASME, 38(4), pp. 1003-1006.

D.E. Newland. (1989) *Mechanical Vibration Analysis and Computation*, Longman Scientific & Technical, Harlow, England.

N.M. Newmark. (1959) "A method of computation for structural dynamics", *Journal of the Engineering Mechanics Division*, ASCE, 85, pp. 67-94.

M. Olsson. (1985) "Finite element, modal co-ordinate analysis of structures subjected to moving loads", *Journal of Sound and Vibration*, 99(1), pp. 1-12.

Ontario Highway Bridge Design Code. (1979) Highway Engineering Division, Ontario Ministry of Transportation and Communication, Ontario, Canada.

Ontario Highway Bridge Design Code. (1983) Highway Engineering Division, Ontario Ministry of Transportation and Communication, Ontario, Canada.

G.S. Palani, N.R. Iyer, and T.V.S.R. Appa Rao. (1992) "Efficient finite element model for static and vibration analysis of eccentrically stiffened plates/shells", *Computers and Structures*, 43(4), pp. 651-661.

J. Palamas, O. Coussy, and Y. Bamberger. (1985) "Effects of surface irregularities upon the dynamic response of bridges under suspended moving loads", *Journal Sound and Vibration*, 99, pp. 235-245.

W. N. Patten. (1997) "Semiactive vibration absorbers (SAVA) at the I-35 Walnut Creek Bridge", *Final Report, No. 2125,* FHWA, Oklahoma Department of Transportation, and The University of Oklahoma, Norman, OK.

W.N. Patten, J. Sun, G. Li, J. Kuehn, and G. Song. (1999) "Field test of an intelligent stiffener for bridges at the I-35 Walnut Creek Bridge", *Earthquake Engineering and Structural Dynamics*, 28, pp. 109-126.

S. S. Rao. (1995) *Mechanical Vibrations*, 3rd Edition, Addison-Wesley Publishing Company, Reading, MA.

S.W. Robinson. (1887) "Vibration of bridges", *Transactions of ASCE*, 16, Paper No. 351, pp. 42-65.

126

J. Solnes. (1997) *Stochastic Processes and Random Vibrations: Theory and Practice*, John Wiley & Sons, Chichester, England, p. 257.

C.C. Spyrakos. (1998) "Dynamic load factor in composite highway bridges", *International Conference on Structures Under Shock and Impact*, June 1998 pp. 211-220.

N. Sridharan and A.K. Mallik. (1979) "Numerical analysis of vibration of beams subjected to moving loads", *Journal of Sound and Vibration*, 65(1), pp. 147-150.

R.S. Srinivasan and K. Munaswamy. (1978) "Dynamic response analysis of stiffened slab bridges", *Computers and Structures*, 9(6), pp. 559-566.

R.S. Srinivasan and S.V. Ramachandran. (1976) "Large deflection of clamped skew plates", *Computer Methods in Applied Mechanics and Engineering*, 7(2), pp. 219-233.

Standard Specifications for Highway Bridges. (1989) 14th Edition, American Association of State Highway and Transportation Officials (AASHTO), Washington, D.C.

M.M. Stanisic, J.A. Euler, and S.T. Montgomery. (1974) "On a theory concerning the dynamic behavior of structures carrying moving masses", *Ingenieur-Archiv*, 43(5), pp. 295-303.

G. Stokes. (1849) "Discussion of a differential equation relating to the braking of railway bridges", *Transactions of the Cambridge Philosophical Society*, 8, p. 707.

H.S. Suer. (1955) *Dynamic Response of Simple Span Highway Bridges to Moving Vehicle Loads*, Doctor of Science dissertation, the Massachusetts Institute of Technology, Cambridge.

P. Swannell and C.W. Miller. (1987) "Theoretical and Experimental studies of a bridge-vehicle system", *Proc. Instn Civ. Engrs.*, 83(Part 2), pp. 613-635.

M.R. Taheri and E.C. Ting. (1990) "Dynamic response of plates to moving loads: finite element method", *Computers and Structures*, 34(3), pp.509-521.

G.H. Tan, G.H. Brameld, and D.P. Thambiratnam. (1994) "A three-dimensional vehicle model for bridge-vehicle interaction", 5th *Int. Conf. Recent Advances in Structural Dynamics*, Southampton, UK.

G.H. Tan, G.H. Brameld, and D.P. Thambiratnam. (1998) "Development of an analytical model for treating bridge-vehicle interaction", *Engineering Structures*, 20(1-2), pp. 54-61.

P.V. Thangam Babu and D.V. Reddy. (1971) "Frequency analysis of skew orthotropic plates by the finite strip method", *Journal of Sound and Vibration*, 18, pp. 465-475.

S.P. Timoshenko. (1922a) "Vibrations of beams under moving, pulsating forces", *Philosophical Magazine*, Ser. 6, 43, p. 125-133.

S.P. Timoshenko. (1922b) "On the forced vibration of bridges", *Philosophical Magazine*, Ser. 6, 43, pp. 1018-1019.

S.P. Timoshenko and D.H. Young. (1955) *Vibration Problems in Engineering*, 3rd edition, D. Van Nostrand and Co., New York.

E.C. Ting, J. Genin, and J.H. Ginsberg. (1975) "Dynamic interaction of bridge structures and vehicles", *The Shock and Vibration Digest*, 7(7), pp. 61-69.

E.C. Ting and M. Yener. (1983) "Vehicle-structure interactions in bridge dynamics", *The Shock and Vibration Digest*, 15, pp. 3-9.

M.S. Troitsky. (1976) *Stiffened Plates — Bending, Stability and Vibrations*, Elsevier Scientific Publishing Company, New York.

T.P. Tung, L.E. Goodman, T.Y. Chen, and N.M. Newmark. (1956) "Highway bridge impact problems", *Highway Research Board Bulletin 124*, National Academy of Sciences, Washington, D.C., pp. 111-134.

A.S. Veletsos and T. Huang. (1970) "Analysis of dynamic response of highway bridges", *Journal of the Engineering Mechanics Division*, ASCE, 96(EM5), pp. 593-620.

W. Voigt. (1910) *Lehrbuch der Kristallphysik*, B. G. Teubner, Berlin.

T.L. Wang and D.Z. Huang. (1992) "Computer modeling analysis in bridge evaluation", *Interim Research Report*, Florida Department of Transportation, Report No. FL/DOT/RMC/0542-3394, Tallahassee, FL.

T.L. Wang, D. Huang, M. Shahaway, and K. Huang. (1996) "Dynamic response of highway girder bridges", *Computers and Structures*, 60(6), pp. 1021-1027.

T.L. Wang, M. Shahaway, and D.Z. Huang. (1993) "Dynamic response of highway trucks due to road roughness", *Computers and Structures*, 49(6), pp. 1055-1067.

R.K.L. Wen. (1960) "Dynamic response of breams traversed by two-axle loads", *Journal of Engineering Mechanics Division*, ASCE, 86(EM5), pp. 91-111.

R.K.L. Wen and T. Toridis. (1962) "Dynamic behavior of cantilever bridges", *Journal of the Engineering Mechanics Division*, ASCE, 88(EM4), pp. 27-43.

R. Willis. (1849) *Report of the Commissioners Appointed to Inquire into the Application of Iron to Railway Structures*, Appendix B, Stationery Office, London, England.

J.F. Wilson. (1973) "Response of simple spans to moving mass loads", *AIAA Journal*, 11(1), pp. 4-5.

D.T. Wright and R. Green. (1959) "Highway bridge vibrations I: review of previous studies, *Research Report No. 5, Ontario Joint Highway Research Program*, Queen's University, Kingston, Ontario.

Y. Xiang, S. Kitipornchai, K.M. Liew, and M.K. Lim. (1995) "Vibration of stiffened skew Mindlin plates", *Acta Mechanica*, 112, pp. 11-28.

Y. Yamada and T. Kobori. (1965) "Studies of highway bridge impact due to random moving vehicles", *Transactions of the Japan Society of Civil Engineers*, **119**, pp. 61-70.

Y.B. Yang, S.S. Liao, and B.H. Lin. (1995) "Impact formulas for vehicles moving over simple and continuous beams", *Journal of Structural Engineering*, ASCE, **121**(11), pp. 1644-1650.

Y.B. Yang and B.H. Lin. (1995) "Vehicle-bridge interaction analysis by dynamic condensation method", *Journal of Structural Engineering*, ASCE, **121**(11), pp. 1636-1643.

Y.B. Yang and J.D. Yau. (1997) "Vehicle-bridge interaction element for dynamic analysis", *Journal of Structural Engineering*, ASCE, **123**(11), pp. 1512-1518.

M. Yener and K. Chompooming. (1991) "Formulation of dynamic vehicle-bridge interaction systems", *Structural Engineering and Mechanics Division*, Report No. CEE-SEMD-91-11, Utah State University, Logan, UT.

M. Yener and K. Chompooming. (1994) "Numerical method of lines for analysis of vehicle-bridge dynamic interaction", *Computers and Structures*, Vol. 53, No. 3, pp. 709-726.

H. Zeng and C.W. Bert. (2000) "A differential quadrature analysis of vibration for rectangular stiffened plates", *Journal of Sound and Vibration*, in press.

H. Zeng, J. Kuehn, J. Sun, and H.L. Stalford. (2000) "An analysis of skewed bridge/vehicle interaction using the grillage method", *Proceedings of the*

Fourteenth Engineering Mechanics Conference, ASCE, Austin, TX, May 21-24.

Appendix I

Vehicle coupled force vector, and gravity vector,

stiffness, damping, and mass matrices

Coupled force vector:

$$F_{bv} = \begin{bmatrix} k_{t1}w_1 \div c_{t1}\dot{w}_1, k_{t2}w_2 \div c_{t2}\dot{w}_2, k_{t3}w_3 \div c_{t3}\dot{w}_3, k_{t4}w_4 \div c_{t4}\dot{w}_4, \\ k_{t5}w_5 \div c_{t5}\dot{w}_5, k_{t6}w_6 \div c_{t6}\dot{w}_6, 0,0,0,0 \end{bmatrix}^T$$

Gravity vector:

$$G_v = \begin{bmatrix} -m_1, -m_2, -m_3, -m_4, -m_5, -m_6, -b_2 M_1, \\ a_1 c_2 M_2 - (b_1 - a_2)M_1, -d_2 c_1 M_2, -d_1 c_1 M_2, -a_2 c_2 M_2 - a_2 M_1 \end{bmatrix}^T \times g$$

with g being the gravity acceleration.

Symmetric Stiffness matrix:

$K_v=$

```
[[k_t1 + k_s1, 0,  0,  0,  0,  0,  -k_s1,  0,  0,  0,  0],
 [0,  k_t2 + k_s2,  0,  0,  0,  0,  0,  -k_s2,  0,  0,  0],
 [0,  0,  k_t3 + k_s3,  0,  0,  0,  0,  0,  -k_s3,  0,  0],
 [0,  0,  0,  k_t4 + k_s4,  0,  0,  0,  0,  0,  -k_s4,  0],
 [0,  0,  0,  0,  k_t5 + k_s5,  0,  0,  0,  0,  0,  -k_s5],
 [0,  0,  0,  0,  0,  k_t6 + k_s6,  -k_s6,  k_s6,  0,  0,  -k_s6],
 [-k_s1,  0,  0,  0,  0,  -k_s6,  k_s6 + k_s1,  -k_s6,  0,  0,  k_s6],
 [0,  -k_s2,  0,  0,  0,  k_s6,  -k_s6,  k_s2 + k_s6,  0,  0,  -k_s6],
 [0,  0,  -k_s3,  0,  0,  0,  0,  0,  k_s3,  0,  0],
 [0,  0,  0,  -k_s4,  0,  0,  0,  0,  0,  k_s4,  0],
 [0,  0,  0,  0,  -k_s5,  -k_s6,  k_s6,  -k_s6,  0,  0,  k_s6 + k_s5]];
```

Symmetric Damping matrix:

Replacing "k" with "c" in stiffness matrix gives damping matrix C_v.

Symmetric mass matrix:

$M_v=$

$[[m_1, \ 0, \ 0, \ 0, \ 0, \ 0, \ 0, \ 0, \ 0, \ 0, \ 0],$

$[0, \ m_2, \ 0, \ 0, \ 0, \ 0, \ 0, \ 0, \ 0, \ 0, \ 0],$

$[0, \ 0, \ m_3, \ 0, \ 0, \ 0, \ 0, \ 0, \ 0, \ 0, \ 0],$

$[0, \ 0, \ 0, \ m_4, \ 0, \ 0, \ 0, \ 0, \ 0, \ 0, \ 0],$

$[0, \ 0, \ 0, \ 0, \ m_5, \ 0, \ 0, \ 0, \ 0, \ 0, \ 0],$

$[0, \ 0, \ 0, \ 0, \ 0, \ m_6, \ 0, \ 0, \ 0, \ 0, \ 0],$

$[0, \ 0, \ 0, \ 0, \ 0, \ 0, \ (M_v)_{7,7}, \ (M_v)_{8,7}, \ 0, \ 0, \ (M_v)_{11,7}],$

$[0,0,0,0,0,0, \ (M_v)_{8,7} \ (M_v)_{8,8}, \ (M_v)_{9,8}, \ (M_v)_{10,8}, \ (M_v)_{11,8}],$

$[0,0,0,0,0,0, \ 0, \ (M_v)_{9,8} \ (M_v)_{9,9}, \ (M_v)_{10,9}, \ (M_v)_{11,9}],$

$[0,0,0,0,0,0, \ 0, \ (M_v)_{10,8}, \ (M_v)_{10,9}, \ (M_v)_{10,10}, \ (M_v)_{11,10}],$

$[0,0,0,0,0,0, \ (M_v)_{11,7}, \ (M_v)_{11,8}, \ (M_v)_{11,9}, \ (M_v)_{11,10}, \ (M_v)_{11,11}]];$

with

$$(M_v)_{7,7} = b_2^2 M_1 + \frac{I_{\theta 1}}{l_b^2} \ ;$$

$$(M_v)_{8,7} = b_2 M_1 (b_1 - a_2) - \frac{I_{\theta 1}}{l_b^2} \ ;$$

$$(M_v)_{11,7} = b_2 a_2 M_1 \ ;$$

$$(M_v)_{8,8} = (b_1 - a_2)^2 M_1 + a_1^2 c_2^2 M_2 + \frac{I_{\theta 1}}{l_b^2} + \frac{I_{\alpha 1}}{l_a^2} + \frac{a_1^2 I_{\theta 2}}{l_c^2} \ ;$$

$$(M_v)_{9,8} = a_1 c_1 c_2 d_2 M_2 - \frac{a_1^2 I_{\theta 2}}{l_c^2} \ ;$$

134

$$(M_v)_{10.8} = a_1 c_1 c_2 d_1 M_2 - \frac{a_1 a_2 I_{\theta 2}}{l_c^2} \; ;$$

$$(M_v)_{11.8} = (b_1 - a_2) a_2 M_1 + a_1 a_2 c_2^2 M_2 - \frac{I_{\alpha 1}}{l_a^2} \div \frac{a_1 a_2 I_{\theta 2}}{l_c^2} \; ;$$

$$(M_v)_{9.9} = (d_2 c_1)^2 M_2 \div \frac{I_{\alpha 2}}{l_d^2} \div \frac{a_1^2 I_{\theta 2}}{l_c^2} \; ;$$

$$(M_v)_{10.9} = d_1 d_2 c_1^2 M_2 - \frac{I_{\alpha 2}}{l_d^2} \div \frac{a_1 a_2 I_{\theta 2}}{l_c^2} \; ;$$

$$(M_v)_{11.9} = a_2 c_1 c_2 d_2 M_2 - \frac{a_1 a_2 I_{\theta 2}}{l_c^2} \; ;$$

$$(M_v)_{10.10} = (d_1 c_1)^2 M_2 \div \frac{I_{\alpha 2}}{l_d^2} \div \frac{a_2^2 I_{\theta 2}}{l_c^2} \; ;$$

$$(M_v)_{11.10} = a_2 c_1 c_2 d_1 M_2 - \frac{a_2^2 I_{\theta 2}}{l_c^2} \; ;$$

$$(M_v)_{11.11} = a_2^2 c_2^2 M_2 \div \frac{I_{\alpha 1}}{l_a^2} \div \frac{a_2^2 I_{\theta 2}}{l_c^2} \div a_2^2 M_1 .$$

Appendix II

Computer code VehiclePack written in Matlab®

% VehiclPack() numerically integrates the equations of motion

%   of vehicle by using Newmark's method.

```
function [Fvb,Xv_out,Xvd_out,Xvdd_out]=...
    VehiclePack(Xcon,dtime,Xv_ini,Xvd_ini,Xvdd_ini,M_v,K_v,C_v,G_v,F_v);
```

% input of VehiclePack:

%	Xcon:	displacement and velocity of contact points
%		[w1,w2,...,w1d,w2d,...]
%	dtime:	time increment
%	Xv_ini:	initial displacement vector
%	Xvd_ini:	initial velocity vector
%	Xvd_ini:	initial acceleration vector
%	M_v:	mass matrix of vehicle
%	K_v:	stiffness matrix of vehicle
%	C_v:	damping matrix of vehicle
%	G_v:	gravity force vector
%	F_v:	interactive force vector

% output of VehiclePack:

%	Fvb:	tire forces vector
%	Xv_out:	displacement vector
%	Xvd_out:	velocity vector
%	Xvdd_out:	acceleration vector

```
alpha=1/6;beta=1/2; % two constants in Newmark's method


Xv_out=inv(M_v/alpha/dtime^2+C_v*beta/alpha/dtime+K_v)*...
   (G_v+F_v*Xcon+M_v*(Xv_ini/alpha/dtime^2+Xvd_ini/alpha/dtime+...
   (1/2/alpha-1)*Xvdd_ini)+C_v*(Xv_ini*beta/alpha/dtime+...
   (beta/alpha-1)*Xvd_ini+(beta/alpha-2)*dtime/2*Xvdd_ini));
Xvdd_out=(Xv_out-Xv_ini)/alpha/dtime^2-Xvd_ini/alpha/dtime-...
   Xvdd_ini*(1/2/alpha-1);
Xvd_out=Xvd_ini+(1-beta)*dtime*Xvdd_ini+beta*dtime*Xvdd_out;


Fvb1=F_v*(Xcon-[Xv_out(1:6);Xvd_out(1:6)]);
Fvb=Fvb1(1:6);
```

Appendix III

Computer code BVPack written in Matlab®

```
%%%%%%%%%%%%%%%%%%%%%%%%%%%%%%%%%%%%%%%%%%%%%
% As an example, Rock Truck running on the west lane        %
% at the speed of 30 m/s with Poor bridge entrance          %
% is simulated by the following program.                    %
% by Huan Zeng, November, 2000.                                      %
%%%%%%%%%%%%%%%%%%%%%%%%%%%%%%%%%%%%%%%


clear all;close all;
Nmode=5;


for i=1:Nmode
   eval(['load W'num2str(i) '.prn']);
end


load KK0.prn;load MM0.prn;
[Vector,Value]=eig(KK0,MM0);
w0=sqrt(diag(Value));
[w0,w_ind]=sort(w0);
w0=real(w0);
w=w0;
% modal damping from test.
ksi=[0.024,0.014,0.016,0.018,0.014,0.014, 0.022,0.025,0.022,0.025];
```

```
T0=clock;

T_DOF=11;T_DOF2=22;
CON_DOF=6; CON_DOF2=12; % Contact points

lb2kg=1/2.202;ft2m=12*0.0254;in2m=0.0254;

alpha=pi/4;ta=tan(alpha);sa=sin(alpha);ca=cos(alpha);
b=34*ft2m;
a=400*ft2m;

L=a;
L_pro1=a/4;
L_pro2=b*sin(alpha);
L_pro3=a/4;
L_pro=L_pro1+L_pro2+L+L_pro3;

VehicleDyn; % return matrix , K_v, C_v, F_v, and G_v;

VELOCITY=30;T_CONTACT=L/VELOCITY;
T_pro1=L_pro1/VELOCITY;
T_pro2=L_pro2/VELOCITY;
T_pro3=L_pro3/VELOCITY;
T_pro=L_pro/VELOCITY;

dtime=T_CONTACT/5000;

N_pro1=fix(T_pro1/dtime);
```

```
N_pro2=fix(T_pro2/dtime);
N_pro3=fix(T_pro3/dtime);
N_pro=fix(T_pro/dtime);


% generate sample profile
Ar_VG=5e-6; % Very Good
Ar_G=20e-6; % Good
Ar_A=80e-6; % Average
Ar_P=256e-6; % Poor


Pkey='VGVG';
Zprofile=psd(N_pro,L_pro,Ar_VG);
plot(Zprofile);


Z0=[ones(CON_DOF,1);zeros(CON_DOF,1)];


T_FINAL=T_pro;


time=0:dtime:T_FINAL;
NSTEP_FINAL=length(time);


% Travel path
XF=zeros(6,NSTEP_FINAL);
YF=zeros(6,NSTEP_FINAL);


B1=3*b/4*sin(alpha);
B2=b/2*sin(alpha);
```

140

```
q=zeros(Nmode,NSTEP_FINAL);
q_dot=q;


%%%              Initialization          %%%


Xcon=zeros(CON_DOF2,1);
Zv_ini=[-0.03196770851071 -0.02175054828472 ...
    -0.01309502313343 -0.01309503434948 ...
    -0.02175054781848 -0.03196771169376 ...
    -0.06208659296437 -0.06492270869329 ...
    -0.11458805762317 -0.11458829300190 -0.06492270708460]';
Zvd_ini=zeros(T_DOF,1);
Zvdd_ini=inv(M_v)*(G_v+F_v*Xcon-C_v*Zvd_ini-K_v*Zv_ini);
Z=zeros(CON_DOF2,1);


% Initial coupled force;
Fvb1=F_v*(Xcon-[Zv_ini(1:6);Zvd_ini(1:6)]);
Fvb=zeros(6,NSTEP_FINAL);
Fvb(:,1)=Fvb1(1:6);


L12=4.7;L23=5.7;
y1=zeros(12,NSTEP_FINAL);


%%    Coupling Loop


for Itime=2:(NSTEP_FINAL-2)
  if((Itime)<(N_pro1))
    Xcon=Zprofile(Itime)*Z0;
```

```
y1(:,Itime)=Xcon;


% Response of Vehicle
[Fvb(:,Itime+1),Zv_ini,Zvd_ini,Zvdd_ini]=...
   VehiclePack(Xcon,dtime,Zv_ini,Zvd_ini,Zvdd_ini,...
   M_v,K_v,C_v,G_v,F_v);
 bb(:,Itime)=[Fvb(:,Itime+1);Zv_ini];


elseif(time(Itime)<T_pro1+T_pro1+T_CONTACT)


% 1,6: front axle
% 2,5: middle axle
% 3,4: rear axle
XF(1,Itime)=VELOCITY*time(Itime)-L_pro1-b*sin(alpha)/2;
XF(2,Itime)=XF(1,Itime)-L12;
XF(3,Itime)=XF(2,Itime)-L23;
XF(6,Itime)=VELOCITY*time(Itime)-b*sin(alpha)/4;
XF(5,Itime)=XF(6,Itime)-L12;
XF(4,Itime)=XF(6,Itime)-L23;


YF(1,Itime)=B1;YF(2,Itime)=B1;YF(3,Itime)=B1;
YF(4,Itime)=B2;YF(5,Itime)=B2;YF(6,Itime)=B2;


for iX=1:CON_DOF
  if XF(iX,Itime)<0 ; XF(iX,Itime)>L
    XF(iX,Itime)=0;
    YF(iX,Itime)=0;
    Fvb(iX,Itime)=0;
```

```matlab
        Z(iX,1)=1;
    end
end


% Bridge response


for n=1:Nmode
    for IL=1:6
        %delmen(IL,1)=get_xy(Wn,XF(IL,Itime),YF(IL,Itime));
        eval(['delme'num2str(n)                '(IL,1)=get_xy(W'num2str(n)
',XF(IL,Itime),YF(IL,Itime));']);
    end
end


Xcon=Z*Zprofile(Itime);


for n=1:Nmode
    eval(['delme=delme'num2str(n) ';']);
    Qi=sum(delme.*Fvb(:,Itime));
    q(n,Itime)=z1_quad2(Qi,dtime,w(n),ksi(n),q(n,Itime-1),q_dot(n,Itime-1));
    q_dot(n,Itime)=z1_quad_dot2(Qi,dtime,w(n),ksi(n),q(n,Itime-
1),q_dot(n,Itime-1));
    Xcon=Xcon+[delme*q(n,Itime);delme*q_dot(n,Itime)];
end


y1(:,Itime)=Xcon;


% Response of Vehicle
```

```matlab
    [Fvb(:,Itime+1),Zv_ini,Zvd_ini,Zvdd_ini]=...
       VehiclePack(Xcon,dtime,Zv_ini,Zvd_ini,Zvdd_ini,...
       M_v,K_v,C_v,G_v,F_v);
    bb(:,Itime+1)=[Fvb(:,Itime+1);Zv_ini];
  else
    % Free vibration of bridge
    for n=1:Nmode
       Qi=0;
       q(n,Itime)=z1_quad2(Qi,dtime,w(n),ksi(n),q(n,Itime-1),q_dot(n,Itime-1));
       q_dot(n,Itime)=z1_quad_dot2(Qi,dtime,w(n),ksi(n),q(n,Itime-
1),q_dot(n,Itime-1));
    end


    Xcon=[ones(CON_DOF,1);zeros(CON_DOF,1)]*Zprofile(Itime);


    y1(:,Itime)=Xcon;


    % Free Vibration of Vehicle


[Fvb(:,Itime+1),Zv_ini,Zvd_ini,Zvdd_ini]=VehiclePack(Xcon,dtime,Zv_ini,Zvd_
ini,Zvdd_ini,M_v,K_v,C_v,G_v,F_v);
    bb(:,Itime+1)=[Fvb(:,Itime+1);Zv_ini];


    Fvb(:,Itime+1)=zeros(CON_DOF,1);
  end % if


end % Itime
```

```
bb(:,Itime+2)=[Fvb(:,Itime+1);Zv_ini];


Tf=clock;
RUNTIME0=Tf(4:6)-T0(4:6);
disp([' Running time is about: 'num2str(RUNTIME0(1))...
    'hours 'num2str(RUNTIME0(2)) ' minutes '...
    num2str(RUNTIME0(3)) ' seconds'])


get_deflect;


%%%%% END OF MAIN PROGRAM %%%%%



%%%%%%%%%%%%%%%%%%%%%%%%%%%%%%%%%%
%            get_deflection subroutine            %
%%%%%%%%%%%%%%%%%%%%%%%%%%%%%%%%%%
yQ=zeros(20,NSTEP_FINAL); % stors time history of 20 locations.


% G#1, 1st mid-span
ptx(1)=L/8;pty(1)=0;


% G#1, 2nd mid-span
ptx(2)=L/4+L/8;pty(2)=0;


% G#1, 3rd mid-span
ptx(3)=2*L/4+L/8;pty(3)=0;


% G#1, 4th mid-span
```

```
ptx(4)=3*L/4+L/8;pty(4)=0;


% G#2

ptx(5:8)=ptx(1:4)+b/4*cos(alpha); pty(5:8)=b/4*sin(alpha)*ones(1,4);


% G#3

ptx(9:12)=ptx(1:4)+b/2*cos(alpha); pty(9:12)=b/2*sin(alpha)*ones(1,4);


% G#4

ptx(13:16)=ptx(1:4)+3*b/4*cos(alpha); pty(13:16)=3*b/4*sin(alpha)*ones(1,4);


% G#5

ptx(17:20)=ptx(1:4)+b*cos(alpha); pty(17:20)=b*sin(alpha)*ones(1,4);


for u=1:20
  for n=1:Nmode
    eval(['temp(u,n)=get_xy(W'num2str(n) ',ptx(u),pty(u));']);
  end
end


for u=1:20
  for n=1:Nmode
    qXY(n,:)=temp(u,n)*q(n,:);
  end
  yQ(u,:)=sum(qXY(1:Nmode,:));
end


%%%%%%%%%%%%%%%%%%%%%%%%%%%%%%
```

```
% PSD function                                    %
%%%%%%%%%%%%%%%%%%%%%%%%%%%%%%%%%%

function PSD_return=PSD(N,L,At)

w0=1/2/pi;
fmin=1/L; fmax=2.5e4;
x=L/N:L/N:L;
dw=(fmax-fmin)/N;
the=rand(1,N)*2*pi;
temp=zeros(1,N);w=temp;r=w;

for n=1:N
  w(n)=(n-1/2)*dw;
end

for i=1:N
  for n=1:N
    temp(n)=sqrt(4*At*(w(n)/w0)^(-2)*dw)*cos(w(n)*x(i)+the(n));
  end
  PSD_return(i)=sum(temp);
end
```